ความต้านทานการสึกหรอแบบขัดสีของเหล็กหล่อไฮโปยูเทคติค 26 เปอร์เซ็นต์โดยมวลโครเมียมที่เติมโมลิบดีนัม

นายอรรถสิทธิ์ ชูประจง

วิทยานิพนธ์นี้เป็นส่วนหนึ่งของการศึกษาตามหลักสูตรปริญญาวิศวกรรมศาสตรมหาบัณฑิต
สาขาวิชาวิศวกรรมโลหการ ภาควิชาวิศวกรรมโลหการ
คณะวิศวกรรมศาสตร์ จุฬาลงกรณ์มหาวิทยาลัย
ปีการศึกษา 2554

ABRASIVE WEAR RESISTANCE OF HYPOEUTECTIC 26 MASS% CHROMIUM CAST IRON CONTAINING MOLYBDENUM

Mr. Attasit Chooprajong

A Thesis Submitted in Partial Fulfillment of the Requirements

for the Degree of Master of Engineering Program in Metallurgical Engineering

Department of Metallurgical Engineering

Faculty of Engineering

Chulalongkorn University

Academic Year 2011

Thesis Title	ABRASIVE WEAR RESISTANCE OF HYPOEUTECTIC 26 MASS% CHROMIUM CAST IRON CONTAINING MOLYBDENUM
By	Mr. Attasit Chooprajong
Field of Study	Metallurgical Engineering
Thesis Advisor	Associate Professor Prasonk Sricharoenchai
Thesis Co-advisor	Professor Yasuhiro Matsubara

Accepted by the Faculty of Engineering, Chulalongkorn University in Partial Fulfillment of the Requirements for the Master's Degree

…….. Dean of the Faculty of Engineering
(Associate Professor Boonsom Lerdhirunwong, Dr.Ing.)

THESIS COMMITTEE

…….. Chairman
(Assistant Professor Sawai Danchaivijit, Ph.D.)

……. Thesis Advisor
(Associate Professor Prasonk Sricharoenchai, D.Eng.)

…….. Thesis Co-Advisor
(Professor Yasuhiro Matsubara, D.Eng.)

…….. Examiner
(Professor Takateru Umeda, D.Eng.)

…….. External Examiner
(Assistant Professor Sudsakorn Inthidech, D.Eng.)

อรรถสิทธิ์ ชูประจง : ความต้านทานการสึกหรอแบบขัดสีของเหล็กหล่อไฮโปยูเทคติค 26 เปอร์เซ็นต์โดยมวลโครเมียมที่เติมโมลิบดีนัม. (ABRASIVE WEAR RESISTANCE OF HYPOEUTECTIC 26 MASS% CHROMIUM CAST IRON CONTAINING MOLYBDENUM) อ. ที่ปรึกษาวิทยานิพนธ์หลัก : รศ. ดร. ประสงค์ ศรีเจริญชัย,อ. ที่ปรึกษาวิทยานิพนธ์ร่วม : Prof. Yasuhiro Matsubara, 123 หน้า.

เหล็กหล่อไฮโปยูเทคติค 26 เปอร์เซ็นต์โดยมวลโครเมียมที่ไม่เติมและเติมโมลิบดีนัมถูกเตรียมขึ้นเพื่อศึกษาความต้านทานการสึกหรอแบบขัดสี ได้ชุบแข็งชิ้นงานที่ผ่านการอบอ่อนจาก 1323 K และจากนั้นอบคืนตัวที่อุณหภูมิ 3 ระดับระหว่าง 673 ถึง 823 K เป็นเวลา 7.2 ks คือ อุณหภูมิที่ให้ความแข็งสูงที่สุด (H_{Tmax}), อุณหภูมิต่ำกว่า H_{Tmax} (L-H_{Tmax}) และอุณหภูมิสูงกว่า H_{Tmax} (H-H_{Tmax}) ประเมินผลความต้านทานการสึกหรอแบบขัดสีโดยใช้การทดสอบการสึกหรอแบบขัดสี Suga (ชนิดสองบอดี้) และการทดสอบการสึกหรอแบบขัดสีล้อยาง (ชนิดสามบอดี้)

พบว่าความแข็งและสัดส่วนเชิงปริมาตรของออสเตนไนท์เหลือค้าง (V_γ) ในชิ้นงานที่ผ่านกรรมวิธีทางความร้อนแปรผันตามปริมาณโมลิบดีนัมและเงื่อนไขของกรรมวิธีทางความร้อน ความสัมพันธ์เชิงเส้นระหว่างน้ำหนักที่สูญเสียและระยะทางเป็นเส้นตรงในทุกชิ้นงาน ได้อัตราการสึกหรอ (Rw) ต่ำที่สุดทั้งในชิ้นงานสภาพชุบแข็ง และ H_{Tmax} ได้ Rw สูงที่สุดทั้งในชิ้นงาน L-H_{Tmax} และ H-H_{Tmax} ค่า Rw ลดลงตามความแข็งที่เพิ่มขึ้น ในการทดสอบการสึกหรอแบบขัดสี Suga ได้ค่า Rw ต่ำที่สุดในชิ้นงานที่ V_γ ประมาณ 10 เปอร์เซ็นต์ ค่า Rw ลดลงตามปริมาณโมลิบดีนัมที่เพิ่มขึ้น ในการทดสอบการสึกหรอแบบขัดสีล้อยาง ได้ค่า Rw ต่ำที่สุดในชิ้นงานที่ V_γ 10 เปอร์เซ็นต์เช่นกัน อย่างไรก็ตามค่า Rw ไม่ขึ้นกับปริมาณโมลิบดีนัม

ภาควิชา...วิศวกรรมโลหการ.....ลายมือชื่อนิสิต.....
สาขาวิชา...วิศวกรรมโลหการ..... ลายมือชื่อ อ.ที่ปรึกษาวิทยานิพนธ์หลัก.....
ปีการศึกษา....2554..... ลายมือชื่อ อ.ที่ปรึกษาวิทยานิพนธ์ร่วม .....

5170517121 : MAJOR METALLURGICAL ENGINEERING
KEYWORDS : HYPOEUTECTIC 26% CHROMIUM CAST IRON / ABRASIVE WEAR RESISTANCE / HEAT TREATMENT / MOLYBDENUM EFFECT / HARDNESS / VOLUME FRACTION OF RETAINED AUSTENITE

ATTASIT CHOOPRAJONG : ABRASIVE WEAR RESISTANCE OF HYPOEUTECTIC 26 MASS% CHROMIUM CAST IRON CONTAINING MOLYBDENUM. ADVISOR : ASSOC. PROF. PRASONK SRICHAREONCHAI, D.Eng., CO-ADVISOR : PROF. YASUHIRO MATSUBARA, D.Eng., 123 pp.

Hypoeutectic 26 wt% Cr cast irons without and with Mo were prepared in order to investigate their abrasion wear resistance. The annealed specimens were hardened from 1323 K and then tempered at three levels of temperatures between 673 and 823 K for 7.2 ks, the temperature giving the maximum hardness (H_{Tmax}), temperature lower than that at H_{Tmax} (L-H_{Tmax}) and temperature higher than that at H_{Tmax} (H-H_{Tmax}). The abrasive wear resistance was evaluated using Suga abrasion wear test (two-body-type) and Rubber Wheel abrasion wear test (three-body-type).

It was found that hardness and volume fraction of retained austenite (V_γ) in the heat-treated specimens varied by the Mo content and the heat treatment condition. A linear relation was obtained between wear loss and wear distance in all specimens. The lowest wear rate (Rw) was obtained in both the As-hardened and the H_{Tmax} specimens. The highest Rw was obtained in both the L-H_{Tmax} and the H-H_{Tmax} specimens. Rw decreased with increasing hardness. In Suga abrasion wear test, the lowest Rw obtained in the specimens with around 10% V_γ. The Rw decreased with an increase in Mo content. In Rubber Wheel abrasion wear test, the lowest Rw obtained also in the specimen with 10% V_γ. However, the Rw was independent on Mo content.

Department : Metallurgical Engineering Student's Signature .....
Field of Study : Metallurgical Engineering Advisor's Signature .....
Academic Year : 2011 Co-advisor's Signature .....

ACKNOWLEDGEMENT

First of all, I would like to thank my thesis advisor, Associate Professor Prasonk S., for his decisions to let me join the collaboration group of Professor Y. Matsubara in Kurume National College of Technology (KNCT). I thank Associate Professor Prasonk S. for his decision to have given me the great opportunity to study abroad and valuable suggestions since I just decided to study the master degree.

For this research, I could never have done it without the help, support and guidance of a lot of people. I wish to thank my advisor, Professor Y. Matsubara, for his kindness and guidance, without him this research would not have been possible. I would like to thank Assistant Professor Sudsakorn I. for his guidance and support over the year since my first experiment at Faculty of Engineering, Mahasarakham University. I would also like to thank Professor N. Sasaguri and Professor K. Yamamoto for their advice and support not only about the research but also daily life care while I was working on this research at Department of Materials Science and Engineering, KNCT.

I am grateful to Mr. Phasit A. from Kawara Steel Co., Ltd for his friendship and help when I was investigating abrasion wear test at Isobe Iron Works Co., Ltd. My thank also goes to the technician of KNCT, Mr. K. Nanjo, in providing me all lessons for equipments which I was supposed to use for this research in Japan. I would like to take this opportunity to thank my teacher, Mr. Suvanchai P., for his help and suggestion for using of equipments at our laboratory in Thailand.

CONTENTS

Page

Page

LIST OF TABLES

LIST OF FIGURES

CHAPTER I
INTRODUCTION

1.1 Background

Alloyed white cast irons containing 15-30 mass% Cr (hereafter shown by %) have been employed as abrasion wear resistant materials for more than 50 years. The microstructures of these alloys consist of hard eutectic carbides and strong matrix structure providing the excellent wear resistance and suitable toughness. It is well known that 15% to 20% Cr cast irons have been commonly used for rolling mill rolls in the steel plants, while cast irons with 25% to 28% Cr have been applied to rollers and tables of pulverizing mills in the mining and cement industries. High Cr cast irons with hypoeutectic composition are preferable than those with hypereutectic composition because they are free from precipitation of massive primary carbides that reduce the toughness. [1]

In the hypoeutectic cast iron, as-cast microstructure consists of primary matrix and eutectic M_7C_3 carbide. Austenite which is stable at high temperature under an equilibrium condition will transform to ferrite and carbides or pearlite on the way of cooling. Under non-equilibrium condition, however, the austenite may remain stable or partially transforms to pearlite or martensite depending on the chemical composition and the cooling rate. [1,2] Austenite is favored by high cooling rate, high Cr/C ratio and additions of alloying elements such as Ni, Cu and Mo. [1-3] The supersaturation of Cr and C in austenite decreases the martensite start temperature (Ms), and resultantly, the austenite could be remained even at room temperature.

Austenite has high toughness and it can be work-hardened to increase the surface hardness during service, but is limited to the spalling wear resistance. Improved service performance could be obtained by heat treatment and addition of some alloying elements to provide martensitic matrix with higher wear resistance. In the most cases, a suitable martensitic matrix produced by heat treatment used to provide an increase of abrasion wear resistance. To obtain a martensitic matrix, the cast iron is

held in austenite region at 900-1100 ^{o}C to enable secondary carbide precipitation in austenite (so-called as destabilization of austenite) and followed by fan air cooling to room temperature. The precipitation of secondary carbides in the matrix during heat treatment must be related to the wear resistance and somewhat to the mechanical properties. [4] The retained austenite should be normally limited less than 5 vol% by single or multiple tempering to avoid the spalling during service. [1,3] In practical applications of high Cr cast iron, adequate heat treatment must be given to the cast iron to get optimal combination of the hardness and the toughness which is mainly controlled by quantity of retained austenite. Since quantitative measurement of retained austenite for high Cr cast iron has been performed successfully by X-ray diffraction method [5-8], it is possible to connect the wear resistance and other properties with the amount of retained austenite.

The purpose of alloy addition is to suppress the formation of pearlite in the as-cast condition and to improve the hardenability in the post heat treatment. Since Cr is presented in both the eutectic and secondary carbides, the rest of Cr is retained in the matrix to suppress the pearlite transformation and increase the hardenability. Therefore, the supplementary addition of the third alloying elements such as Mo, Ni, Cu are needed to harden the matrix fully. [1] The effect of additional alloying element to high Cr cast iron has been extensively reported. [2-4,6,9-19] It was reported that the highest hardness after heat treatment of 26% Cr cast iron was obtained by Mo addition. [3] This is because Mo can form its special carbide of Mo_2C or M_2C type with extremely high hardness as eutectic and secondary carbides, and this lead to improve the wear resistance. [11]

The abrasive wear is a type of wear that is brought about by means of hard particles. Moreover, these particles act to concentrate the stress, leading to operate a plastic deformation in the matrix on the surface of the cast iron. The wear rate which is measured by the wear loss depends on several factors, microstructure, kind of abrasive particle, type of relative or mutual movements, chemical reaction and

temperature. [1] Abrasive wear results in a high cost for annual replacement in mining, ore treatment, cement and other industries.

Abrasive wear may be divided into two types; two-body-type and three-body-type. [20] In the two-body-type abrasive wear process, the wear takes place when the hard angular abrasive particles contact the wear surface, e.g., hammer and liner of impact crusher. The local stresses between abrasive particles and wear surface are high enough to crush the particles, leading up to the heavy plastic deformation on the wear surface. As the wear progresses, the tips of particles are fixed on the wear surface, and the matrix is removed first. In this case, therefore, the high surface hardness enough to resist the penetration of particles and the sufficient toughness enough to resist cracking are required. In order to evaluate the two-body-type abrasive wear, an abrasive paper, which is made by high hardness abrasive particles such as SiC or Al_2O_3 fixed on the paper by a glue, are generally used. Suga wear tester is suitable to evaluate the two-body-type abrasive wear resistance.

In the three-body-type abrasive wear, the wear environment consists of two counter materials and abrasive particles. The stress in this case is lower than that in the case of two-body-type abrasion wear. The stress is not high enough to crush the abrasive particles. It occurs in the application where moving particles come freely into wearing surfaces. Typical applications involving this type of wear are for ball and rod mills, pulverizers, like vertical mill and roll crushers. [21] The toughness of materials composed for these surroundings do with to be smaller than that composed for the two-body-type abrasion and is likely obtained by the materials as hard as possible. The suitable wear testing machine for three-body-type abrasion wear is a Rubber Wheel wear tester where SiO_2 particles are used as the abrasives.

Many laboratory tests have been carried out to evaluate the abrasion wear resistance of high Cr cast irons. However, the test data did not often validly to simulate correctly the wear behavior occurred in the industrial applications. Therefore, it is considered that the systematic and detailed studies on the abrasive wear behavior

are necessary. Particularly, the systematic investigation of Mo addition to the heat-treated high Cr cast irons on the wear behavior is much more important.

There are many researches on the wear resistance of high Cr cast irons [4,7,8,11], and recently a study on the heat treatment behavior of hypoeutectic high Cr cast iron with various Mo contents has been reported. [3] The abrasive wear behavior of heat-treated hypoeutectic 16% Cr cast iron with different Mo content was studied by the previous work. [7,8] However, the research on the abrasion wear behavior of heat-treated hypoeutectic 26% Cr cast iron containing molybdenum using two-body-type and three-body-type wear testers has not been investigated.

In this study, hypoeutectic 26% Cr cast irons varying Mo content were prepared and they were heat-treated. Then, two types of abrasion wear tests, Suga abrasion wear test and Rubber Wheel abrasion wear test, are conducted. The relationships between abrasion wear, hardness, volume fraction of retained austenite (V_γ) and molybdenum content are investigated. In addition, the wear behaviors are discussed in connection with the matrix structure in the cast iron.

1.2 Objective of Research

To clarify the effects of Mo content on heat treatment behavior, hardness, volume fraction of retained austenite (V_γ) and matrix structure, and finally the relations between such parameters and wear resistance, two-body-type and three-body-type abrasive wear tests were carried out.

1.3 Scopes of Research

The experiments have been done as follows:

1.3.1 To heat-treat specimens by annealing, hardening and tempering. For the tempering, three levels of temperatures, the temperatures giving the maximum hardness (H_{Tmax}) in the tempering curve and the lower and higher tempering temperatures than that of H_{Tmax} (L-H_{Tmax} and H-H_{Tmax}), were determined referring to the tempered hardness curves reported by S.Inthidech. [3]

1.3.2 To measure the micro-hardness and macro-hardness in the as-cast and heat-treated states.

1.3.3 To measure the volume fraction of retained austenite (V_γ) in the as-cast and heat-treated states.

1.3.4 To investigate the behavior of abrasive wear using Suga abrasion wear test and Rubber Wheel abrasion wear test.

1.3.5 To evaluate the wear resistance associated with the variation of hardness, volume fraction of retained austenite (V_γ) and matrix structure connect to Mo content.

1.3.6 To observe the microstructure by Optical Microscope (OM) and Scanning Electron Microscope (SEM).

1.3.7 To discuss the effects of hardness, volume fraction of retained austenite (V_γ) and Mo content on abrasive wear resistance.

1.3.8 To discuss the wear resistance comparing the test results of heat-treated 26% Cr cast irons with those of 16% Cr cast irons.

1.4 Advantages of Research

1.4.1 This research reveals the characteristics in two-body-type and three-body-type abrasion wear of 26% Cr cast iron with different Mo content.

1.4.2 This research clarifies the relationship between hardness, volume fraction of retained austenite (V_γ) and abrasive wear resistance.

1.4.3 This research clarifies the effect of heat treatment condition and Mo content on abrasive wear resistance.

1.4.4 These data are keenly profitable for practical heat treatment to improve wear resistance of 26% Cr cast iron with Mo

CHAPTER II
LITERATURE SURVEY

High Cr cast irons with hypoeutectic composition are commonly used as abrasion wear resistant materials. The 15-30% Cr cast irons are popular as the cast irons for abrasive wear resistance. The alloys containing 25-28% Cr have been especially developed for materials with abrasion and corrosion resistance. The high Cr cast irons are generally used with austenitic or martensitic matrix. The purpose of Mo addition is to suppress the transformation of pearlite in the as-cast state and to improve the hardenability during subsequent heat treatment.

In the mining industry, the life of parts and components of machines are subjected to the services conditions in which the materials are received. They are mainly abrasion wear and impact stress. It is well known that the abrasive wear is very severe during operation. Therefore, the improvement of wear resistant materials contributes to not only the reduction of cost but also that of downtime and the time of maintenance. The performance of high Cr cast iron depends on the function of microstructure, material properties, abrasion wear resistance, corrosion resistance and etc. Although the high Cr cast irons with hypo- and hypereutectic compositions have been used, the hypoeutectic irons have been used mainly as the components. The research and development of microstructure of cast iron has been done from the viewpoint of alloying and processing. The main challenge was the studies on carbide structure, such as volume fraction, size and morphology of carbides, alloying and solidification. The improvement of the matrix structure has been carried out through subsequent thermal process so-called heat treatment.

2.1 Solidification and Microstructure of High Chromium Cast Iron

High Cr cast irons are based on Fe-C-Cr system. Alloying elements such as Mo, Ni and Mn are usually added to the cast iron. The chemical compositions of several cast irons for abrasion resistance are shown in Table 2.1.

Table 2.1 Chemical composition of abrasion wear resistance cast irons. [10]

Class	Type	Designation	C	Mn	Si	Ni	Cr	Mo	P	S	Cu
I	A	Ni-Cr-HC	2.8-3.6	2.0	0.8	3.3-5.0	1.4-4.0	1.0	0.3	0.15	-
	B	Ni-Cr-LC	2.4-3.0	2.0	0.8	3.3-5.0	1.4-4.0	1.0	0.3	0.15	-
	C	Ni-Cr-GB	2.5-3.7	2.0	0.8	4.0	1.0-1.5	1.0	0.3	0.15	-
	D	Ni-HiCr	2.5-3.6	2.0	2.0	4.5-7.0	7.0-11.0	1.5	0.1	0.15	-
II	A	12% Cr	2.0-3.3	2.0	1.5	2.5	11.0-14.0	3.0	0.1	0.06	1.2
	B	15%Cr-Mo	2.0-3.3	2.0	1.5	2.5	14.0-18.0	3.0	0.1	0.06	1.2
	D	20%Cr-Mo	2.0-3.3	2.0	1.0-2.2	2.5	18.0-23.0	3.0	0.1	0.06	1.2
III	A	25%Cr	2.3-3.3	2.0	1.5	2.5	23.0-30.0	3.0	0.1	0.06	1.2

LC = low carbon, HC = high carbon, GB = graphite bearing

The solidification of high Cr cast irons have been studied by many researchers. [6,9-15,17,22-29] Thorpe and Chicco [22] constructed the liquidus surface phase diagram of Fe-Cr-C system using accurate experimental technique and high purity materials, and it is as shown in Fig. 2.1. The majority of chemical composition of commercial cast iron for abrasion wear resistance is 12-30% Cr and 2.0-3.6% C. In the hypoeutectic cast irons, the microstructure consists of primary austenite (γ_p) and eutectic structure of austenite (γ_E) and carbides. The reaction is described as followed,

$$L \rightarrow \gamma_E + M_7C_3 \qquad \text{or} \qquad \gamma_E + (CrFe)_7C_3$$

Although most of high Cr cast iron finishes solidifying completely within the eutectic region, a quasi-peritectic at low temperature may be occur if liquid remains after the eutectic reaction. This reaction is described as follow,

$$M_7C_3 + L \rightarrow M_3C$$

The M_3C carbides appear at the shell of M_7C_3 carbide as intervening between M_7C_3 carbide and liquid. The high Cr cast irons with hypereutectic composition are generally used as hard facing alloy being added by some strong carbide formers.

In the range of less than 10% Cr, eutectic of γ and M_3C carbide is precipitated as follows,

$$L \rightarrow \gamma + M_3C$$

The crystal lattice of M_7C_3 carbide is hexagonal, whereas the M_3C carbide is orthorhombic. The hardness of M_7C_3 carbide is 1400-1800 HV and it is much harder than that of M_3C carbide with 800-1100 HV. [6] As Cr content increases, the eutectic line moves to high temperature and low C sides, and therefore, the C content in austenite decreases. From Fig. 2.1, the eutectic carbon content in 12% Cr cast iron is about 4.0% while for 30% Cr cast iron is around 2.8%.

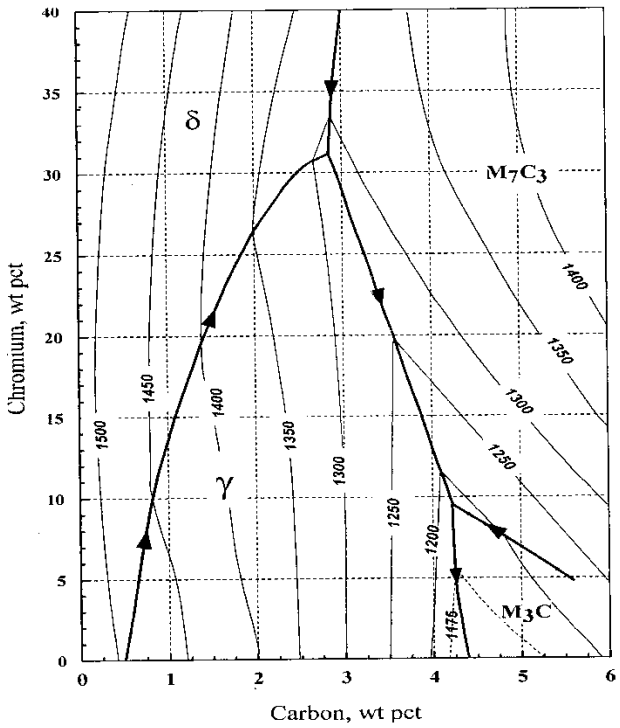

Fig. 2.1 Liquidus surface phase diagram of Fe-Cr-C system. [22]

Generally, the wear resistance and the mechanical properties of high Cr cast iron depend on the type, morphology and that distribution of carbides on matrix structure. [1] In hypoeutectic cast iron, the eutectic is randomly nucleated in the liquid after solidification of primary austenite dendrite, and then grows with a cellular interface to solidify as a colony structure. The eutectic carbides develop in rod-like shape and the rods of carbide join together to form an interconnected colony structure with lamella cross-section. [2]

The rod-like M_7C_3 carbides become finer with increasing the Cr content and the rate of solidification. In addition, the size of eutectic colony is also decreased and the carbide spacing is also reduced with an increase in the Cr content and rate of solidification. G. Powell observed the carbide morphology of high Cr cast iron by SEM and reported that both the rod-like and blade-like of M_7C_3 carbides in the white cast iron with Cr content more than 12% were not completely discontinuous but interconnected. [13] Dogan found that the eutectic colony in eutectic cast iron contains completely rod-like M_7C_3 carbides, whereas the hypoeutectic and hypereutectic high Cr cast irons have both rod-like and blade-like carbides. [14] It was found that slower growth rates (smaller undercooling) favored to solidify in the morphology of blade-like carbides, whereas faster growth rates (larger undercooling) favored that of the rod-like carbides. Volume fraction of carbide can be calculated as a function of the carbon and chromium contents of the alloy. Maratray [16] demonstrated the following equations,

$$\text{Volume fraction of carbide } (V_C) = 12.33x\%C + 0.55x\%Cr - 15.2 \qquad \text{[Eq. 2.1]}$$

From the equation, V_C increases with an increase in C and Cr contents. Laird suggested that it needs caution if this equation is availed because of limited accuracy. [27] Dupin found that there is some the difference in the V_C between the surface and core regions of the casting. [23]

The carbides morphology is closely related to the fracture toughness. The high fracture toughness is obtained in the cast iron with fine eutectic carbide. In order to refine the eutectic carbide, the rapid cooling has been used to increase the

nucleation of carbide and to suppress the growth of carbide. By contrast, slow cooling results in larger dendrite arm spacing and coarser the eutectic carbides. [17]

Alloy addition has been used to modify the carbide structure. Boron additions of 0.1-0.3% decreased the solubility of carbon in austenite and increased the number of carbide nuclei. As a result, it produced a large number of fine carbides in as-cast structure. [30] The effect of V on the eutectic colony size was investigated by Y. Matsubara and et al. [28] It was reported that V reduces the eutectic freezing range and the size of eutectic carbides as well as that of eutectic colony is refined.

As introduced earlier, matrix structure is very important factor affecting the abrasive wear resistance. In hypoeutectic cast iron, the as-cast matrix consists of primary austenite dendrites and eutectic of (γ_E and carbide), as example shown in Fig. 2.2. [6] The austenitic matrix was obtained in the 26% Cr cast iron without and with Mo. Fully austenitic matrix gives adequate resistance to the abrasive wear under the conditions which allow austenite to work-harden during service. However, too much austenite promotes the spalling wear. Therefore, heat treatment is necessary to control the amount of austenite for higher wear resistance.

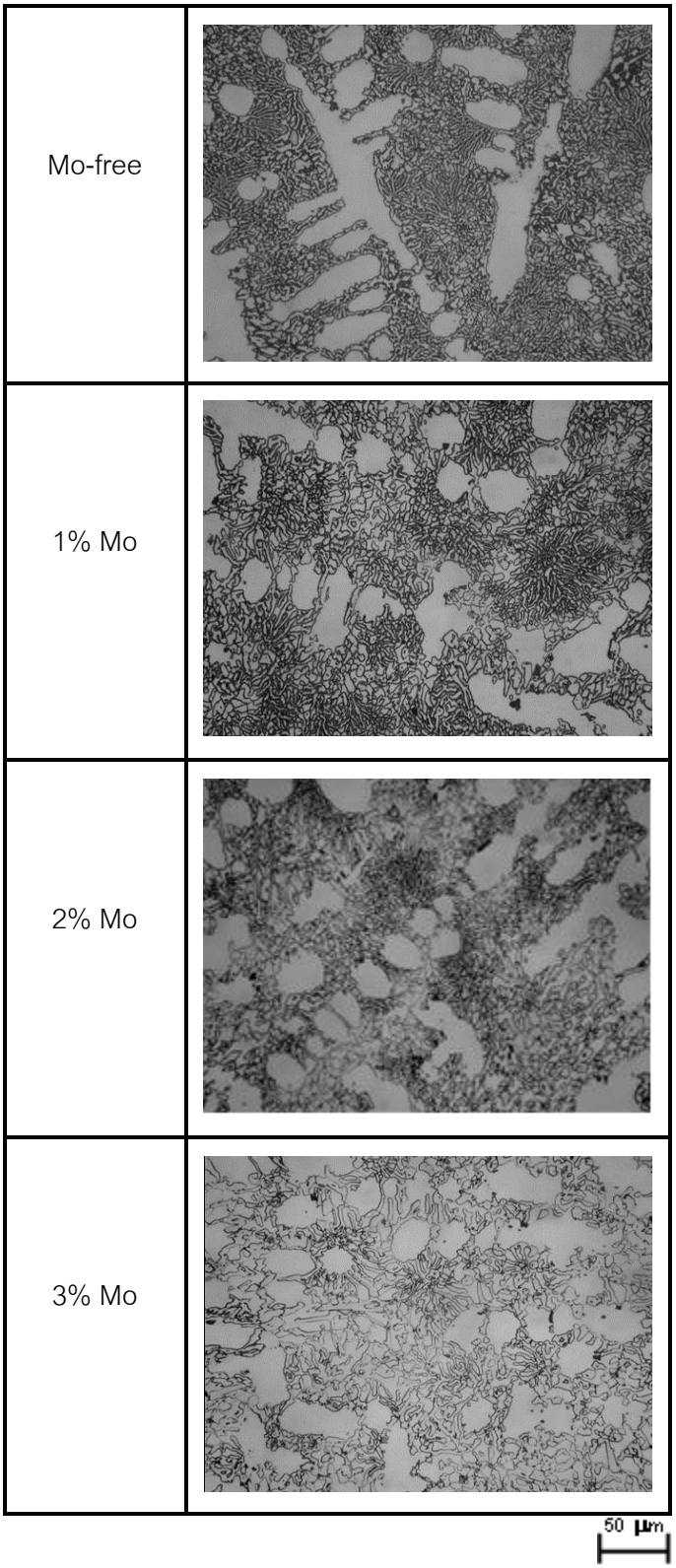

Fig. 2.2 As-cast microstructures of 26% Cr hypoeutectic cast irons without and with Mo. [6]

As shown in Fig. 2.2, the austenite remains stable in the matrix of each iron. This is because the supersaturation of C and Cr stabilized austenite and depress the Ms temperature below room temperature. G. Laird II [17] reported that Cr retards the transformation from austenite to pearlite. Resultantly, a large amount of austenite remains in the matrix and it leads to low hardness. However, fully austenitic matrix in the as-cast state is desirable under a certain wear circumstances that gives a work-hardened wear surface. A fully austenitic matrix is obtained when [32]

1. Ms temperature is below room temperature.
2. Sufficient alloying elements are added to avoid the pearlite and bainite transformation.
3. Cooling rate after austenitization is high enough not to precipitate secondary carbides in the matrix.

In most cases, the martensitic matrix is preferred to provide high wear resistance. For optimum wear resistance, strength and toughness, an iron with high C and fully martensitic matrix is required. A certain amount of martensite is usually present in the as-cast microstructure, predominantly in localized regions adjacent to the eutectic carbides where the depletion of C and Cr from austenite raised the Ms temperature. If the cooling rate of the casting is slow enough, partial transformation of austenite to pearlite or bainite may take place. [4]

Alloying elements such as Ni, Cu, and Mo are added to high Cr cast irons to increase the hardenability and to prevent austenite from pearlite transformation in the case of heavy section castings. Generally, the alloying element affects the properties of cast iron in two ways. First, it is partially distributed to the austenite during solidification and determines the matrix structure in both the as-cast and heat-treated states. This may improves the properties of matrix. Second, the element remaining in the melt is consumed for the formation of eutectic. In this case, the alloying element except for the element distributed into eutectic austenite has no longer any effect on the hardenability. [6] Though, the alloying elements such as Mn, Mo, Ni and Cu are normally added to increase the hardenability, the strong carbide formers such as Mo, V and W

have been used for special applications when much the higher hardness is required. [33] Laird et al [27] measured the Cr content in the matrix of high Cr cast iron in the as-cast state using electron microprobe analysis. Then, the Cr concentration in the matrix of 3.2%C-28.8%Cr cast iron was only 12.5%. Therefore, a reasonable amount of alloying elements must be added to get sufficient hardenability.

Austenite tends to reject or accept a certain alloying element when it solidifies. The growing austenite will reject C, Cr, Mo, V and Nb which are ferrite forming elements but accept Cu, Ni and Mn which are austenite forming ones. However, Mn dissolves into austenite and carbide. If a large amount of strong carbide forming elements like Mo and V are added into cast iron, they are possible to form special carbides of Mo_2C and VC which has much higher hardness than chromium carbide (M_7C_3). [6] There is a report showing that the special carbides are formed when the content of Mo or V exceeds 2%. [23,24] Mo is added to high Cr cast iron between 0.5-3.5%. However, it should be added more than 1% for effectiveness. [23] Mo acts to suppress the pearlite transformation and improves the hardenability. As shown in Fig. 2.3, the austenitic in the matrix increases when the Mo content is increased. In addition, Mo has little effect on the Ms temperature, while other elements decrease it largely. Mo is relatively expensive, therefore, the decrease of Mo addition was considered. The addition of Cu or Ni instead of Mo is now popular to delay the pearlite transformation and improve the hardenability, because they don't form carbide but dissolve into matrix. [17] Inoculation of Ti refines the eutectic structure. [35]

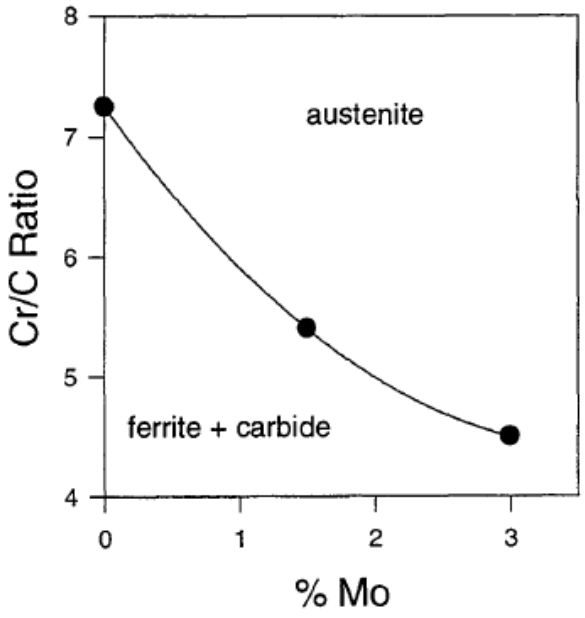

Fig. 2.3 Relationship between Cr/C ratio and Mo content on matrix structure of high chromium cast irons. [16]

The tendency for alloying element to segregate to matrix was observed by Laird. [27] The parameter of segregation ratio (Sr) for each alloying element is introduced using the following equation,

$$S_r = \frac{\%X_{Carbide}}{\%X_{Matrix}}$$

Where %X is the weight percent of each alloy. The results of Sr value using the electron microprobe analysis are summarized in Table 2.2. A high Sr value was obtained in the elements of C and Cr. This suggested that they are strongly segregated to carbides. The Sr values of Cu, Ni and Si are zero. It is indicated that these alloys almost dissolve in the matrix. Dupin [23] investigated the alloy distribution in the austenite dendrite of 17%Cr-2%C cast iron. The results are shown in Fig. 2.4. A slight increase in C and Cr content from the center of dendrite toward the periphery of dendrite can be distinguished. A narrow band near eutectic carbides depleted of C and Cr is due to their diffusion into the eutectic carbides. However, the opposite result is observed by Si.

Table 2.2 Segregation ratios for various alloying element in high chromium cast irons. [27]

Alloy	C	Si	Ni	Cu	Mo	Cr	Mn
15Cr 1Mo 3C	5.4	0.0	0.23	n/a	n/a	4.8	1.3
18Cr 2.2C	6.2	0.0	0.0	0.0	n/a	4.3	1.2
20Cr 2Mo 1Cu 3C	6.1	0.0	0.0	0.0	2.2	4.5	1.0
29Cr 3C	8.8	0.0	0.0	0.0	n/a	4.6	0.8

n/a = not analysed

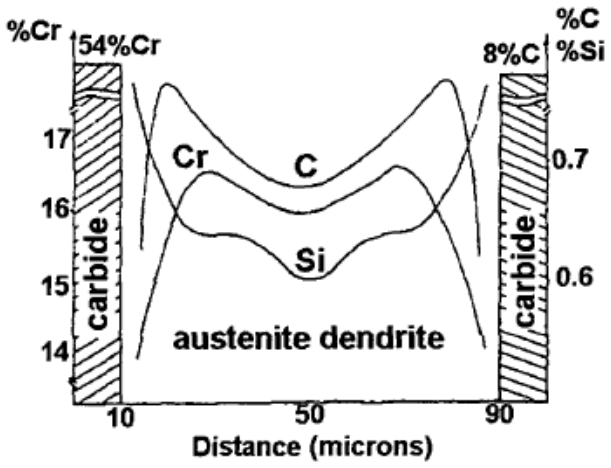

Fig. 2.4 Distribution of alloying elements in austenite dendrite. [23]

2.2 Heat Treatment of High Chromium Cast Iron

It is well known that heat treatments of high Cr cast irons are widely taken to improve the wear resistance of parts and components in the mining and mineral industries. Various solid state transformations occur during heat treatment. The primary purpose of heat treatment is to destabilize the austenite. So that the matrix transforms to martensite on cooling. Other heat treatments like sub-critical heat treatment and cryogenic treatment aim to reduce the amount of retained austenite. The annealing treatment is given to the high Cr cast irons to improve machinability.

2.2.1 Annealing

High Cr cast irons with martensite in the matrix and eutectic carbide are difficult to machine because of their high hardness. [1,5,7,34] This problem can be solved by a full annealing. The high Cr cast iron was annealed at 900-1000 ^{o}C, followed by furnace cooling to below A_1 temperature, and then holding at this temperature for 10-50 hours depending on the chemical composition. [1] The matrix structure after full annealing consists of coarse pearlite or carbides and ferrite. In the 19% Cr cast iron annealed at 900-950 ^{o}C, the coarse secondary carbides were observed and the hardness was lowered by about 150 HV than the as-cast hardness. [1] After machining, the cast iron will be hardened after destabilization treatment and then tempered. Annealing prior to destabilization affects on the morphology and distribution of secondary carbides. Furthermore, the annealing can reduce the destabilization time. [1,34] Higher Mo content in the cast iron gave finer secondary carbides in the annealed matrix, and the hardness increased from about 350 HV in Mo-free 25% Cr cast iron to 460 HV in that with 2.5% Mo.

2.2.2 Hardening

Hardening is performed after the destabilization treatment of austenite so that the austenite can transform into martensite. Since the matrix in as-cast high Cr cast iron is austenitic due to supersaturation of C and Cr, a destabilization is necessary to cause the martensite transformation. In the heat treatment process, firstly, the austenite is destabilized by isothermal treatment at high temperature. A usual destabilization temperature for as-cast high Cr cast iron ranges about 950-1100 ^{o}C for 1-6 hours depending on alloy content. Powell [27] reported that the secondary carbide precipitation occurred while holding at 1000 ^{o}C for 25 minutes. However, at least two hours is need for high Cr cast iron with alloying elements. [1] If the holding time is too long in the case of heavy section casting, the number of secondary carbides is decreased by Ostwald ripening process.

In the case of high Cr cast iron, the destabilization occurs as follows,

$$\gamma \rightarrow \gamma^{*} + \text{Secondary carbides } (M_{23}C_6,\ M_7C_3,\ \text{nil or very less } M_3C)$$

This time, γ^{*} is destabilized to be lower alloy concentration than that in the as-cast state. The types of secondary carbides could be $M_{23}C_6$ and/or M_7C_3 depending on chemical composition and holding temperature. For 25% to 30% Cr cast irons, the $M_{23}C_6$ carbides are mainly formed, whereas M_7C_3 and $M_{23}C_6$ carbides form in 15% to 20% Cr cast irons. [37] It has been reported that the precipitation of secondary carbide produces in two stages, the $M_{23}C_6$ carbide precipitates first and then transform to M_7C_3 when it is held for a long time. [26,27,37] As a result of the secondary carbides precipitation, the C and Cr content in austenite is reduced and the Ms temperature is raised. The high Cr cast irons are usually hardened by fan air cooling after destabilization treatment to room temperature. An important requirement is that the cast iron must show sufficient hardenability to avoid the pearlite transformation during cooling.

Fig. 2.5 shows the typical as-hardened microstructure of 16% Cr cast iron with 3% Mo. In the matrix, the secondary carbides, martensite and small amount of retained austenite can be observed. [7] The M_2C carbides are clearly detected in the SEM micrographs of 3% Mo specimen. [6] Powell [26] reported that the secondary carbides which precipitated in the matrix are mostly $M_{23}C_6$ carbides co-existing with small amount of M_7C_3 carbides.

The destabilization temperature has a major effect on the amount of retained austenite and final hardness. Maratray and Poulalion [38] showed that the main factors controlling the amount of retained austenite are chemical composition, holding temperature and cooling rate. For the high Cr cast iron, the maximum hardness is achieved at the destabilization temperature between 950-1050 ^{o}C as shown in Fig. 2.6. The maximum hardness has been obtained at about 20% V_{γ}. [3,38] S. Inthiech [3] showed that the proportion of retained austenite after destabilization at 1050 ^{o}C was greater than that at 1000 ^{o}C destabilization.

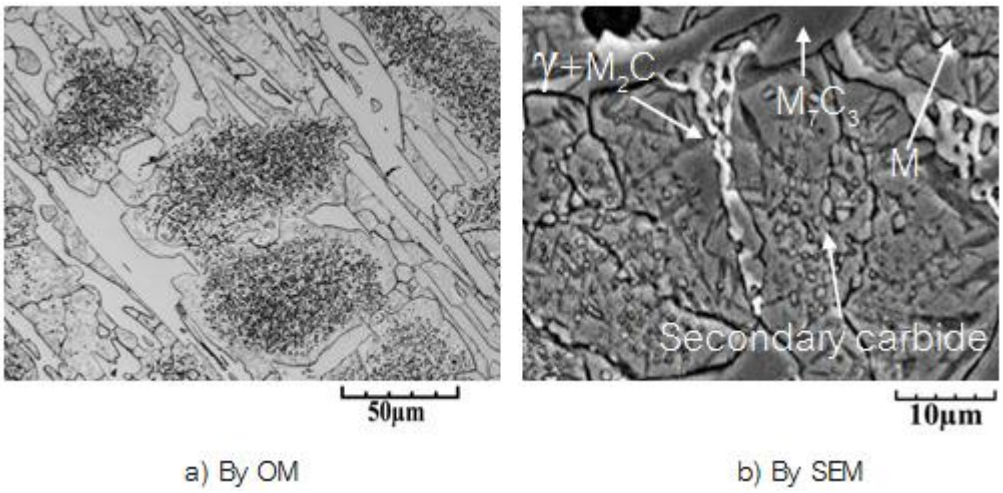

Fig. 2.5 Microphotographs of as-hardened specimens with Mo by OM and SEM. [7]

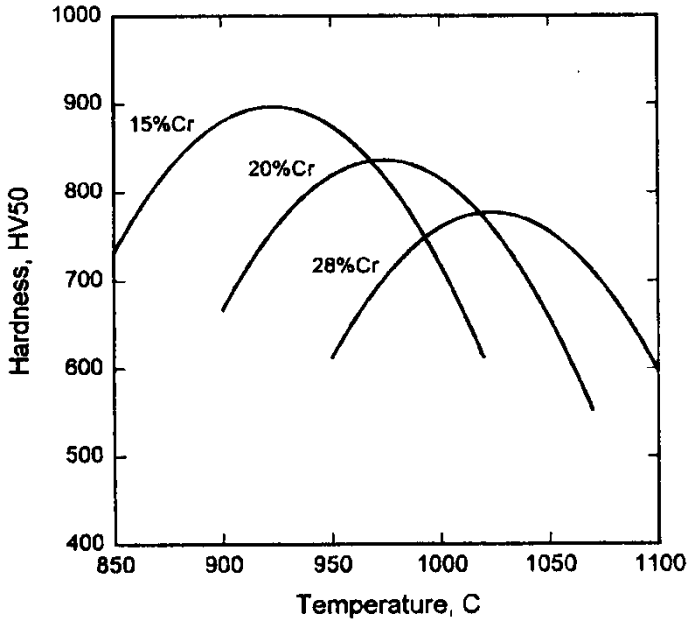

Fig. 2.6 Effect of destabilization temperature on the maximum hardness of high chromium cast irons. [33]

Maratray [16] suggested that an optimal destabilization temperature for maximum hardness in air hardening arises from as follows,

1. At high temperature, the solubility of carbon in austenite is high. The high carbon content depresses the Ms temperature producing the large amount of retained austenite after air cooling.

2. At low temperature, the carbide precipitation reduces the carbon content in austenite. The low carbon martensite forms during cooling and the relative low hardness is obtained.

From Fig. 2.7, the maximum hardness is obtained at about 1025 ^{o}C. The amount of retained austenite (V_{γ}) increases with increasing the austenitizing temperature.

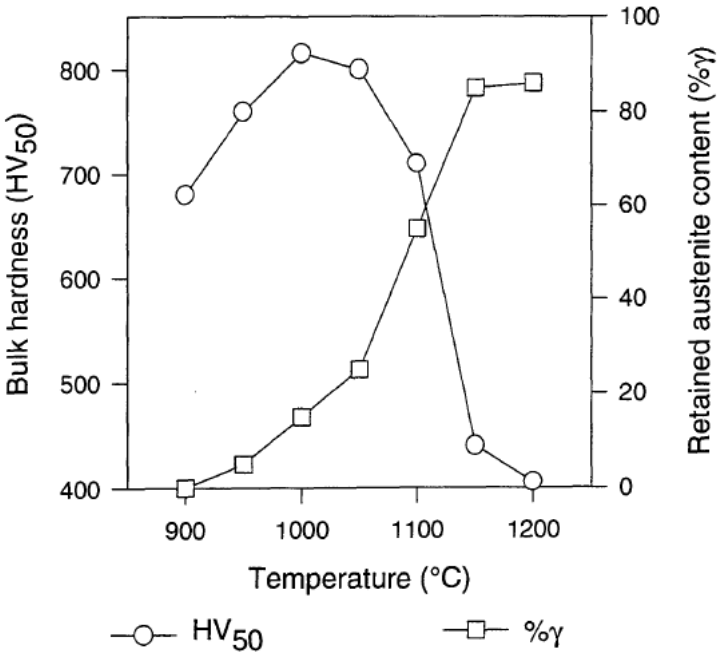

Fig. 2.7 Effect of destabilization temperature on hardness and volume fraction of retained austenite. [16]

The addition of alloying element also affects the amount of retained austenite due to the stabilization of austenite. The carbon content in the matrix has greatest influence on the Ms temperature. Increasing the carbon content can increase the hardenability and the hardness. However, it also increases the amount of retained austenite. There is a report concerning Ms temperature or hardenability by S.Inthidech. [6] The hardenability increases with an increase in Cr/C value and with an addition of Ni, Cu and Mo. The volume fraction of retained austenite in the as-hardened state of 16% Cr cast iron was increased by Ni, Cu and Mo additions but decreased by V addition as shown in Fig. 2.8. Cu and Ni almost dissolve in the austenite and lower the Ms temperature. Mo and V, strong carbide forming elements, prefer to dissolve in the eutectic carbides during solidification. Only the rest of elements consumed in carbide formation dissolves in the austenite and affects the Ms temperature.

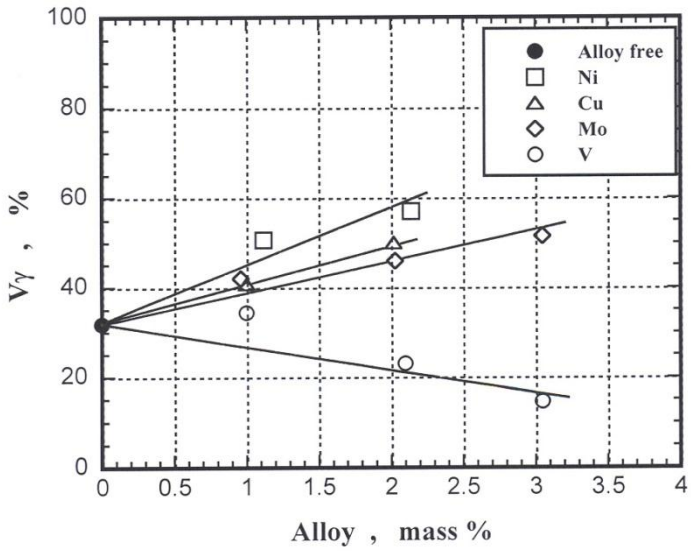

Fig. 2.8 Effects of alloying elements on the volume fraction of retained austenite (V_γ) in the as-hardened state of 16% Cr cast iron. [6]

2.2.3 Tempering

Tempering is the final heat treatment stage to produce the desired properties of materials. Tempering is always recommended after hardening. The main purpose is to decompose martensite and retained austenite to control the hardness, of course, the residual stress caused by hardening should be reduced by tempering. The main reaction is to destabilize the retained austenite to bring about the martensite transformation on cooling. Sudsakorn [6] reported that the secondary hardening in tempering of high Cr cast iron is considered to occur by the following reactions;

I. Decomposition of as-hardened martensite, that is to say, precipitation of secondary carbides from martensite. Finally, this ends with “carbide reaction”.

II. Decomposition of retained austenite in the as-hardened state, in other words, precipitation of carbides from retained austenite.

III. Transformation of retained austenite after precipitation of secondary carbides into martensite during cooling.

Each reaction acts the part of an increase in hardness. However, the increasing degree of hardness could be greater in the reactions (I) and (III), but the effect of reaction (II) is probably small. Martensite formation after tempering is attributed to the precipitation of secondary carbides in the retained austenite during tempering. Because of the reduction of C and Cr contents in the retained austenite, Ms temperature increases and martensite transformation appears on cooling to room temperature.

The tempering temperature and holding time must be carefully chosen to avoid over-tempering that leads to a decrease in hardness and strength of the matrix. Tempering temperature between 200 and 450 ^{o}C is too low to make the retained austenite transform, and temperature in the range of 500 to 600 ^{o}C is appreciated. [1] Maratray [38] reported that in the range of tempering temperature from 480 ^{o}C (753K) to 650 ^{o}C (923 K), $M_{23}C_6$ carbide is more stable than M_7C_3 carbide and so $M_{23}C_6$ carbide could precipitate from retained austenite at the temperature over 480 ^{o}C (753 K). [34] Sare and Arnold [4] said that tempering treatment of 27% Cr cast iron at 500 ^{o}C (773 K) reduced the retained austenite below 10 vol%. In 15% Cr cast irons with C content less than 1.5%, the toughness is increased with increasing the tempering temperature. [1] For over 1.5% C, the toughness is not controlled by varying the tempering temperature but controlled by the amount of eutectic carbides.

The effect of alloying elements on the hardness and V_γ during tempering was reported by S. Inthidech. [3] It was found that the hardness curve showed the secondary hardening. The degree of secondary hardening was greatest in Ni bearing specimen followed by Cu, Mo and V, respectively and the cast iron with Mo showed the highest hardness. Fig. 2.9 shows the tempering behavior of 26% Cr cast irons with and without Mo. The tempered hardness curves show evident secondary hardening due to the precipitation of secondary carbides and the transformation of austenite to martensite. The degree of secondary hardening increases with increasing of Mo

content. The amount of retained austenite decreases when the tempering temperature rises. The maximum hardness is obtained at the tempering temperature 500-525 ^{o}C. The temperature over this temperature, the hardness is decreased due to the coarsening of secondary carbides. It is also found that the cast irons with large amount of retained austenite give a large degree of secondary hardening and the hardness is higher than that in its as-hardened state.

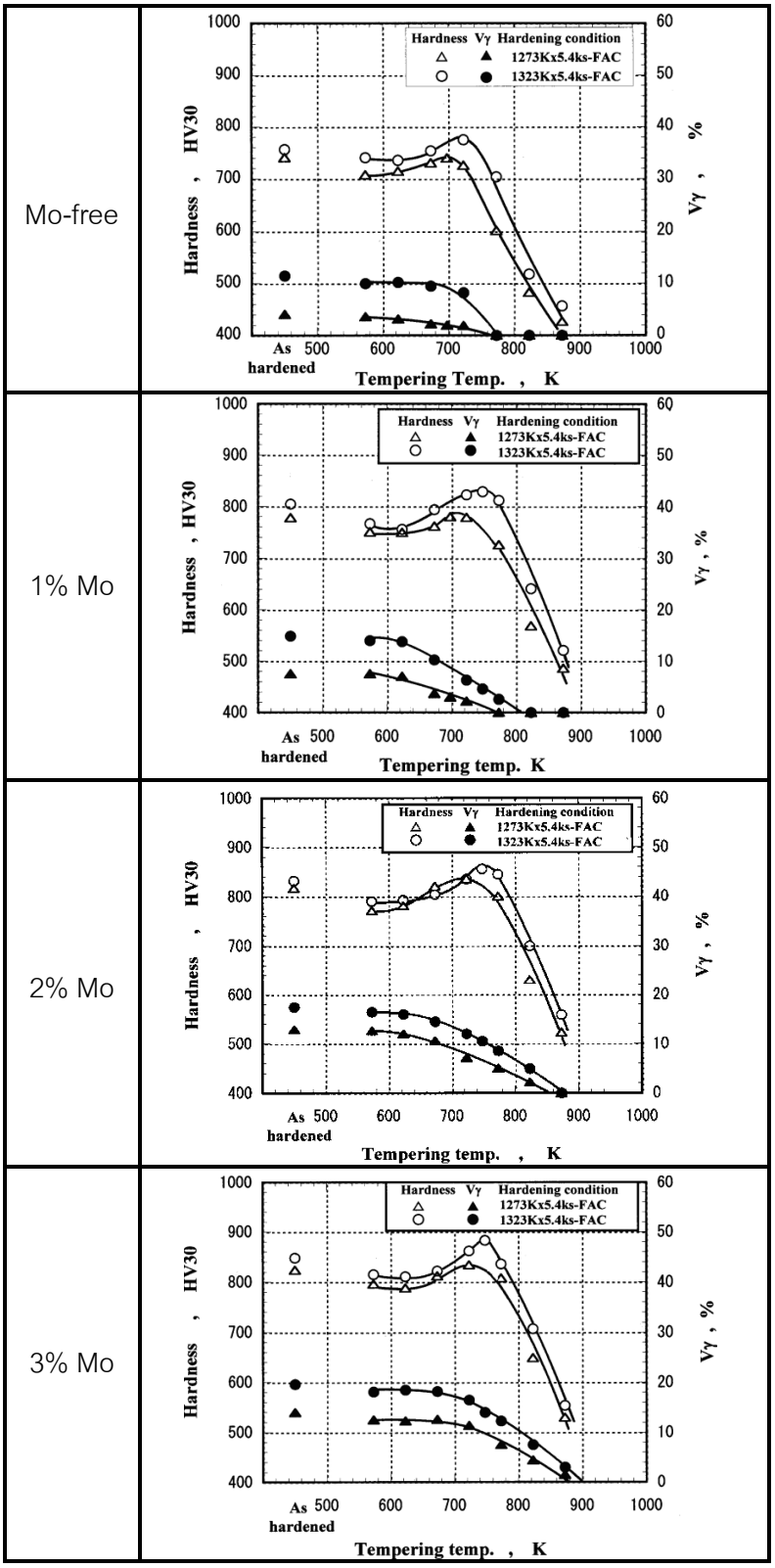

Fig. 2.9 Relationship between hardness, volume fraction of retained austenite (V_γ) and tempering temperature of 26% Cr cast irons with and without Mo. [3]

2.3 Abrasive Wear

2.3.1 Concept and classification of abrasive wear

Wear can be defined as the removal of materials from the surface of body moving in contact with another material or counterpart. The rate of wear depends on several factors such as surface microstructure, type of materials, relative movement, chemical action, service circumstance like moisture and temperature. Abrasive wear occurs due to the action of abrasive particles or fragment on the surface of component. It occurs usually in the various kinds of machines which are used for digging, crushing, milling or pulverizing and rolling in the fields of mining, iron and steel, electric power plant and cement industries. Abrasive wear can be described as two basic types, two-body-type and three-body-types as shown in Fig. 2.10. Two-body-type abrasive wear occurs when two working surfaces are contacted to grind those angular materials. The stress in this wear process is high enough to crush the particles. On the other hands, three-body-type abrasive wear occurs in the portion where freely moving particles exist between the surfaces of components. The stress is not high enough to cause crushing of the abrasive particle. This type of wear takes place in the ball mills and tube mills in the cement, steel and mining industries.

2.3.2 Abrasive wear resistance

There are many mechanisms for abrasive wear. Fig. 2.11 shows the ideal cross section of wear grove. Area A1 is a size of wear groove, while A2 is a size of materials welled plastically to the side of groove. The wear rate (Rw) is calculated using the following relation, [40]

$$Rw = \frac{(A_1 - A_2)}{A_1}$$

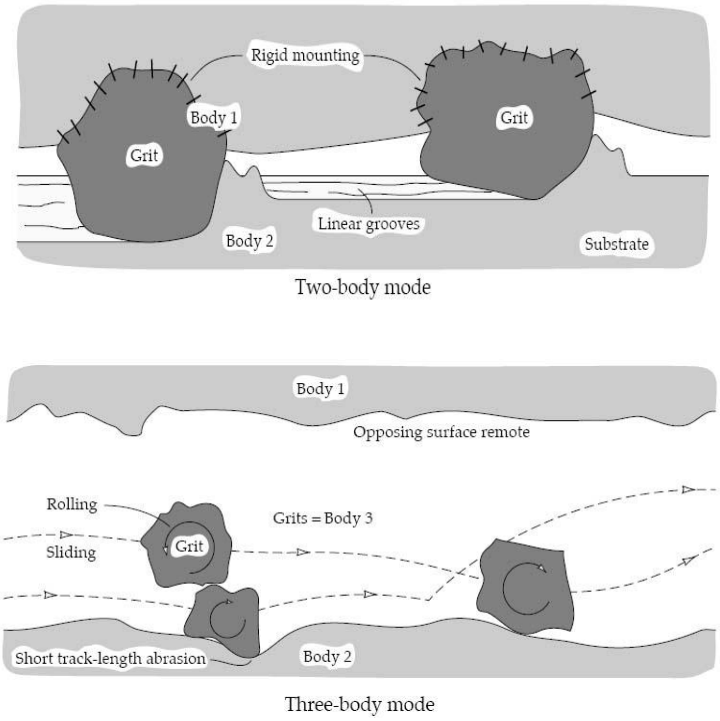

Fig. 2.10 Main type of wear. [39]

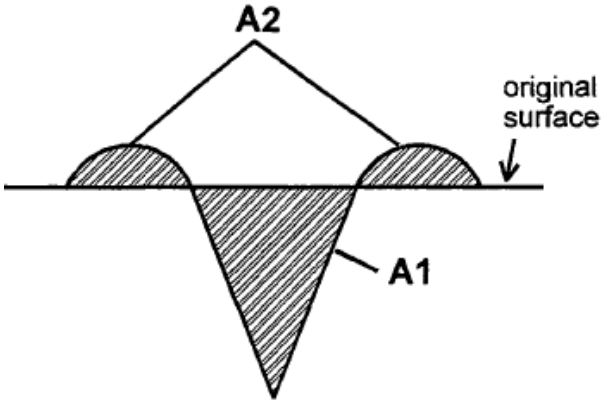

Fig. 2.11 Ideal cross section of wear groove. [40]

The mechanism of wear can be summarized as follows,

1. Ploughing: the material displaces either side of the wear groove as shown in Fig. 2.12 (a). There is no materials remove directly in the wear process. So, the area of A2 equals to area of A1.

2. Cutting: the material is removed as debris of microchip without displacement. Volume of wear loss equals to that of material removal as shown in Fig. 2.12 (b).

3. Fragmentation: cracks form the surrounding and at the surface of wear groove as shown in Fig. 2.12 (c). This crack leads to formation of spall and removal of material. The volume of wear loss may exceed the volume wear groove.

It has been suggested that the parallel movement between abrasive material and worn surface produces the ploughing and cutting, while relative vertical motion leads to fragmentation. The plastic deformation behavior of materials also determines the wear mechanism.

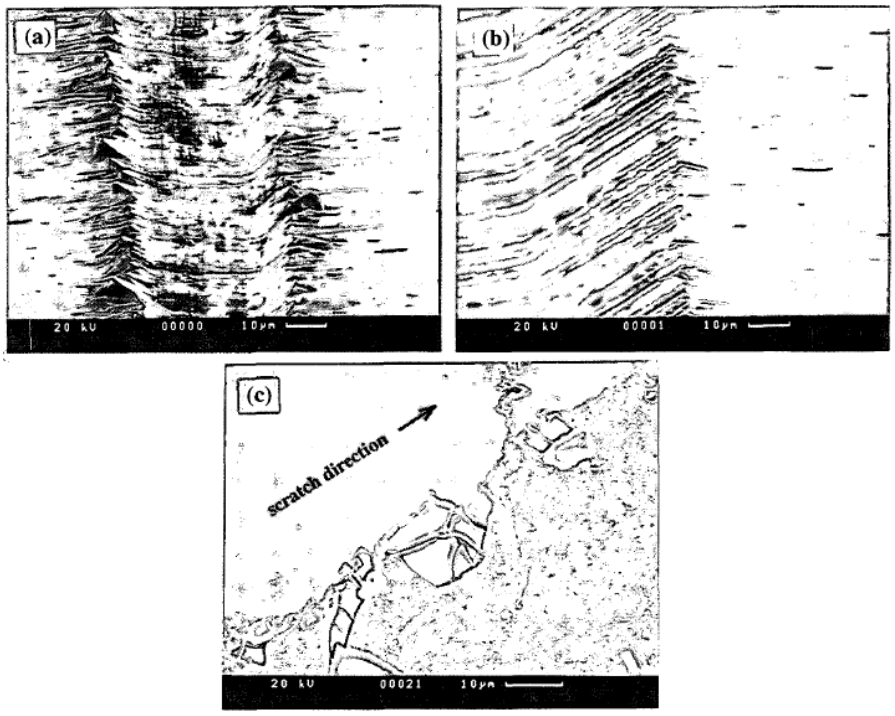

Fig. 2.12 Example of ploughing, cutting and fragmentation in the worn surface using scratch test. [41]

There are several methods to investigate the wear resistance of materials, and they are summarized in Fig. 2.13. For each test, standard condition of load, dimension of specimen, wear distance are used and the mass loss due to abrasion wear is measured. It is well known that there are many factors to determine the wear resistance. The microstructure plays very important role. In high Cr cast iron, the microstructure varies depending on size of casting or solidification rate, alloy addition and heat treatment conditions.

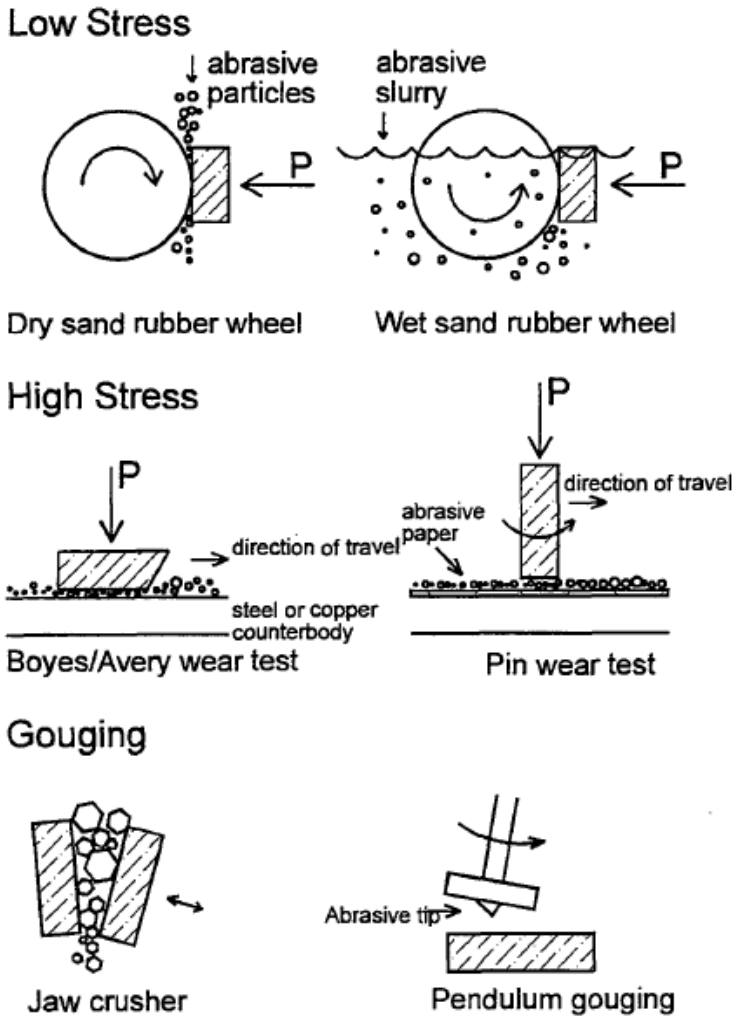

Fig. 2.13 Schematic drawings of abrasive wear tests. [20]

In general, wear resistance is related to the type and morphology of carbides and the matrix structure. [17-19,42] The effects of carbide type and its hardness can be apparently estimated comparing the hardness of carbides with that of the abrasive materials. It is well known that high Cr cast iron contains the eutectic carbides of M_7C_3 type which has a higher hardness than that of the abrasive materials like quartz and garnet. This cast iron shows the excellent wear resistance against these minerals. The addition of Mo, V or Nb to high Cr cast iron can improve the abrasion wear resistance due to the increase in the hardness. It was reported that the rate of wear increased with an increase in the hardness and with a decrease in the size of abrasive particles. [1,40,43] Table 2.3 shows the relative hardness of abrasive materials and carbides in high Cr cast iron. The hardness of M_7C_3 carbide is higher than those of quartz and garnet which commonly encountered in service of mining industry. However, the hardness of M_7C_3 carbide is lower than the hardness of silicon carbide and alumina. From these points of view, it is considered that addition of V which forms very hard vanadium carbide provides the excellent wear resistance.

Table 2.3 Hardness of abrasive materials related to hardness of microstructure of high Cr cast iron. [20]

Abrasive Material	Hardness		Microstructural Constituent
	Knoop	HV	
	2660	2800	Vanadium carbide
Silicon carbide	2585	2500-2600	
Corundum (Al_2O_3)	2020	1800-2000	
	1735	1200-1800	M_7C_3-type carbide
		1060-1240	M_3C-type carbide
Garnet	1360		
Quartz (silica)	840	900-1280	
		770-800	High-carbon martensite
		350-400	Austenite

Under high stress abrasion, the effect of volume fraction of carbide (Vc) on wear resistance depends on the hardness of abrasive materials. If softer abrasive material than carbide hardness is used, the wear resistance increases with increasing Vc. However, when the harder abrasive material is used, an increase in Vc do not show the significant effect on wear resistance. As shown in Fig. 2.14, it is found that the wear loss increases with an increase in Vc when SiC is used. This is because the harder abrasive material could indent into carbides leading to spalling and pitting. The inverse relation is obtained when garnet is used as abrasive material. [40]

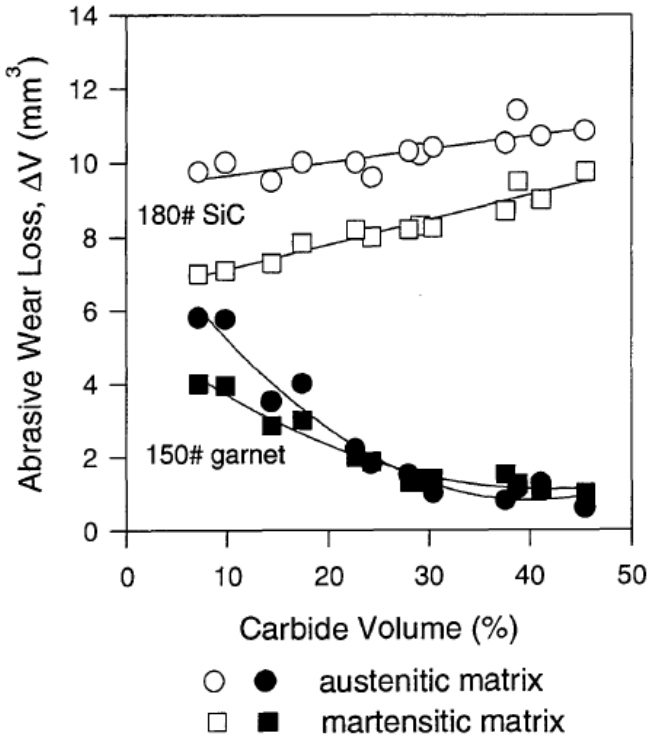

Fig. 2.14 Effect of volume fraction of carbide on abrasive wear loss. [40]

Dogan et al. [14] reported that the carbides aligned appareled to the wear surface give the best wear resistance by a pin on disk abrasion test. He also studied the abrasion wear resistance of as-cast 15% and 26% Cr cast irons. As shown in Fig. 2.15, the wear rate decreased with increasing the volume fraction of carbide when matrix is the same. It can be also concluded that the abrasive wear resistance of as-cast 26% Cr cast iron, which has more austenite in the matrix and high volume fraction of carbide, is better than that of as-cast 15% Cr cast iron with bainitic and pearlitic matrix and with lower volume fraction of carbide. In the same way, wear resistance increases with an increase in the macro-hardness as shown in Fig. 2.16. It has been reported that the increasing of the carbide volume fraction resulted in the decrease of wear rate to the soft abrasives such as hematite and phosphate rock, because of protection of the matrix by carbides in eutectic microstructure. [43]

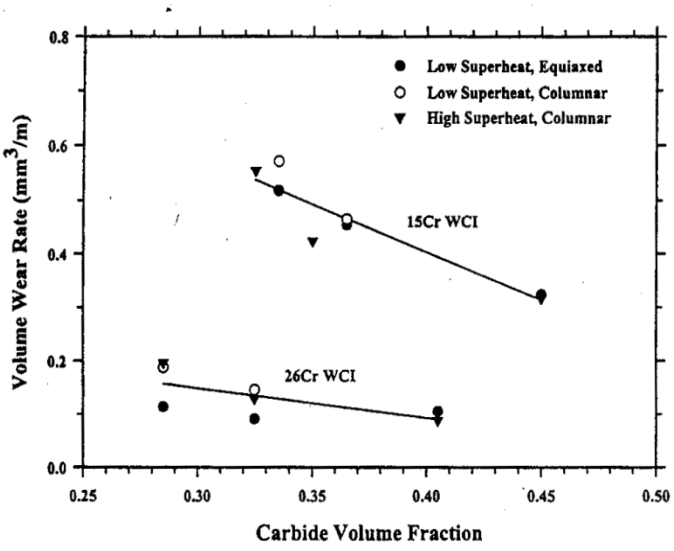

Fig. 2.15 Relationship between wear rate and volume fraction of carbide of high chromium cast irons. [14]

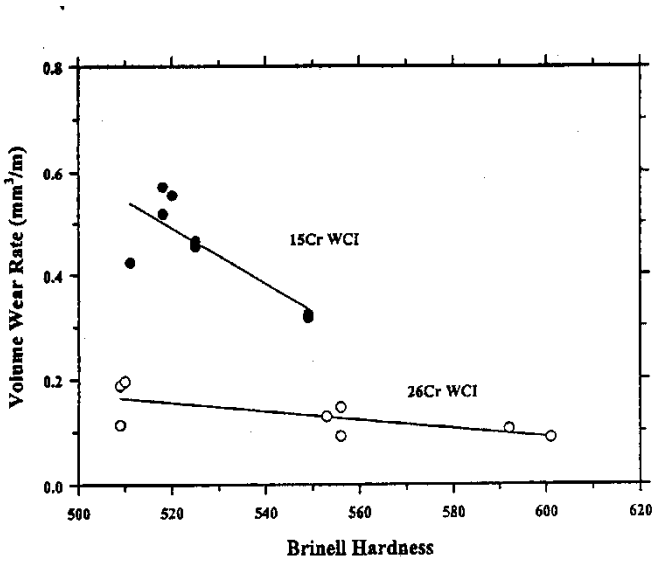

Fig. 2.16 Relationship between wear rate and hardness of high chromium cast irons. [14]

As described previously, the volume fraction of carbide has shown the strong influence on the wear resistance. The 30% volume fraction of carbide provides the best abrasion wear resistance in the heat treated white cast iron. [35] Although wear resistance is generally increased with increasing the volume fraction of carbides, the wear behavior varies depending on the wear system or wear mechanism under the service condition.

It has been said that the higher the matrix hardness, the greater is the wear resistance. The matrix influences on the degree to protect the carbide. If the matrix is not protected and preferentially removed, the carbide may fracture and spall. It was reported that the pearlitic matrix showed the poor wear resistance. [44] The austenitic matrix is preferred under the harder abrasive material, while the martensitic matrix shows the best wear resistance with softer abrasive material. [15] This occurs according to the work hardening effect.

The heat-treated high Cr cast irons with martensitic matrix have a higher wear resistance but sometimes poorer toughness than austenitic and pearlitic matrix. [1,4,9,10,14,18,19,29,31,34-36] By Dogan et al, [15] the pearlitic matrix has extremely

poor wear resistance compared with the matrix mixed with austenite and martensite. An austenitic matrix leads to better abrasion wear resistance compared with the pearlitic matrix because of work-hardening ability of austenite on the worn surface. Sare et al [4] reported that the volume fraction of retained austenite which gives the highest wear resistance lies in 40-50% for gouging abrasion as shown in Fig. 2.17. Sare et al [34] also studied on high stress abrasion pin test and reported that the largest wear resistance is obtained in the as-hardened state containing volume fraction of retained austenite more than 20%. As shown in Fig. 2.18, the results of a pin-on-disk test result by Zum Gahr [40], showed that an increase in retained austenite leads to greater wear rate with garnet as abrasive. When SiC is used, by contrast, the wear loss decreases with increasing of retained austenite. It could be due to the stain-induced-martensite and high toughness of austenite.

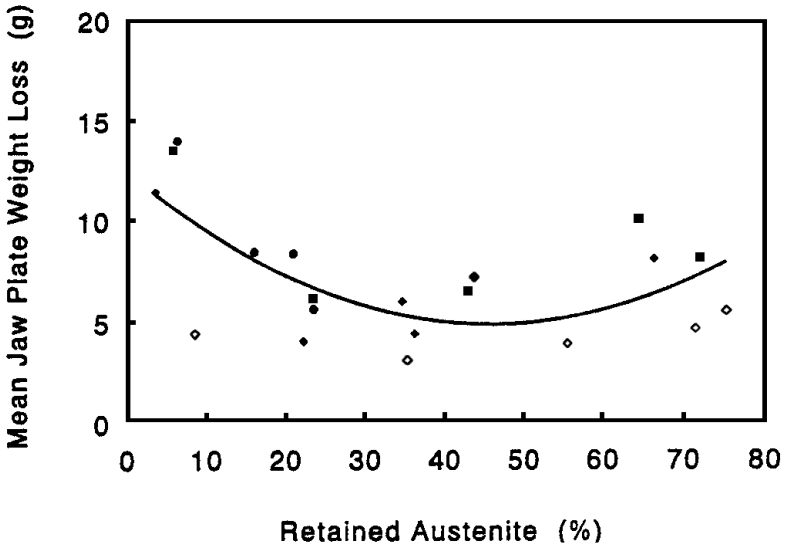

Fig. 2.17 Relationship between mean weight loss (g) and volume fraction of retained austenite by jaw plate test. [4]

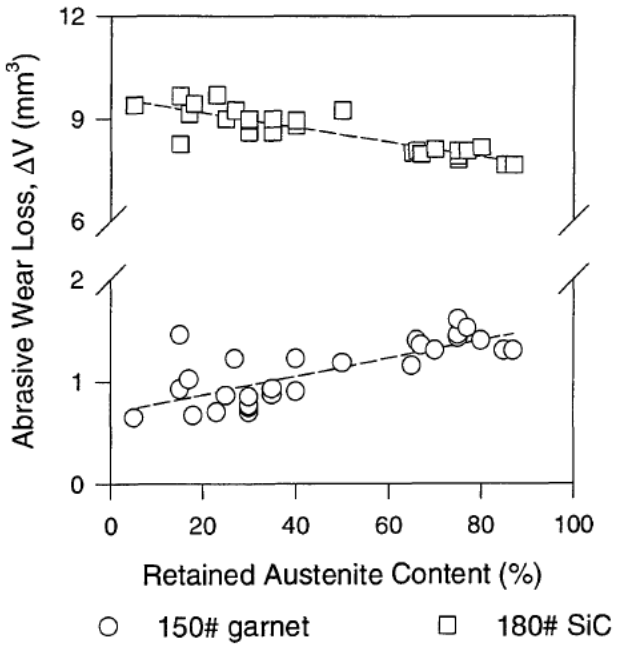

Fig. 2.18 Effect of retained austenite content on abrasive wear loss of 2.9% C-19% Cr-2.35% Mo cast iron. [40]

It was found that the wear resistance was related to carbon content. As shown in Fig. 2.19, the wear loss decreased as the C content increased to 3% at about eutectic composition of 30% Cr cast iron, and then became steady. It has been suggested that as C content increases, the volume fraction of carbides increased high enough to protect the matrix. In fact, the toughness will decrease when the C content increases over eutectic composition, but the wear resistance is balanced due to the precipitation of brittle hyper-eutectic carbides.

Phasit et al [8] used Suga abrasion wear tester and Rubber Wheel abrasion wear tester to investigate the two-body-type and three-body-type abrasion wear behaviors in hypoeutectic 16% Cr cast iron containing molybdenum. It was found that the wear rate was decreased with an increase in Mo content because Mo improves the hardenability in the heat treatment and promotes the precipitation of Mo carbides with high hardness. Sudsakorn et al [7] studied the abrasive wear of hypoeutectic 16% Cr cast iron containing Mo. The data are not so scattered as Sare's results [4] as shown in Fig. 2.20, and the smallest wear rate was obtained at 20 to 25% V_γ. Fig. 2.21 shows

the effect of hardness and Mo content on the wear rate. It is clear from this results that the wear rate decreased proportionally as the macro-hardness is increased regardless of Mo contents of cast irons. When the wear rate is connected to the Mo content, as shown in Fig. 2.22, however the wear rate trends to decrease totally with increasing the Mo content. It can be suggested that an increase in Mo content up to 3% improves the wear resistance of hypoeutectic 16% Cr cast iron. Using a ball mill test, the effects of carbide volume fraction and matrix structure on the abrasive wear resistance of high Cr cast iron balls tested were investigated by Albertin and Sinatora.[43] As shown in Fig. 2.23, it was found that the martensitic matrix showed the highest wear resistance against three kinds of abrasives of phosphate rock, hematite and quartz. When the ratio of hardness of the abrasive and matrix (H_a/H_m) is taken into consideration, it was found that the wear resistance decreased as the H_a/H_m increased as shown in Fig. 2.24. [43]

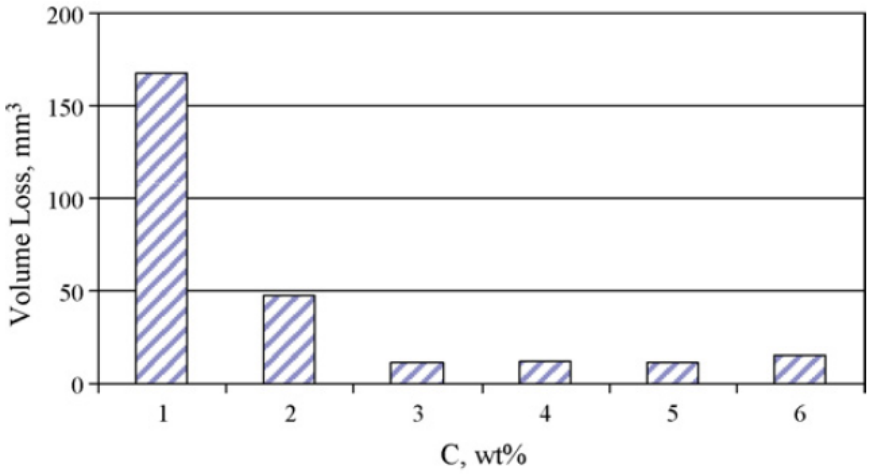

Fig. 2.19 Relationship between wear loss and C content of 30% Cr cast iron. [29]

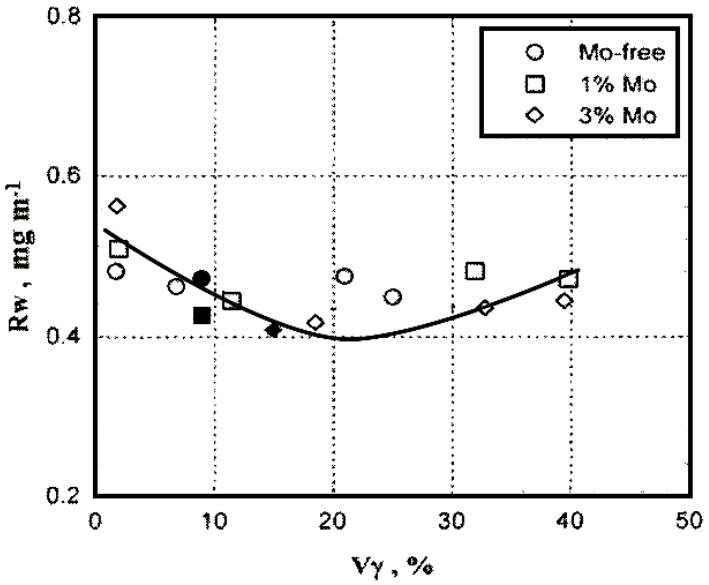

Fig. 2.20 Relation between wear rate (Rw) and volume fraction of retained austenite (V_γ) of hypoeutectic 16% Cr cast iron. [7]

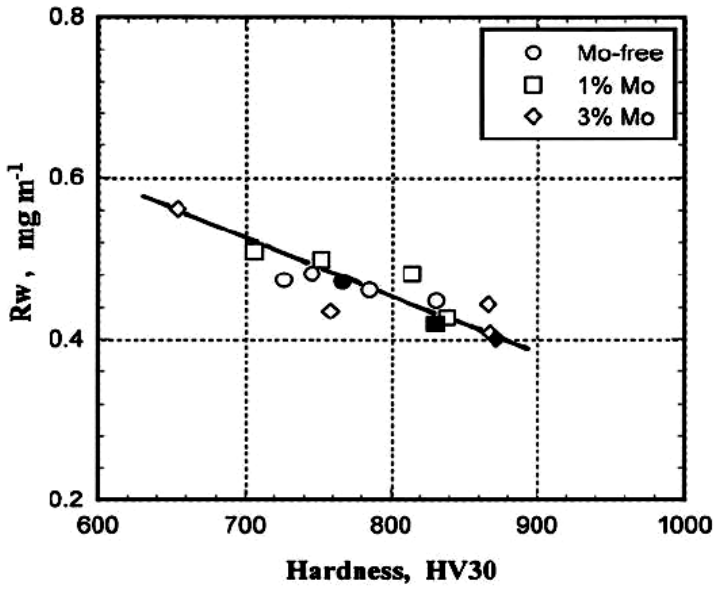

Fig. 2.21 Effect of Mo content on relationship between the wear rate (Rw) and macro-hardness of hypoeutectic 16% Cr cast iron. [7]

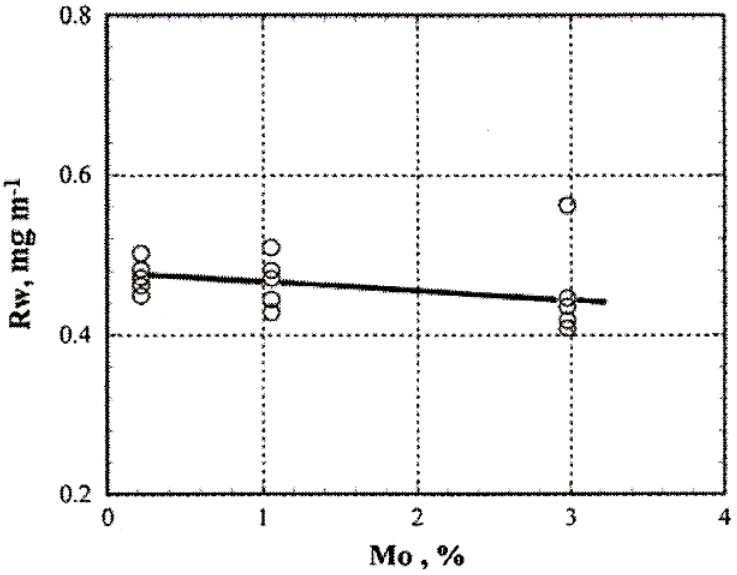

Fig. 2.22 Effect of Mo content on the wear rate (Rw) of hypoeutectic 16% Cr cast iron. [7]

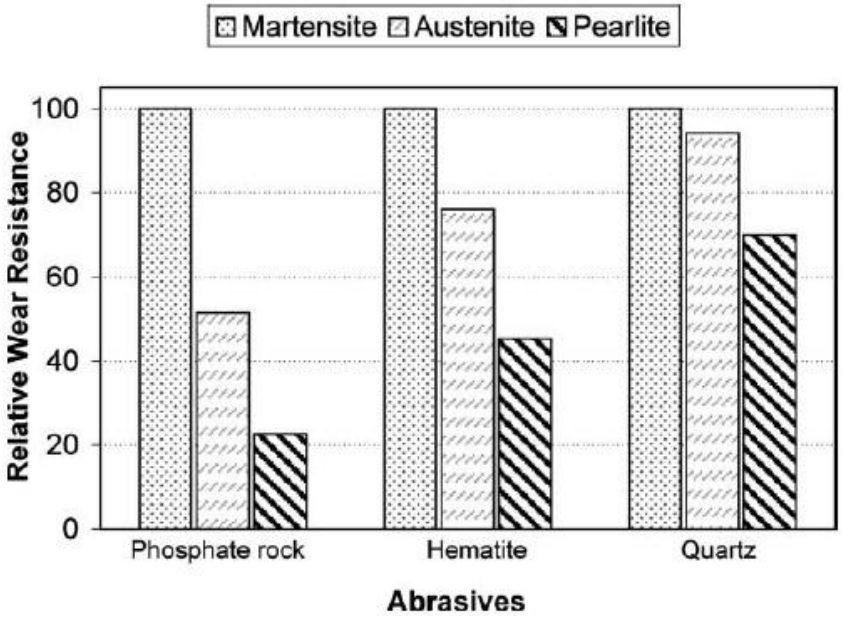

Fig. 2.23 Effect of matrix structure on relative wear resistance of high Cr cast irons. Ball mill test. [43]

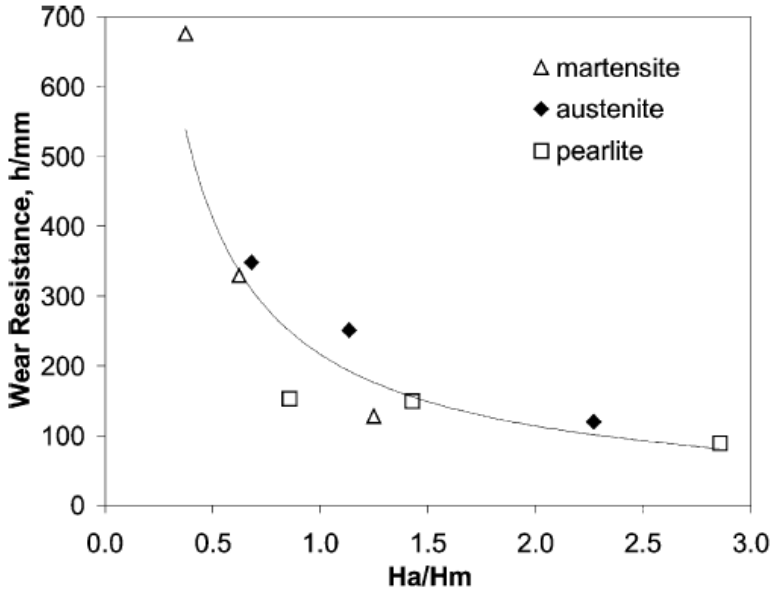

Fig. 2.24 Effect of ratio of abrasive hardness and matrix hardness (Ha/Hm) on the wear resistance. [36]

CHAPTER III
EXPERIMENTAL PROCEDURES

3.1 Preparation of Test Specimens

The charge calculations are carried out for the target chemical compositions as shown by Aim row in Table 3.1. Hypoeutectic 26% Cr cast irons with and without molybdenum are produced using a 30 kg capacity high frequency induction furnace with alumina lining. Raw materials such as mild steel, pig iron, ferro-alloys and pure metals are used as charge materials. The charge materials are melted down and superheated up to 1853 K. After holding at the temperature, each melt is poured from 1793 to 1773 K into preheated CO_2 Y-block mold with a cavity size of 50x50x200 mm, and the surface of the top riser is immediately covered with dry exothermic powder to prevent the riser from fast cooling.(Fig. 3.1(a)). The analyzed chemical compositions of each specimen are also shown by chemistry row in Table 3.1.

Table 3.1 Chemical composition of specimens.

Specimens		Alloy (mass%)				
		C	Cr	Si	Mn	Mo
Mo-free	Aim	2.65	26.00	0.50	0.55	0.00
	Chemistry	2.66	26.08	0.47	0.55	0.18
1% Mo	Aim	2.65	26.00	0.50	0.55	1.00
	Chemistry	2.64	26.12	0.50	0.56	1.02
2% Mo	Aim	2.65	26.00	0.50	0.55	2.00
	Chemistry	2.63	25.92	0.44	0.45	1.97
3% Mo	Aim	2.65	26.00	0.50	0.55	3.00
	Chemistry	2.71	25.98	0.47	0.53	2.96

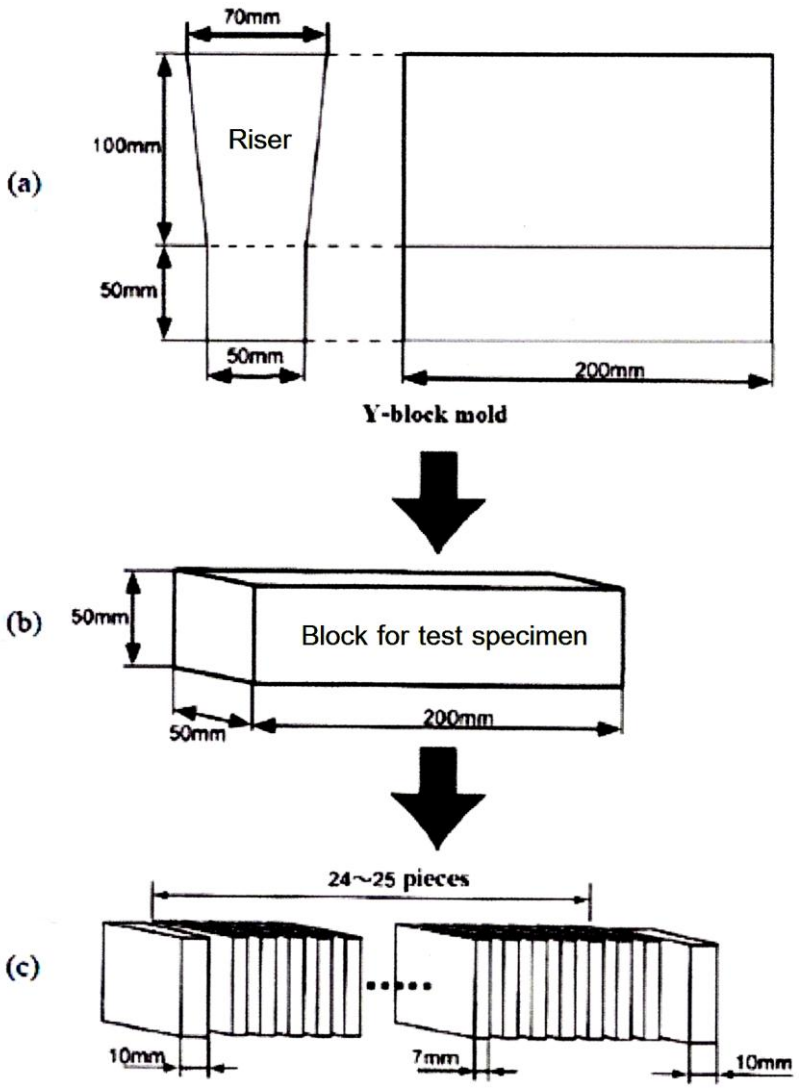

Fig. 3.1 Process of making test pieces. [8]

The riser portion is cut off from Y-block (Fig. 3.1(b)) and the substantial block (b) is supplied for annealing to remove the casting stress and micro-segregation produced during solidification. The substantial block is coated with an anti-oxidation solution to prevent the block from oxidation and decarburization during heat treatment. The block is annealed at 1173 K for 18 ks and then cooled in the furnace to the room temperature. The block is sectioned at 7 mm in thickness by wire-cutting machine to obtain test pieces. (Fig. 3.1(c)).

3.2 Heat Treatment Conditions of Test Pieces

The conditions of heat treatment are listed in Table 3.2.

3.2.1 Hardening

The annealed test pieces were also coated by the anti-oxidation solution, and then they were austenitized at 1323 K for 5.4 ks and hardened by fan air cooling.

3.2.2 Tempering

The hardened test pieces are tempered in a furnace at 3 levels of temperatures between 673 and 823 K, a temperature just at H_{Tmax}, a temperature lower than that at H_{Tmax} (L-H_{Tmax}) and an higher temperature than that at H_{Tmax} (H-H_{Tmax}) for 7.2 ks. The specimens were cooled to room temperature by fan air cooling. The three tempering temperatures were determined according to the tempering curves shown in the reference. (Fig. 3.2) [3] The selected temperatures are summarized in Table 3.3. The test piece tempered at L-H_{Tmax} was selected to have higher retained austenite and lower hardness than that at H_{Tmax} and the test piece at H-H_{Tmax} has much lower retained austenite and hardness.

Table 3.2 Heat treatment conditions.

Heat treatment	Annealing	Hardening	Tempering
Temperature (K)	1173	1323	3 levels between 673 and 823
Holding time (ks)	18.0	5.4	7.2
Cooling condition	Furnace cooling	Fan air cooling	Fan air cooling

Table 3.3 Heat treatment temperature.

Specimens	Tempering temperature (K)		
	$L\text{-}H_{Tmax}$	H_{Tmax}	$H\text{-}H_{Tmax}$
26%Cr Mo-free	673	723	773
26%Cr-1%Mo	673	748	800
26%Cr-2%Mo	673	748	800
26%Cr-3%Mo	673	748	823

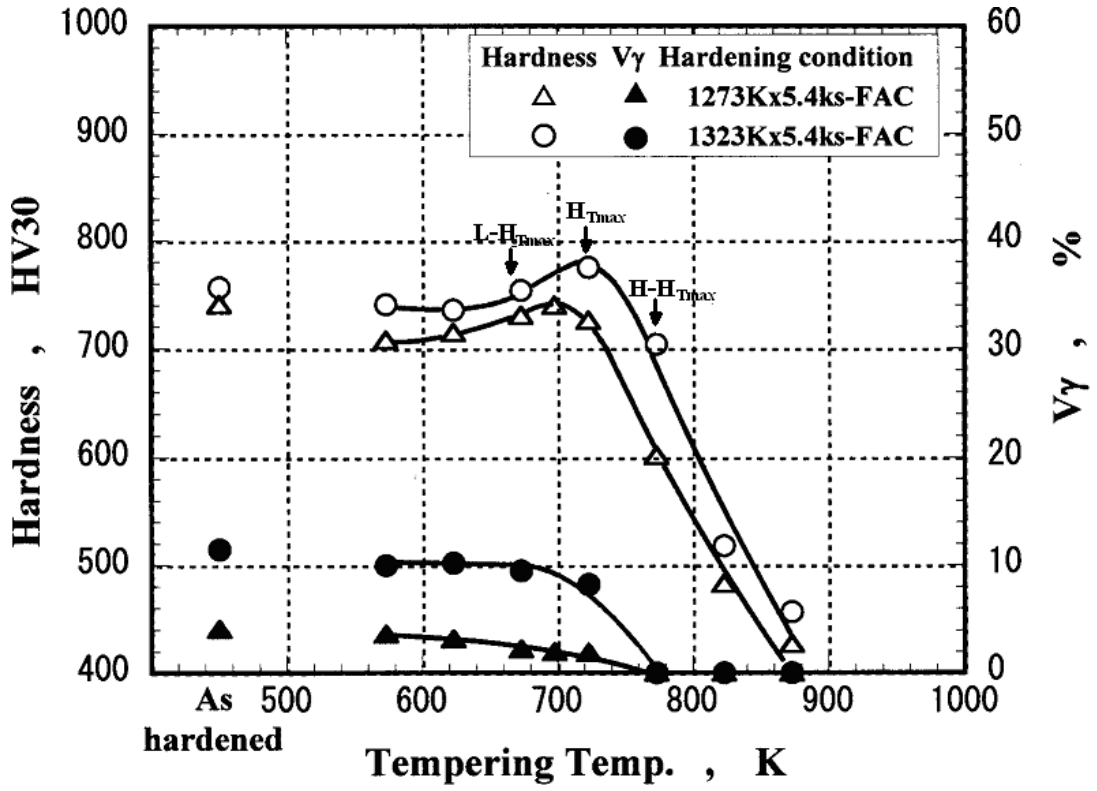

Fig. 3.2 Schematic graph to select tempering temperatures.

3.3 Microstructure Observation of Test Specimens

3.3.1 Optical microscope (OM)

To observe the microstructure of specimens by an Optical Microscope (OM), test piece is polished using emery papers in the order of #180, 320, 400, 600 and 800, and then finished with fine alumina powder of 0.3 μm in diameter. The microstructure is revealed using etchant A shown in Table 3.4.

3.3.2 Scanning electron microscopy (SEM)

For detailed observation, the microphotographs are taken using a Scanning Electron Microscope (SEM). A polished specimen is etched lightly using etchant A to reveal the microstructure. The SEM microphotographs were taken with high magnifications mainly focusing on the carbide morphology and worn surfaces of wear tested test pieces.

3.4 Measurement of Hardness

The polished specimen is lightly etched using etchant A to reveal dendrite and eutectic structure. The measurement of macro-hardness is carried out by a Vickers hardness tester with a load of 30 kgf, and micro-hardness of matrix is measured by Micro-Vickers hardness tester with a load of 100 g. More than five indentations are taken at random and the measured values are averaged.

Table 3.4 Use of etchant.

Type	Etchant	Etching method	Attack
A	Picric acid 1 g, HCl 5 cc, Ethanol 100 cc	Immersion at room temperature	Carbide and matrix

3.5 Measurement of Volume Fraction of Retained Austenite

The volume fraction of retained austenite (V_γ) is obtained by X-ray diffraction method using a special goniometer with automatic rotating and swinging sample stage. Mo-Kα characteristic line with a wavelength of 0.007 nm (0.711 A°) filtered by Zr is used as a source of X-ray beam. The diffraction peaks used for V_γ calculation are (200) and (220) planes for ferrite (α) or martensite (M) and (220) and (311) planes for austenite (γ).

3.5.1 Equipment and measuring condition

The measurement of V_γ by X-ray diffraction method was developed for block of steel and high Cr white iron. [5-8] The measuring condition is displayed in Table 3.5. In this experiment, the simultaneously rotating and swinging sample stage is employed to cancel the influence of preferred orientation or textural configuration of austenite existed in the cast specimen.

Table 3.5 Conditions of X-ray diffraction method to measure the volume fraction of retained austenite (V_γ).

Target metal	Mo
Tube voltage · current	50 kV · 30 mA
Slits	Divergence slit: 1°, Receiving slit: 1.5 mm, Scattering slit: 1°
Filter	Zr
Scanning range(2θ)	24-44 deg
Scanning speed	0.5 deg/min
Step/Sampling	0.01 deg

3.5.2 Calculation of volume fraction of austenite

In this investigation, the diffraction peaks from crystal planes used for the calculation are (200), (220) of ferrite or martensite and (220), (331) of austenite because these four peaks are independent or not interfering from peaks of other phases like carbides. The reason why the α_{211} peak in these patterns is not taken into account is that this peak is overlapped with a strong peak of chromium carbide (M_7C_3). The integrated areas of adopted peaks are obtained using an image analyzer. The calculation of V_γ is done by the three combination of peaks, $\alpha_{200} - \gamma_{311}$, $\alpha_{200} - \Sigma\gamma(220,311)$ and $\Sigma\alpha(200,220) - \gamma_{311}$. The averages of values calculated from three combinations are adopted.

3.6 Abrasion Wear Test

The surface roughness of test pieces is controlled to be less than 3 μm R-max using a grinding machine. The surface roughness is measured three times at random by surface roughness tester to direction perpendicular to grinding direction.

3.6.1 Suga abrasion wear test

A schematic drawing of Suga abrasion wear tester for two-body-type is illustrated in Fig. 3.3. Load of 1 kgf is applied from abrading wheel (44 mm in diameter and 12 mm in thickness) contacted to the test piece. The wheel adhered by a 180 mesh SiC abrasive paper on the circumference moves back and forth for 30 mm distance on the same area of the test piece. Simultaneously, the wheel is rotated intermittently for 0.9 degrees per one stroke, that is, the speed of rotation wheel is 0.230 mm/s. Therefore, the total distance by one revolution or 360 degrees is 30x2x400 mm (24 m). After one test, the specimen is cleaned in an ultrasonic acetone and then dried. The weight of the test piece is measured using a high precision digital balance with 0.1 mg accuracy. The test is repeated for eight times or until total at wear distance 192 m on one test piece.

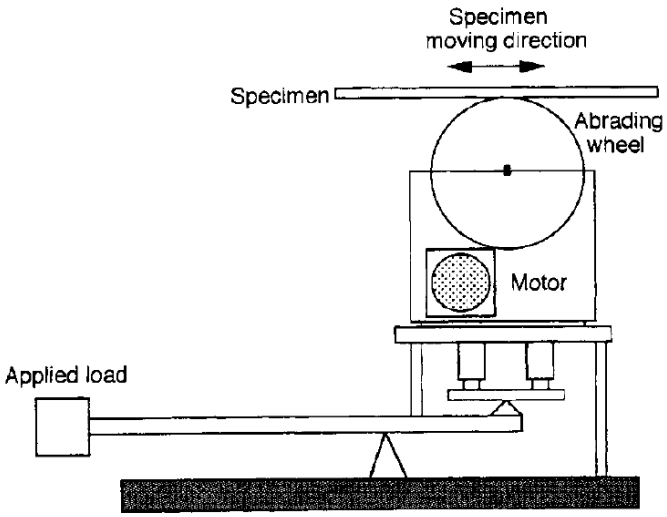

Fig. 3.3 Schematic drawing of Suga abrasion wear tester. [8]

3.6.2 Rubber Wheel abrasion wear test

The schematic drawing of Rubber Wheel abrasion wear tester is shown in Fig. 3.4. The silica sand of AFS 60 grade is used as the abrasives. The sands are fed to the contacting face between the rotating rubber wheel with 250 mm in diameter and test piece. The test is conducted at a rotating speed of 120 rpm. The rate to feed the abrasives is approximate 250-300 g/min. The load applied is 8.7 kgf. After the rubber wheel rotates for 1,000 revolutions or at wear distance 785.5 m, the specimen is got off and cleaned in an ultrasonic acetone and then dried. The weight of the test piece is measured using a high precision digital balance with 0.1 mg accuracy. The test is repeated four times or up to the wear distance 3142 m per one test piece.

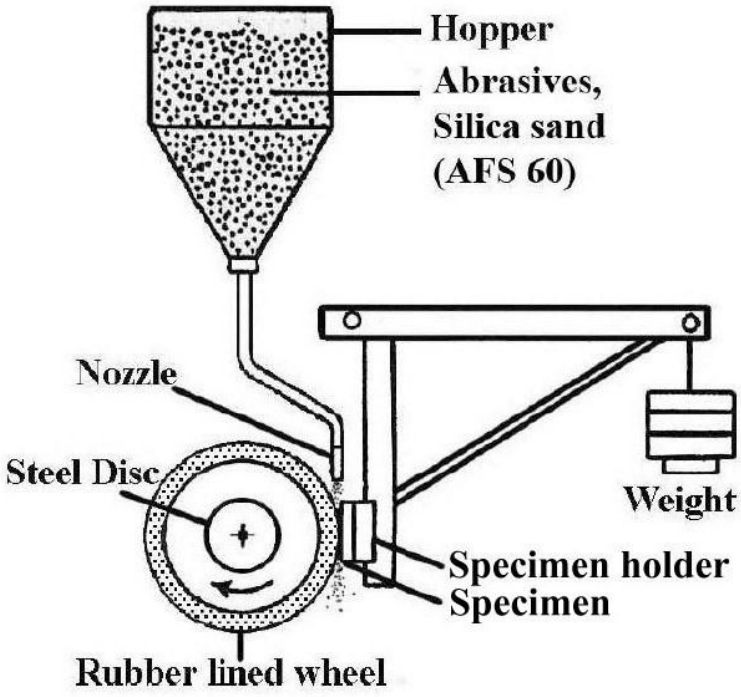

Fig. 3.4 Schematic drawing of Rubber Wheel abrasion wear tester. [8]

3.6.3 Abrasive materials

In this study, the silicon carbide (SiC) with a hardness of 2500-2600 HV is availed as the abrasives for Suga abrasion wear test, while the silica sands (900-1280 HV) of AFS 60 grade is used for Rubber wheel abrasion wear test. The SEM microphotographs with high magnification of both abrasive materials are shown in Fig. 3.5 (a) and (b). The SiC abrasives are fixed strongly to the paper by glue uniformly. Therefore, the abrasive particles cannot move during the test, and the tips of particles always scratch the surface of test piece. In the case of the silica sands, they can move and rotate freely on the surface of test piece. Comparing with the SiC abrasives for Suga abrasion wear test, silica sands are much bigger, sharper and more angular. The details of abrasive materials are summarized in Table 3.6.

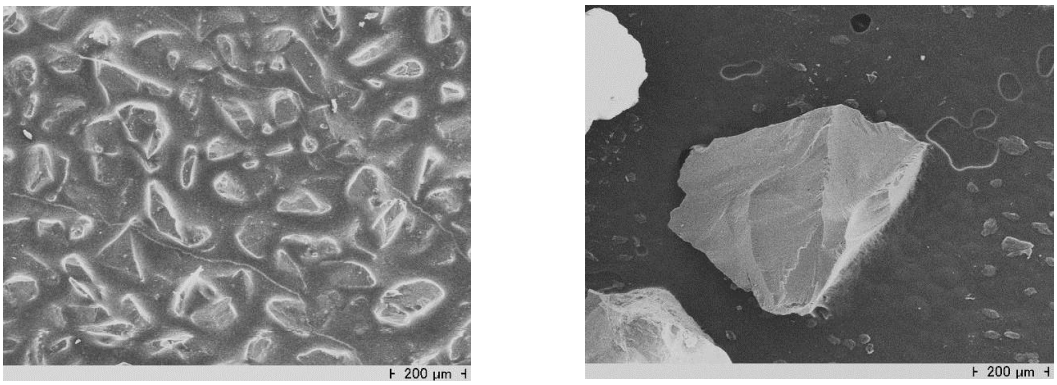

Fig. 3.5 SEM microphotographs of abrasives for Suga and Rubber wheel abrasion wear tests. (a) 180 mesh SiC abrasive paper for Suga abrasion wear test, (b) silica sands of AFS 60 grade for Rubber wheel abrasion wear test.

Table 3.6 Comparison of size and hardness of the abrasive particles used Suga and Rubber Wheel abrasion wear tests. [8]

Abrasives	Size (µm)	Hardness (HV)
SiC (60 mesh)	91.83	2500-2600
SiO_2 (AFS60)	363.83	900-1280

CHAPTER IV
EXPERIMENTAL RESULTS

4.1 Microstructure of Test Specimens

4.1.1 Microscopy in as-cast state

Typical as-cast microstructures of 26% Cr cast irons with and without Mo are respectively presented in Fig. 4.1 using OM and SEM. All the microstructures indicate primary austenite dendrites and eutectics of (γ+M_7C_3). It is found that the size of eutectic M_7C_3 carbide particles increases with an increase in Mo content. The size of eutectic structures are larger in the specimens containing Mo. It is well known that Mo is a strong carbide former and enriched to the final liquid to form the binary or ternary eutectic with Mo carbides. Therefore, the eutectic M_2C carbides could precipitate in the specimen with 3% Mo.

The matrices of all specimens are mostly austenitic. This is because sufficient dissolution of Cr content in the matrix prevents the pearlite transformation during cooling. In addition, Mo which was also distributed to the matrix shifted pearlite transformation to the long time side, and at the same time it depresses the M_s temperature to below room temperature. More Mo content results in an increase of the retained austenite. Some transformation of austenite to martensite could occur adjacent to the eutectic carbides because the depletion of carbon and alloying elements takes place due to the transformation of eutectic carbides.

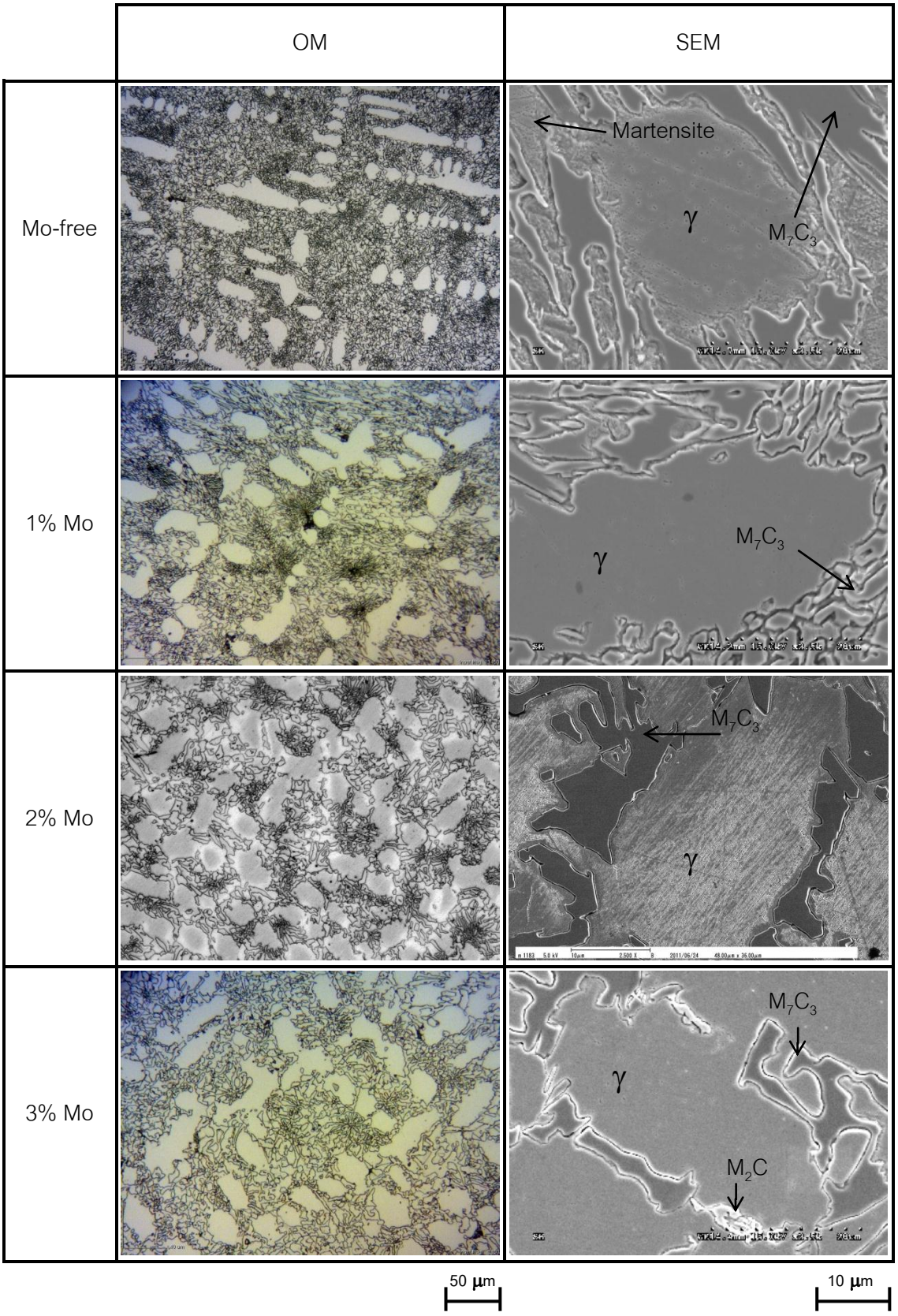

Fig. 4.1 Microstructures of as-cast specimens with different Mo content taken by OM and SEM.

4.1.2 Distribution of alloying elements in as-cast state

During solidification, the alloying elements are distributed to both of austenite and eutectic carbide according to their distribution coefficient. The amount of alloying element dissolved in the austenite determines the solid state transformation. The element remaining in the melt is consumed by formation of eutectic carbide.

Distribution of alloying elements in the as-cast specimens is revealed using Mapping of characteristic lines of X-ray by EPMA, and the results are shown in Fig. 4.2. From the results, it can be qualitatively said that the concentrations of C and Cr are relatively high in the eutectic carbides compared with those in the austenite dendrite or matrix. On the other hand, the concentration of Fe is comparatively high in the matrix. These results confirm that the austenite rejects C and Cr into the liquid and they are consumed to form the eutectic structure. [3] The concentrations of C and Cr adjacent to the eutectic carbide are relatively low in which martensite appears. The concentrations of C and Cr in the eutectic region are higher than those in the matrix region. With respect to Mo content, it is clear from X-ray images in the 3% Mo specimen that Mo is greatly concentrated in the carbides precipitating at the grain boundary.

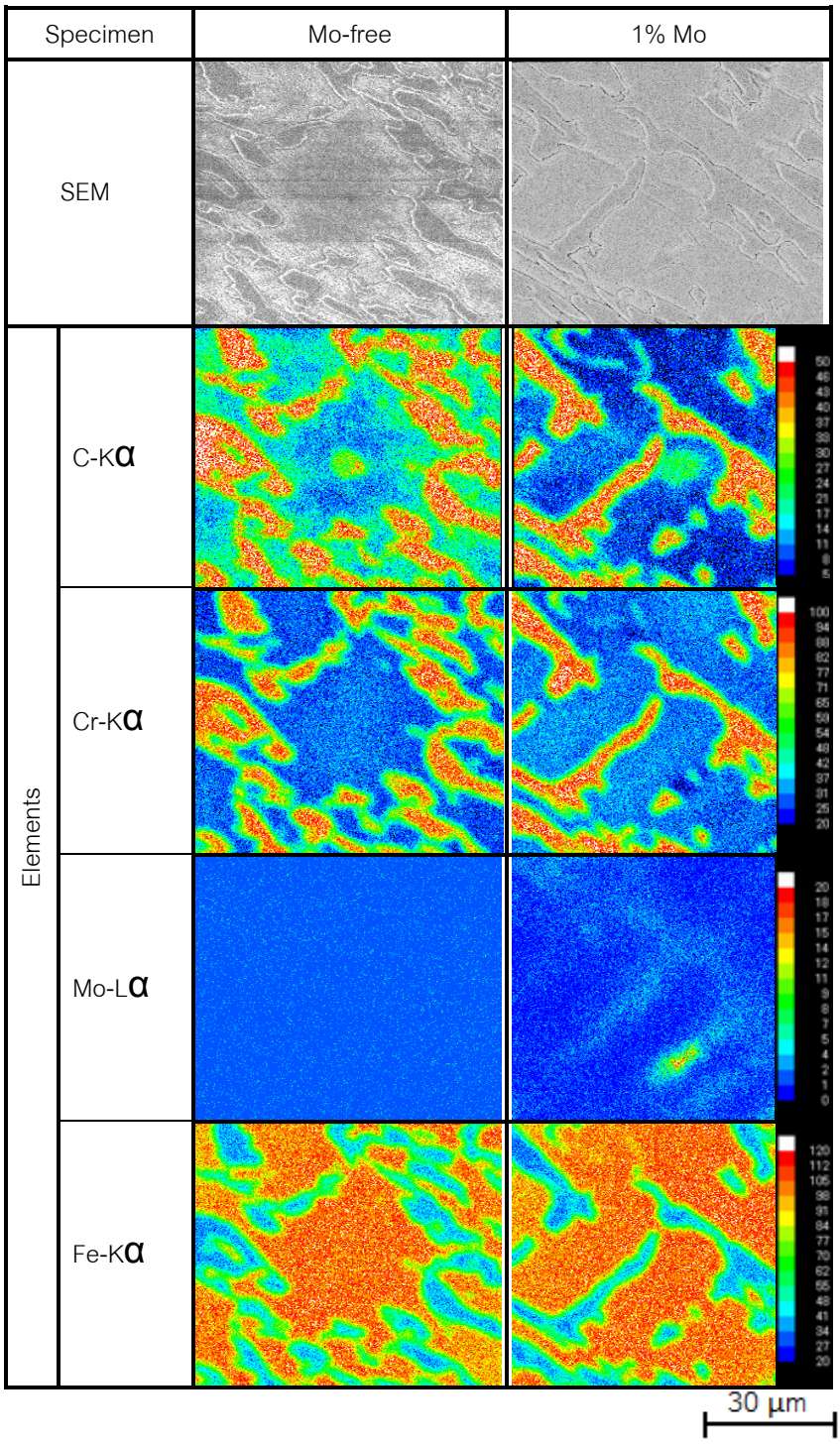

Fig. 4.2 SEM microphotographs and distribution of alloying elements by characteristic X-ray. As-cast state of 26% Cr specimens without and with Mo. (EPMA analysis)

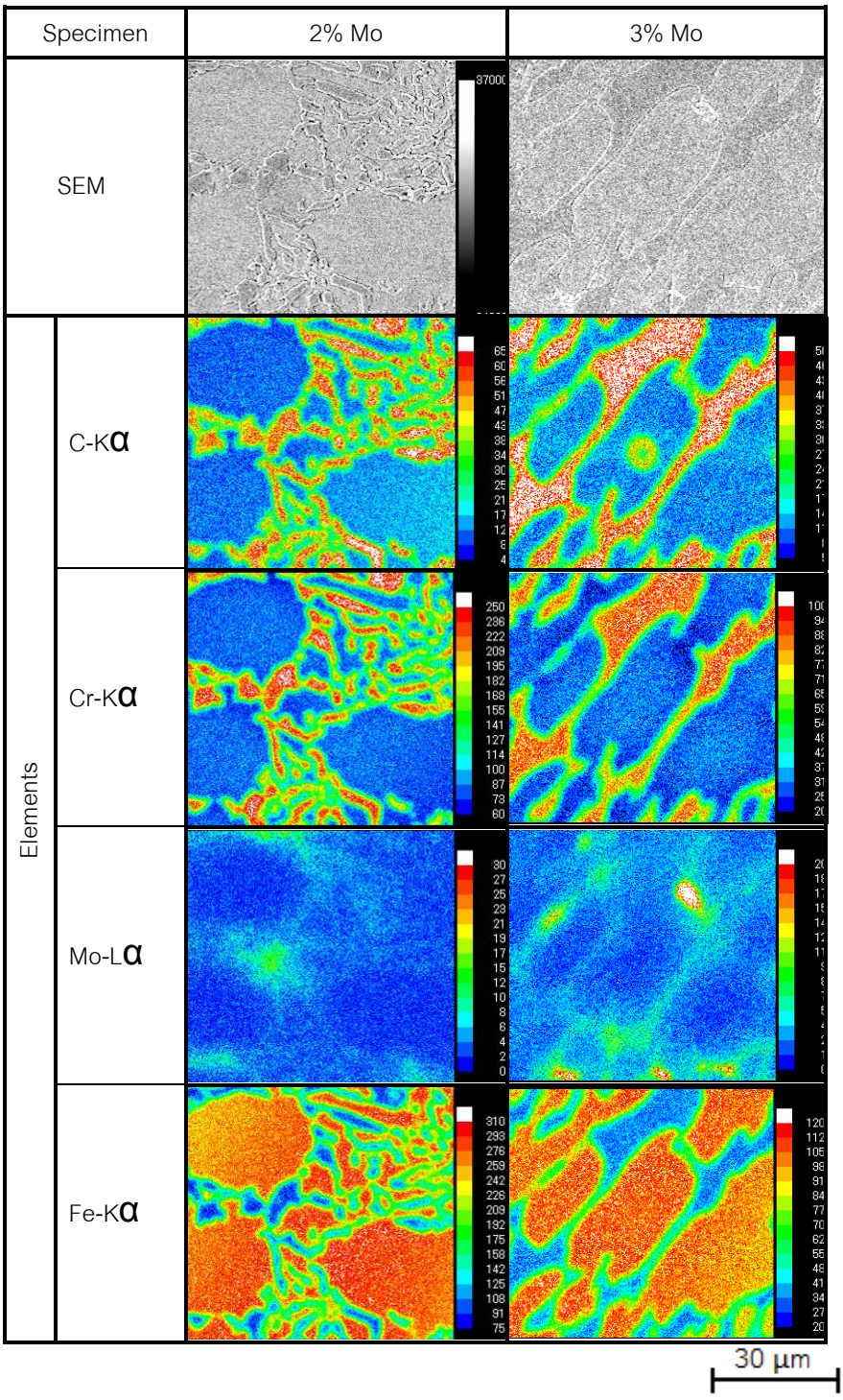

Fig. 4.2 SEM microphotographs and distribution of alloying elements by characteristic X-ray. As-cast state of 26% Cr specimens without and with Mo. (EPMA analysis)

4.1.3 As-hardened state

As-hardened microstructures of all specimens are shown in Fig. 4.3. The eutectic carbides appear unchanged from as-cast condition. On the other hand, it is found that the matrix has transformed to precipitate a large number of fine carbides. The matrices among the carbides should consist of some martensite and retained austenite, but they can not be seen in these photomicrographs. It has been reported that the secondary carbides which precipitated in the as-hardened state of high Cr cast iron are mostly M_7C_3 carbides co-existing with a certain amount of $M_{23}C_6$ carbides. [1,13] The retained austenite which existed in the as-cast state is destabilized to precipitate fine secondary carbides during holding and transforms into martensite during cooling. It is found from SEM photomicrographs that there are a few secondary carbides adjacent to the eutectic carbides. The reason may be that the precipitated carbides were united by diffusion to large and stable eutectic carbides during heat treatment as explained by Ostwald Ripening theory. The eutectic carbides of Mo_2C are observed at the boundary region of austenite in 3% Mo specimen. It is understood from this morphology that these carbides precipitated from the final liquid during solidification.

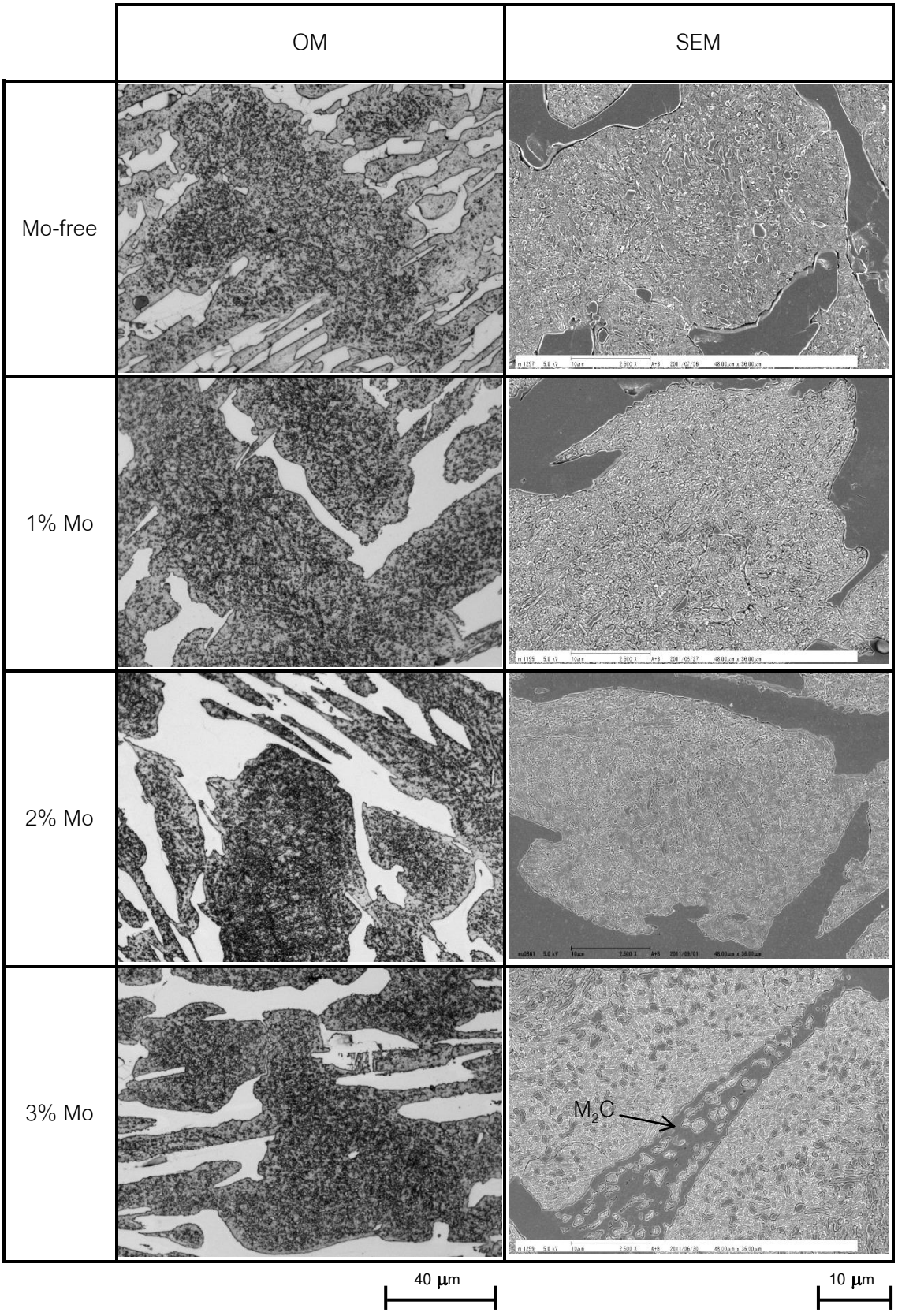

Fig. 4.3 Microstructures of as-hardened specimens with different Mo content taken by OM and SEM.

4.2 Macro-hardness, Micro-hardness and Volume Fraction of Retained Austenite (V_γ) of Test Specimens

4.2.1 As-cast state

The macro-hardness, micro-hardness and V_γ in the as-cast state are listed in Table 4.1. The data showed that the macro-hardness is consistently higher than the corresponding matrix hardness for all specimens. It is natural because the eutectic carbides which commonly have higher hardness are included in the macro-hardness. The hardness are 525-616 HV30 for macro-hardness and 370-414 HV0.1 for micro-hardness, respectively. The V_γ value ranges from 49-83%.

Effects of Mo content on the hardness and V_γ in the as-cast sate are shown in Fig. 4.4. The macro-hardness decreases from 616 HV30 to 525 HV30 and the micro-hardness decreases from 414 HV0.1 to 370 HV0.1 as Mo content increases. By contrast, the V_γ increases from 49% in Mo-free specimen to 78% in 1% Mo specimen, and then increases little at 80 % in 3% Mo specimen. Therefore, it can be said that a decrease in the hardness accompanying by raising the Mo content is due to an increase in the amount of retained austenite.

Table 4.1 Macro-hardness, micro-hardness and volume fraction of retained austenite (V_γ) in the as-cast specimens.

Specimen	Macro-hardness (HV30)	Micro-hardness (HV0.1)	V_γ , %
Mo-free	616	414	49
1% Mo	545	379	78
2% Mo	540	368	79
3% Mo	525	370	83

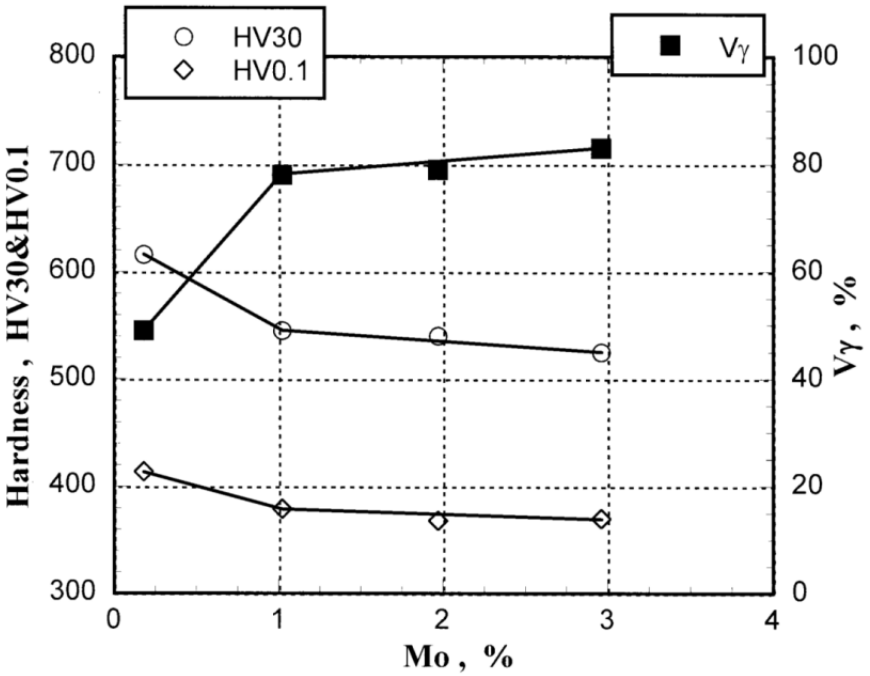

Fig. 4.4 Effect of Mo content on macro- and micro-hardness and volume fraction of retained austenite (V_γ) in the as-cast 26% Cr specimens.

4.2.2 Heat-treated state

Macro-hardness, micro-hardness and V_γ of heat-treated specimens are summarized in Table 4.2. It can be seen that the heat treatment produced a structure harder than that in the as-cast state, regardless of heat treatment condition. The range of hardness values produced was quite large, 300 HV30 at the maximum value. For the heat-treated specimen, the hardness in the as-hardened state is higher than that in the tempered state. The addition of Mo affects on the hardness in the as-hardened state, and it increases the hardness. The hardness range from 743 HV30-810 HV30 for Mo-free and 710-898 HV30 for Mo-bearing specimens, respectively.

The V_γ varies depending on Mo content and heat treatment condition. The V_γ in the as-hardened state is higher than that in the tempered state and it increases with an increase in Mo content. When compared with the as-cast state, however, the V_γ decreased greatly, 49-83% in the as-cast and 1-16% in the heat-treated state. This

result confirmed that the austenite in the as-cast state is destabilized by the precipitation of secondary carbides during holding at austenitizing temperature. The concentrations of C, Cr and Mo in austenite are reduced, leading to an increase of Ms temperature. The V_γ in the as-hardened state is higher than that the tempered state. It is clear that the V_γ value of L-H_{Tmax} specimen is greater than those of H_{Tmax} and H-H_{Tmax} specimens.

Table 4.2 Macro-hardness, micro-hardness and volume fraction of retained austenite (V_γ) of heat-treated specimens with different Mo content.

Specimen		Macro-hardness (HV30)	Micro-hardness (HV0.1)	V_γ , %
Mo content	Heat treatment condition			
Mo-free	As-hardened	810	755	6
	L-H_{Tmax}	743	724	4
	H_{Tmax}	769	741	2
	H-H_{Tmax}	751	726	1
1% Mo	As-hardened	865	762	8
	L-H_{Tmax}	782	737	5
	H_{Tmax}	818	752	4
	H-H_{Tmax}	714	636	1
2% Mo	As-hardened	898	816	16
	L-H_{Tmax}	845	757	9
	H_{Tmax}	866	780	5
	H-H_{Tmax}	854	768	4
3% Mo	As-hardened	873	780	16
	L-H_{Tmax}	831	766	9
	H_{Tmax}	835	768	7
	H-H_{Tmax}	710	616	4

Note ; L-H_{Tmax} : tempered at lower temperature than that at which H_{Tmax} is obtained.

H_{Tmax} : maximum tempered hardness.

H-H_{Tmax} : tempered at higher temperature than that at which H_{Tmax} is obtained.

4.3 Abrasion Wear Test

The heat-treated high Cr cast irons have been used for wear parts in many fields of industries. Therefore, the wear resistance of high Cr cast iron should be evaluated under the different heat treatment and wear conditions. In order to evaluate the wear resistance of heat-treated 26% Cr cast iron, hence, the two types of abrasion test, Suga abrasion wear test as two-body-type and Rubber Wheel abrasion wear test as three-body-type were employed. It is found from previous results that the Mo content and heat treatment condition influence on the hardness and V_γ of which factors are keenly related to the wear resistance. In this section, the effects of Mo content and heat treatment condition on the abrasion wear resistance are described.

4.3.1 Suga abrasion wear test (two-body-type)

In this experiment, series of heat-treated specimens shown in Table 4.2 were used. The relationship between wear loss and wear distance by Suga wear tester is presented in Fig. 4.5 for Mo-free specimen, Fig. 4.6 for 1% Mo specimen, Fig. 4.7 for 2% Mo specimen and Fig. 4.8 for 3% Mo specimen, respectively. The equations of wear loss vs. wear distance for the specimens with different heat treatment are shown at the upper part of each figure. In all of the figures, the wear loss increases in proportion to the wear distance. Total wear losses of specimens with different heat treatment condition at about 192 m wear test are summarized in Table 4.3. Since the linear relations were obtained between wear loss and wear distance in all the specimens, the parameter of wear rate (Rw) which is expressed by the slope of each straight line is introduced. The Rw values of all the specimens are summarized in Table 4.4. It is found that the Rw varies by the heat treatment condition and Mo content.

As-hardened	$W_l = 0.39 \times W_d - 0.123$ (R = 1.00)
L-H_{Tmax}	$W_l = 0.42 \times W_d - 0.799$ (R = 1.00)
H_{Tmax}	$W_l = 0.40 \times W_d - 0.174$ (R = 1.00)
H-H_{Tmax}	$W_l = 0.43 \times W_d - 0.603$ (R = 1.00)

W_l : Wear loss, W_d: Wear distance

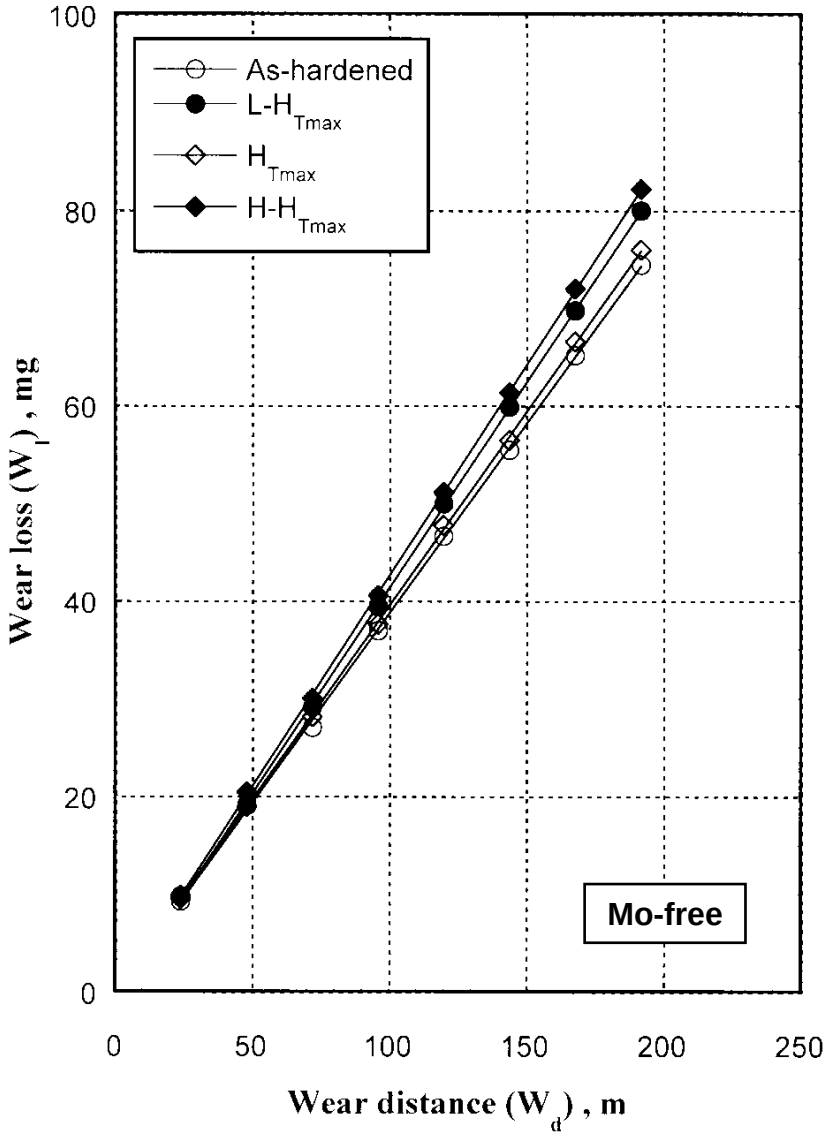

Fig. 4.5 Relationship between wear loss (W_l) and wear distance (W_d) of Mo-free specimens heat-treated by different conditions. Suga abrasion wear test (two-body-type) with load 9.8 N (1 kgf).

As-hardened	$W_l = 0.38 \times W_d + 0.157$ (R = 1.00)
L-H_{Tmax}	$W_l = 0.41 \times W_d - 0.311$ (R = 1.00)
H_{Tmax}	$W_l = 0.37 \times W_d + 0.443$ (R = 1.00)
H-H_{Tmax}	$W_l = 0.43 \times W_d - 0.361$ (R = 1.00)

W_l : Wear loss, W_d : Wear distance

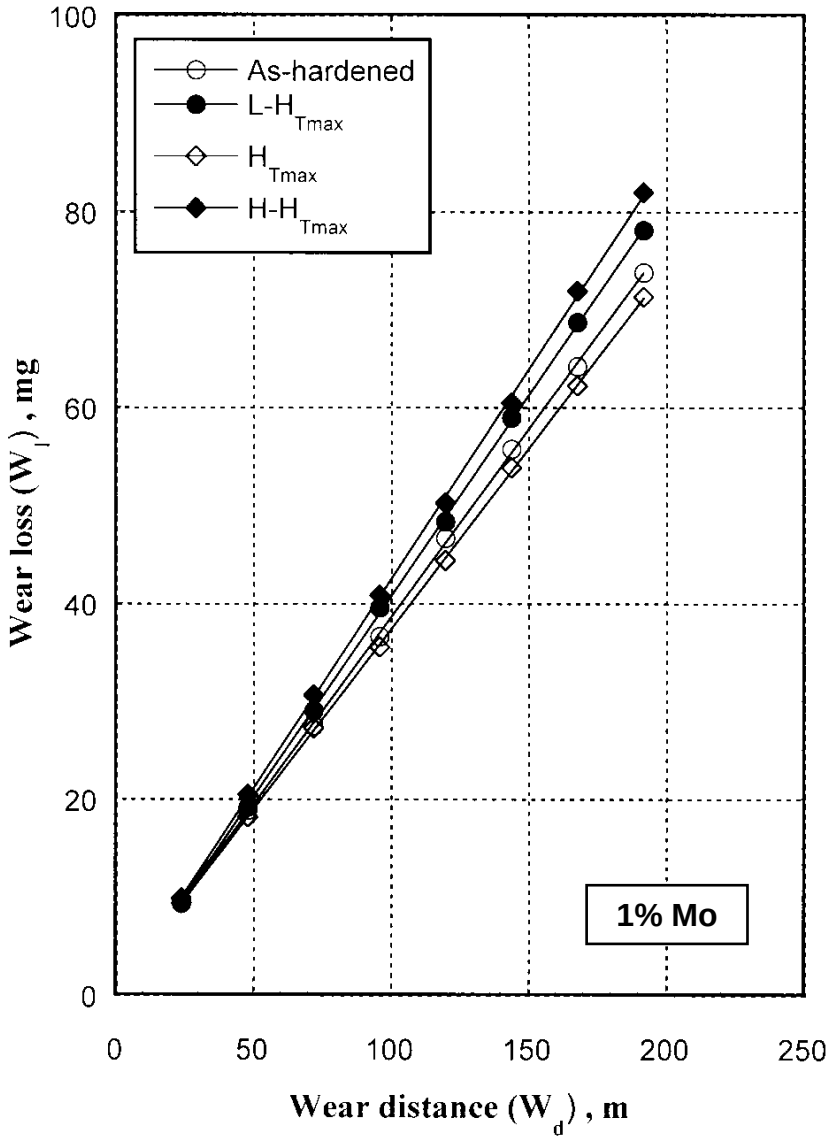

Fig. 4.6 Relationship between wear loss (W_l) and wear distance (W_d) of 1% Mo specimens heat-treated by different conditions. Suga abrasion wear test (two-body-type) with load 9.8 N (1 kgf).

As-hardened	$W_l = 0.34 \times W_d - 0.318$ (R = 1.00)
L-H_{Tmax}	$W_l = 0.35 \times W_d - 0.182$ (R = 1.00)
H_{Tmax}	$W_l = 0.36 \times W_d + 0.689$ (R = 1.00)
H-H_{Tmax}	$W_l = 0.38 \times W_d + 0.979$ (R = 1.00)

W_l : Wear loss, W_d : Wear distance

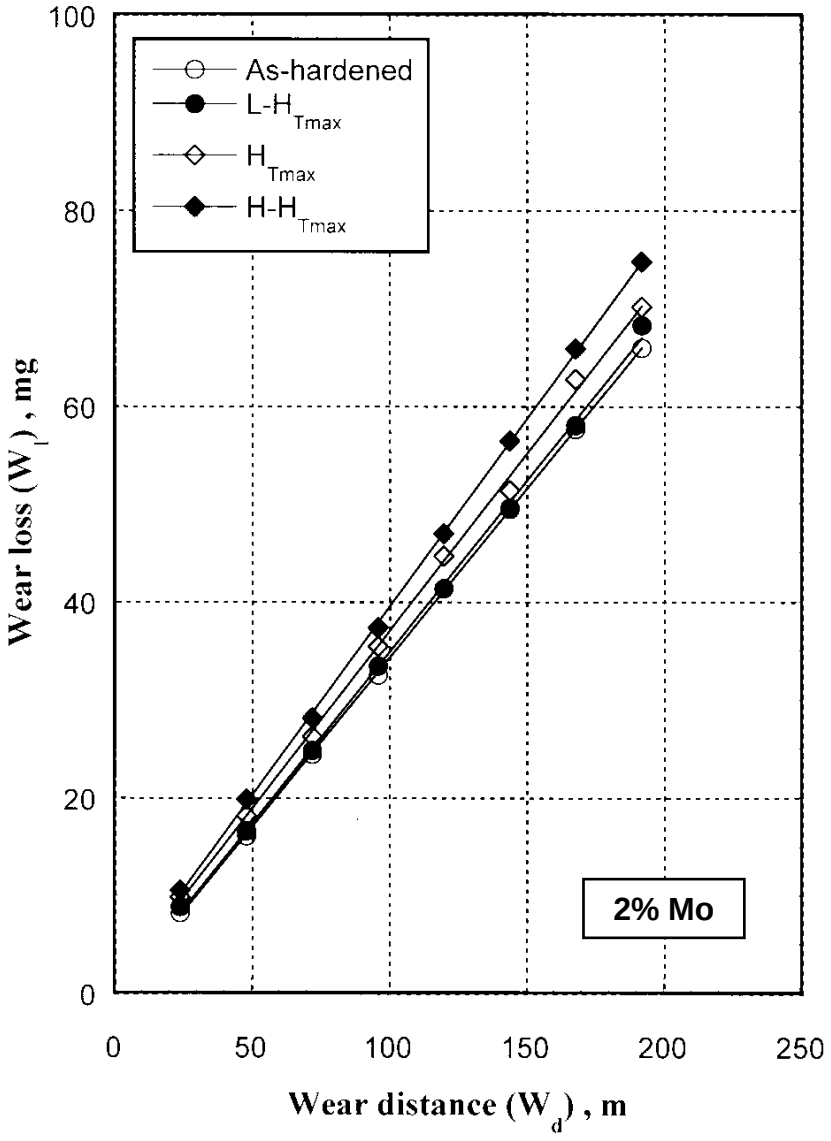

Fig. 4.7 Relationship between wear loss (W_l) and wear distance (W_d) of 2% Mo specimens heat-treated by different conditions. Suga abrasion wear test (two-body-type) with load 9.8 N (1 kgf).

As-hardened	$W_l = 0.37 \times W_d + 0.700$ (R = 1.00)
L-H_{Tmax}	$W_l = 0.38 \times W_d + 0.336$ (R = 1.00)
H_{Tmax}	$W_l = 0.35 \times W_d + 0.039$ (R = 1.00)
H-H_{Tmax}	$W_l = 0.41 \times W_d - 0.121$ (R = 1.00)

W_l : Wear loss, W_d : Wear distance

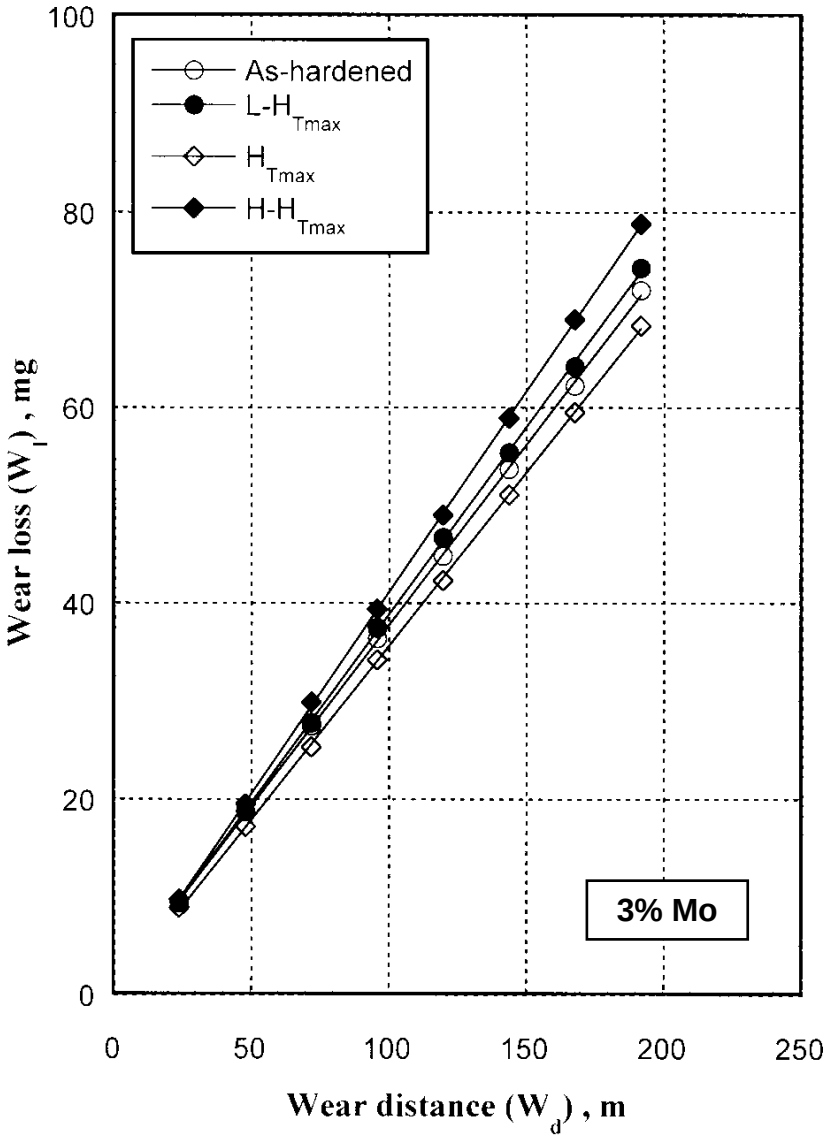

Fig. 4.8 Relationship between wear loss (W_l) and wear distance (W_d) of 3% Mo specimens heat-treated by different conditions. Suga abrasion wear test (two-body-type) with load 9.8 N (1 kgf).

Table 4.3 Total wear loss at 192 m of Suga abrasion wear test with a load of 9.8 N (1 kgf) for specimens with and without Mo.

Specimen	Total wear loss by Suga wear test at 192 m, mg.			
	As-hardened	L-H_{Tmax}	H_{Tmax}	H-H_{Tmax}
Mo-free	74.4	79.9	75.9	82.1
1% Mo	73.7	78.0	71.2	81.9
2% Mo	65.9	68.2	70.1	74.7
3% Mo	71.9	74.2	68.3	78.7

Table 4.4 Wear rate (Rw) by Suga abrasion wear test (two-body-type) of heat-treated specimens with different Mo content. Load : 9.8 N(1kgf).

Specimen	Wear rate (Rw) , mg/m			
	As-hardened	L-H_{Tmax}	H_{Tmax}	H-H_{Tmax}
Mo-free	0.39	0.42	0.40	0.43
1% Mo	0.38	0.41	0.37	0.43
2% Mo	0.34	0.35	0.36	0.38
3% Mo	0.37	0.38	0.35	0.41

The relationship between wear loss and wear distance of Mo-free specimen is presented in Fig.4.5, the total wear loss increases in the order of 74.4 mg in the as-hardened state, 75.9 mg in H_{Tmax}, 79.9 mg in L-H_{Tmax}, and 82.1 mg in H-H_{Tmax} specimens. The smallest Rw value (0.39 mg/m) is obtained in as-hardened specimen followed by H_{Tmax} specimen (0.40 mg/m). The largest Rw value (0.43 mg/m) is obtained in H-H_{Tmax} specimen. Therefore, the highest wear resistance is obtained in the as-hardened specimen and the lowest wear resistance appears in the over-tempering specimen.

As for the results of 1% Mo specimen shown in Fig. 4.6, the relationship between wear loss and wear distance is similar to that of Mo-free specimen, that is, the wear loss increases proportionally with an increase in the wear distance in each heat treatment condition. However, the order of the total wear loss is different from the results of Mo-free specimen, that is, H_{Tmax} specimen (71.2 mg), as-hardened specimen (73.7 mg), L-H_{Tmax} specimen (78.0 mg) and H-H_{Tmax} specimen (81.9 mg). From Table 4.4, the smallest Rw value of 0.37 mg/m is obtained in H_{Tmax} specimen followed by 0.38 mg/m in as-hardened specimen, 0.41 mg/m in L-H_{Tmax} specimen and 0.43 mg/m in H-H_{Tmax} specimen, respectively. Form these results, the highest wear resistance are obtained in the specimen with H_{Tmax} whereas the lowest wear resistance is obtained in H-H_{Tmax} specimen.

From the results of 2% Mo specimen shown in Fig. 4.7, the relation of wear loss vs. wear distance shows the trend similar to other specimens. However, the wear loss is comparably smaller than Mo-free and 1% Mo specimens. The total wear loss values at 192 m are 65.9, 68.2, 70.1 and 74.4 mg in As-hardened specimen, L-H_{Tmax} specimen, H_{Tmax} specimen, and H-H_{Tmax} specimen, respectively. As shown in Table 4.4, the smallest Rw value is 0.34 mg/m in as-hardened specimen. However, the Rw values of others specimens do not make much difference from the smallest value, 0.35mg/m in L-H_{Tmax} specimen and 0.36 mg/m in H_{Tmax} specimen and 0.38 mg/m in the H-H_{Tmax} specimen.

As for the results of 3% Mo specimen shown in Fig. 4.8, the total wear loss values at 192 m are in the order of 68.3 mg in H_{Tmax} specimen, 71.9 mg in as-hardened specimen, 74.2 mg in L-H_{Tmax} specimen and 78.7mg in H-H_{Tmax} specimen, respectively. As shown in Table 4.4, the smallest Rw value 0.35 mg/m is obtained in H_{Tmax} specimen and it is close to the Rw values of as-hardened specimen, 0.37 mg/m and 0.38 mg/m of L-H_{Tmax} specimen. The largest Rw value, 0.41mg/m is obtained in the H-H_{Tmax} specimen.

From above results, it can be concluded that the largest wear resistance is obtained in the as-hardened and H_{Tmax} specimens of which matrix contains large portion of martensite and some retained austenite. The lowest wear resistance or highest Rw is obtained in H-H_{Tmax} specimen where a large portion of martensite was tempered and small amount of austenite is left. It is also found that the wear resistance is improved by Mo addition because Mo improved the hardenability and promoted the secondary hardening.

4.3.2 Rubber Wheel abrasion wear test (three-body-type)

The results of Rubber Wheel wear tester are displayed in Fig. 4.9-4.12 for specimens with different Mo content, respectively. It is found that the wear loss increased in portion to the wear distance in all the specimens and the relation is shown at the upper part of each figure. The total wear loss and Rw value are correspondingly summarized in Table 4.5 and Table 4.6.

The results of the Mo-free specimen are shown in Fig. 4.9. The total wear losses are 146 mg in as-hardened specimen, 208 mg in L-H_{Tmax} specimen, 174 mg in H_{Tmax} specimen and 180 mg in the H-H_{Tmax} specimen, respectively. The smallest Rw value, 0.046 mg/m is obtained in as-hardened specimen followed by the 0.054 mg/m in H_{Tmax} specimen. The largest Rw value, 0.057 mg/m is obtained in H-H_{Tmax} specimen.

Fig. 4.10 shows the results of 1% Mo specimen. The linear relation between wear loss and wear distance is obtained in the same manner as Mo-free

specimen. The total wear losses are in the order of 171mg in H_{Tmax} specimen, 179 mg in as-hardened specimen, 214 mg in L-H_{Tmax} specimen and 247 mg in H-H_{Tmax} specimen. The smallest Rw value, 0.054 mg/m is obtained in H_{Tmax} specimen followed by 0.056 mg/m in as-hardened specimen. The largest Rw value, 0.078mg/m is obtained in H-H_{Tmax} specimen.

In the case of 2% Mo specimen as shown in Fig. 4.11, the total wear losses increase in the order of 149 mg in H_{Tmax} specimen, 165mg in as-hardened specimen, 168 mg in H-H_{Tmax} specimen and 177mg in L-H_{Tmax} specimen. The Rw values are 0.047mg/m in H_{Tmax} specimen, 0.051mg/m in as-hardened specimen, 0.052 mg/m in H-H_{Tmax} specimen and 0.055 mg/m in L-H_{Tmax} specimen, respectively.

In 3% Mo specimen as shown in Fig. 4.12, the order of total wear losses is different from that of 2% Mo specimen. That is, the smallest wear loss, 166 mg is obtained in as-hardened specimen followed by 184 mg in H_{Tmax} specimen, 203 mg in L-H_{Tmax} specimen and 307 mg in H-H_{Tmax} specimen. The smallest Rw value is 0.053 mg/m and the highest value is 0.096 mg/m are obtained in as-hardened and H-H_{Tmax} specimens, respectively.

Here, it can be concluded from the above results that the smallest Rw is obtained in the as-hardened and H_{Tmax} specimens. The largest Rw value is obtained in the H-H_{Tmax} specimen

From these results, it is clear that the Mo content and heat treatment condition greatly influence on the wear rate (Rw) in both Suga abrasion wear test and Rubber Wheel abrasion wear test. This is because the heat treatment can control the matrix structure and the hardness which are important factors to determine the wear resistance. Therefore, the effects of hardness, retained austenite, and Mo content on wear rate are particularly discussed in the next chapter V.

As-hardened	$W_l = 0.046 \times W_d + 3.128$ (R = 1.00)
L-H_{Tmax}	$W_l = 0.067 \times W_d - 3.206$ (R = 1.00)
H_{Tmax}	$W_l = 0.054 \times W_d + 3.542$ (R = 1.00)
H-H_{Tmax}	$W_l = 0.057 \times W_d - 0.351$ (R = 1.00)

W_l : Wear loss, W_d : Wear distance

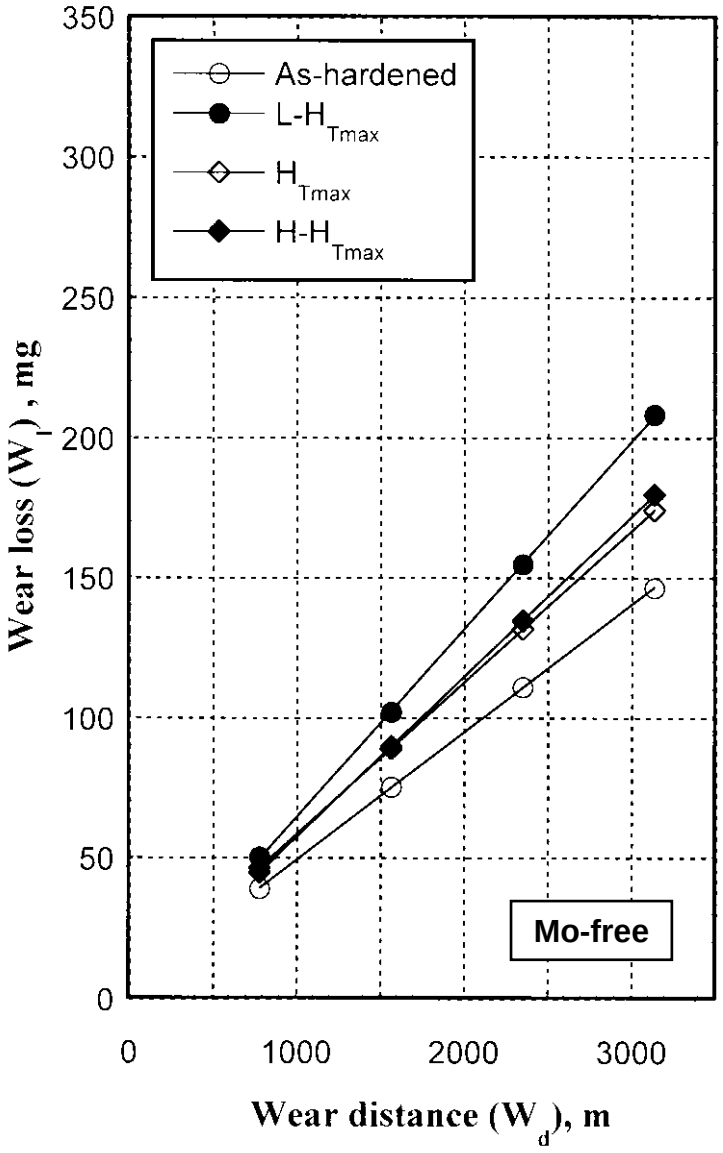

Fig. 4.9 Relationship between wear loss (W_l) and wear distance (W_d) of Mo-free specimens heat-treated by different conditions. Rubber Wheel abrasion wear test (three-body-type) with load 85.3 N (8.7 kgf).

As-hardened	$W_l = 0.056 \times W_d + 4.753$ (R = 1.00)
L-H_{Tmax}	$W_l = 0.068 \times W_d - 1.116$ (R = 1.00)
H_{Tmax}	$W_l = 0.054 \times W_d - 0.508$ (R = 1.00)
H-H_{Tmax}	$W_l = 0.078 \times W_d + 1.969$ (R = 1.00)

W_l : Wear loss, W_d : Wear distance

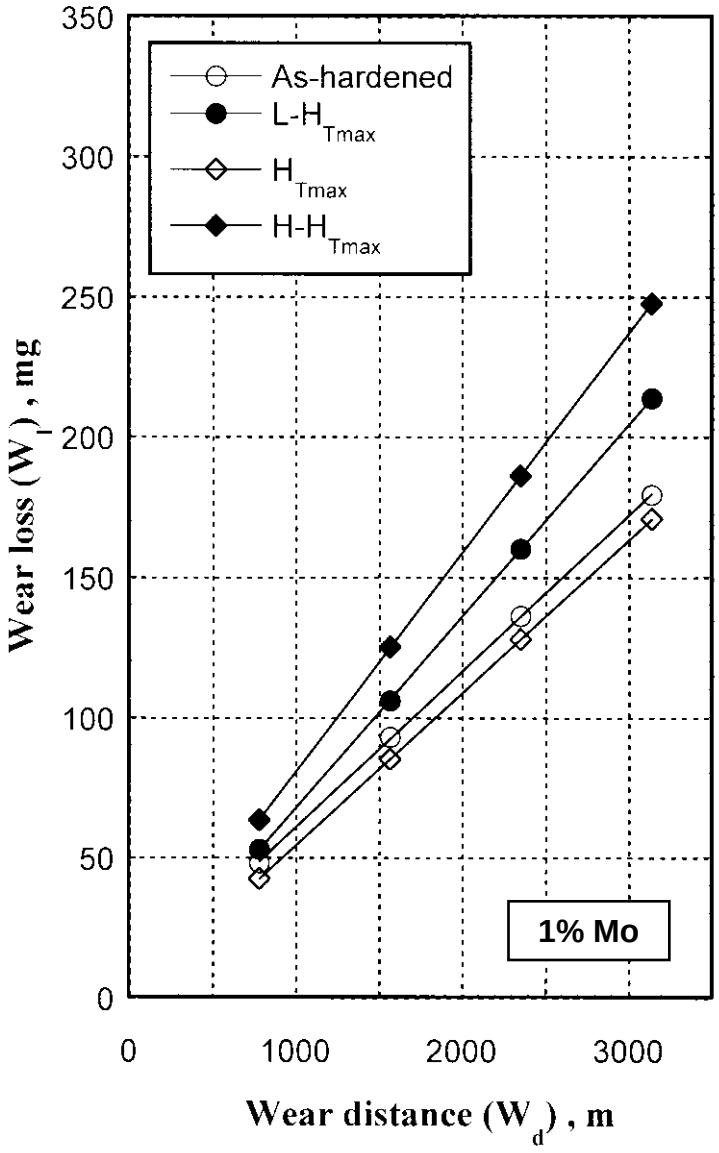

Fig. 4.10 Relationship between wear loss (W_l) and wear distance (W_d) of 1% Mo specimens heat-treated by different conditions. Rubber Wheel abrasion wear test (three-body-type) with load 85.3 N (8.7 kgf).

As-hardened	$W_l = 0.051 \times W_d + 3.636$ (R = 1.00)
L-H_{Tmax}	$W_l = 0.055 \times W_d + 3.783$ (R = 1.00)
H_{Tmax}	$W_l = 0.047 \times W_d + 3.223$ (R = 1.00)
H-H_{Tmax}	$W_l = 0.052 \times W_d + 3.826$ (R = 1.00)

W_l : Wear loss, W_d : Wear distance

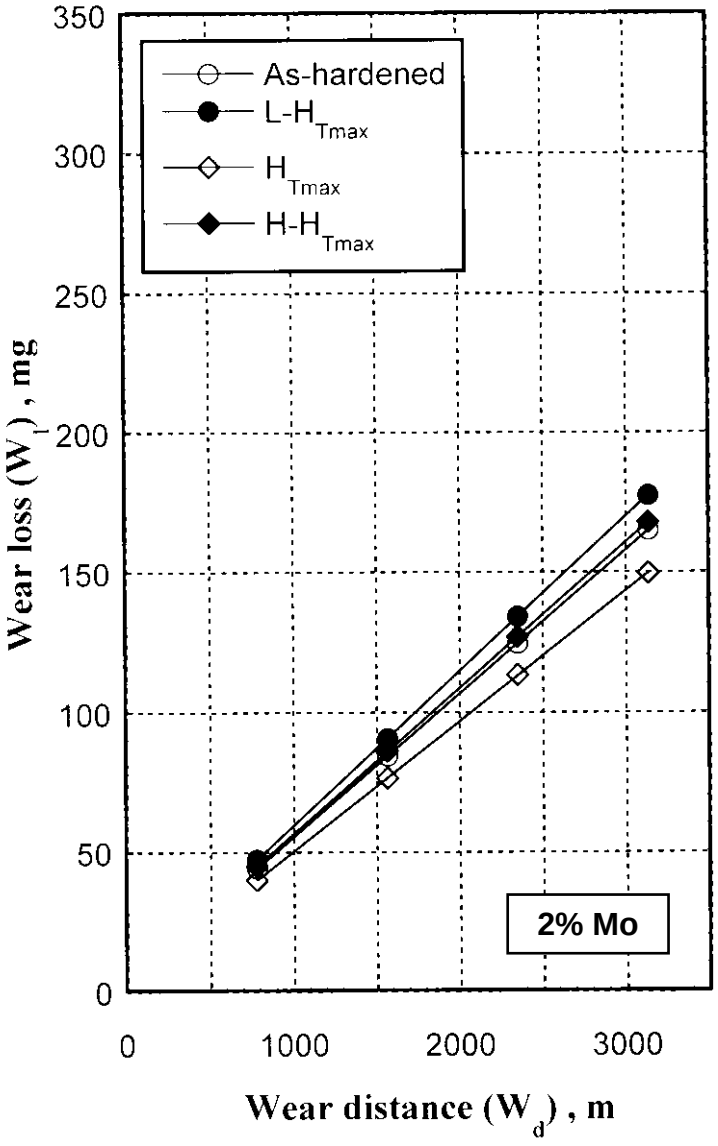

Fig. 4.11 Relationship between wear loss (W_l) and wear distance (W_d) of 2% Mo specimens heat-treated by different conditions. Rubber Wheel abrasion wear test (three-body-type) with load 85.3 N (8.7 kgf).

As-hardened	$W_l = 0.053 \times W_d + 1.321$ (R = 1.00)
L-H_{Tmax}	$W_l = 0.066 \times W_d - 2.947$ (R = 1.00)
H_{Tmax}	$W_l = 0.059 \times W_d - 0.576$ (R = 1.00)
H-H_{Tmax}	$W_l = 0.096 \times W_d + 5.213$ (R = 1.00)

W_l : Wear loss, W_d : Wear distance

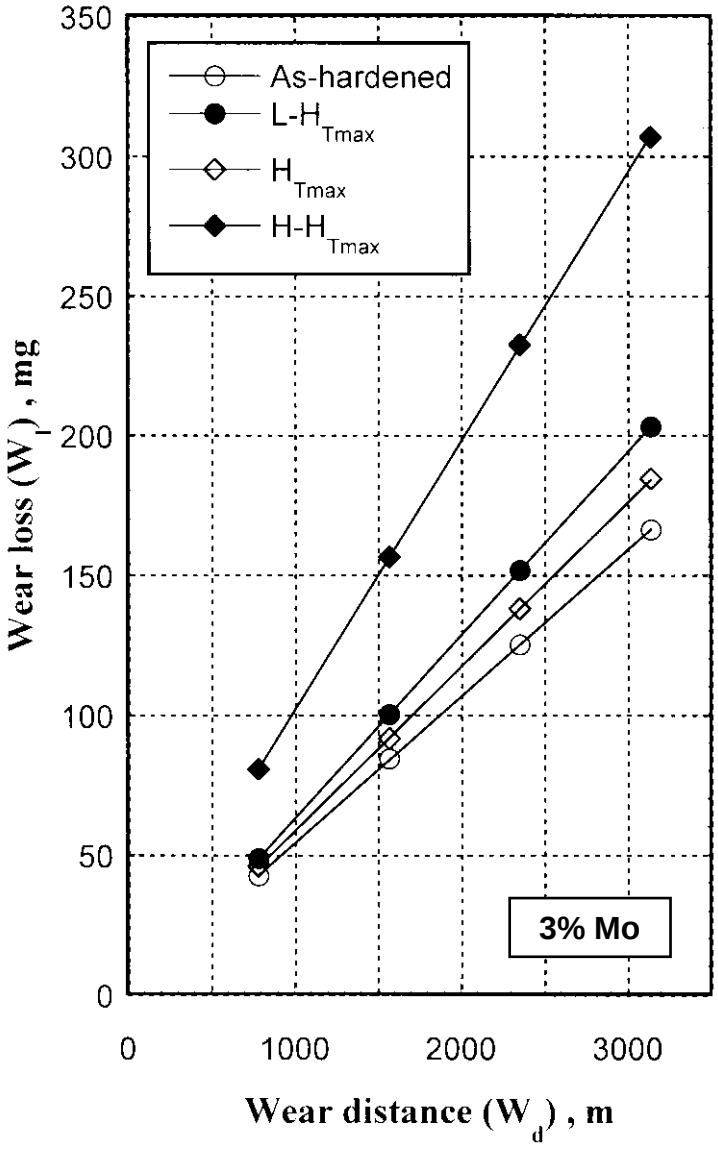

Fig. 4.12 Relationship between wear loss (W_l) and wear distance (W_d) of 3% Mo specimens heat-treated by different conditions. Rubber Wheel abrasion wear test (three-body-type) with load 85.3 N (8.7 kgf).

Table 4.5 Total wear loss at 3143 m of Rubber Wheel abrasion wear test with a load of 85.3 N (8.7 kgf) for specimens with and without Mo.

Heat Treatment Condition	Total wear loss in Rubber Wheel wear test at 3143 m. (mg.)			
	As-hardened	L-H_{Tmax}	H_{Tmax}	H-H_{Tmax}
Mo-free	146	208	174	180
1% Mo	179	213	171	247
2% Mo	165	177	149	168
3% Mo	166	203	184	307

Table 4.6 Wear rate (Rw) by Rubber Wheel abrasion wear test (three-body-type) of heat-treated specimens with different Mo content. Load : 85.3 N (8.7 kgf).

Specimen	Wear rate (Rw) , mg/m			
	As-hardened	L-H_{Tmax}	H_{Tmax}	H-H_{Tmax}
Mo-free	0.046	0.067	0.054	0.057
1% Mo	0.056	0.068	0.054	0.078
2% Mo	0.051	0.055	0.047	0.052
3% Mo	0.053	0.066	0.059	0.096

CHAPTER V
DISCUSSIONS

5.1 Explanation of Abrasion Wear Test Method

5.1.1 Comparison of test methods between Suga abrasion wear test and Rubber Wheel abrasion wear test

In previous chapter, it was described that the abrasion wear resistance (Rw) value in Rubber Wheel abrasion wear test is about eight times smaller than that of Suga abrasion wear test in all the specimens. In order to explain this phenomenon, absolute wear loss per unit area which is the ratio of the total wear loss and the total worn area is introduced. [8] The calculation can be explained as follows,

In Suga abrasion wear test, the test piece was worn by abrasive paper that is fixed to the circumference of wheel with 12 mm in width and it moves forth and back for the stroke distance of 30 mm as shown in Fig. 5.1. So,

$$\text{Worn surface area / stoke} = 12 \times 30 \times 2 \ (mm^2)$$
$$= 720 \ (mm^2)$$

In each test, the wheel is rotated by 0.9 degree every single stroke to provide the new abrasive particles and it takes 400 stokes/test. The test repeated for eight times in the same worn surface area until the wear distance of 192 m. Therefore,

$$\text{Total worn surface area} = 720 \times 400 \times 8 \ (mm^2)$$
$$= 2.304 \times 10^6 \ (mm^2)$$
$$= 2.30 \ (m^2)$$

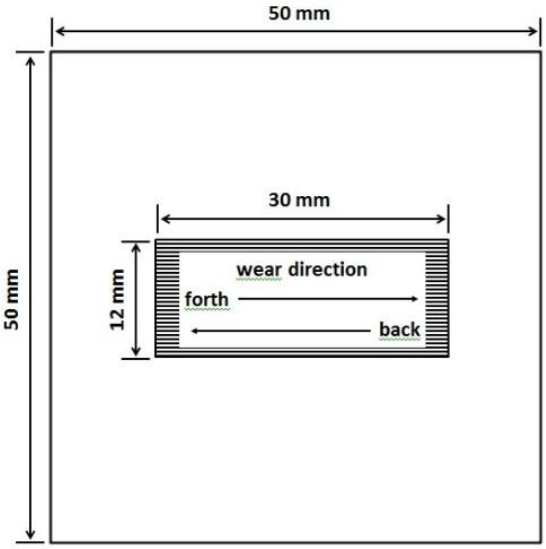

Fig. 5.1 Schematic drawing of worn area in test piece of Suga abrasion wear test.

In Rubber Wheel abrasion wear test as shown in Fig. 5.2, the metallic wheel with width of 15 mm of which circumference is lined by rubber is rotated at the constant rotational speed for 1000 revolutions. Then, the test was repeated for four times at wear distance of 3142 m. Therefore,

$$\text{Total worn surface area} = 2 \times \pi \times \frac{250}{2} \times 15 \times 1000 \times 4 \ (mm^2)$$
$$= 47.12 \times 10^6 \ (mm^2)$$
$$= 47.12 \ (m^2)$$

As an example, the absolute wear loss per unit area in both Suga and Rubber Wheel abrasion wear tests for 1% Mo specimen is summarized in Table 5.1.

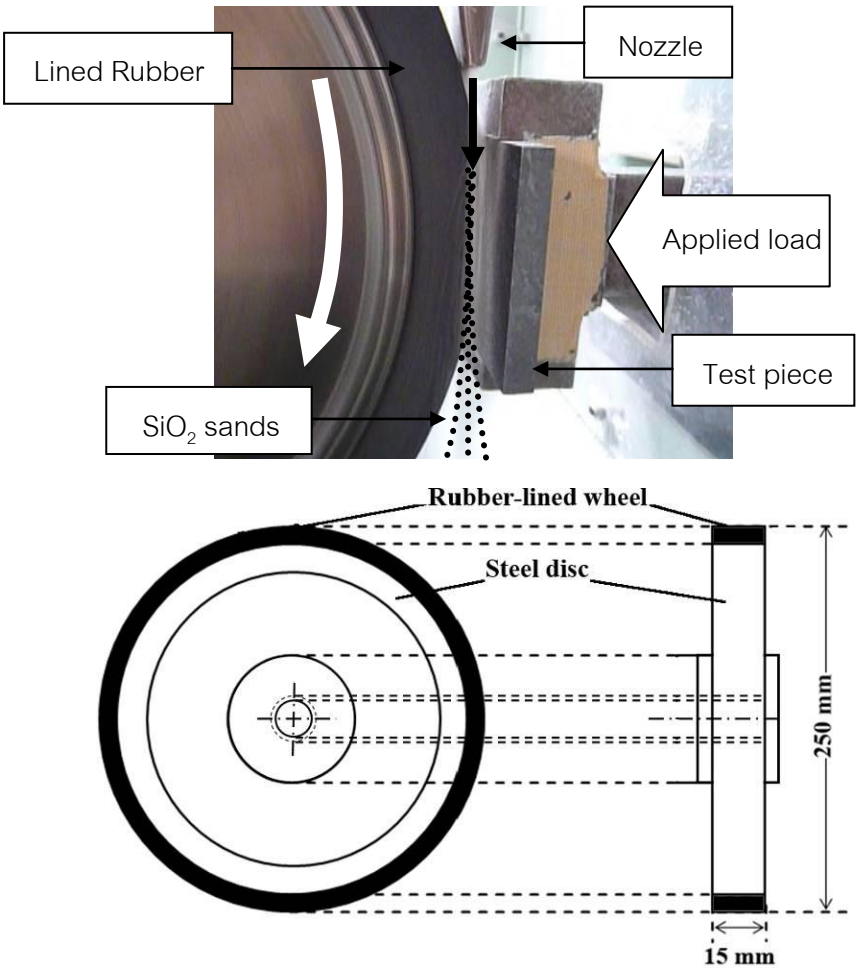

Fig. 5.2 Photograph of main portion of Rubber Wheel abrasion.

Table 5.1 Comparison of wear loss per unit area between Suga abrasion wear test and Rubber Wheel abrasion wear test of 1% Mo specimen.

Heat treatment condition	Absolute wear loss per unit area (mg/m^2) (total wear loss/total worn area)	
	Suga	Rubber Wheel
As-hardened	32.0	3.8
L-H_{Tmax}	33.9	4.4
H_{Tmax}	31.0	3.6
H-H_{Tmax}	35.6	5.3

It is clear from Table 5.1 that the absolute wear loss per unit area of Suga abrasion wear test is greater than that of Rubber Wheel abrasion wear test. The difference is approximately eight times. The highest value is obtained in the H_{Tmax} specimen and the smallest value is obtained in the H-H_{Tmax} specimen. From these results, it can be said that the abrasion wear by Suga abrasion wear test is much more severe than that by Rubber Wheel abrasion wear test. This is because the stress between the particles and the wear surface by Suga abrasion wear test is greater than that by Rubber Wheel abrasion wear test.

5.1.2 Effect of applied load on wear rate (Rw) in Suga abrasion wear test

It is well known that the Rw relates to the applied load or stress between two counterparts. In this section, therefore, the effect of applied load on the wear behavior of 1% Mo specimen is investigated. The test is carried out under the load of 4.9 N (0.5 kgf), 9.8 N (1 kgf) and 29.4 N (3 kgf), respectively. The results are shown in Fig. 5.3 for load of 4.9 N, Fig. 5.4 for load of 29.4 N, whereas the result for 9.8 N was already shown in Fig. 4.6. Under every load, the linear relationships between wear loss and wear distance were obtained by Suga wear tester. The equations for the relationships in the specimens with different heat treatment are also shown at the upper part of each figure. The effect of applied load on the relationship between wear loss (W_l) and wear distance (W_d) is shown in Fig. 5.5. Under any load, the W_l increases in proportion to the W_d and the total wear loss or wear rate (Rw) increases with increasing the applied load.

The effect of load on Rw of 1% Mo specimens is shown in Fig. 5.6 and the relation is expressed at the upper part of the figure. It is found that the Rw increases in proportion to applied load and the inclination is almost the same regardless of heat treatment condition. This suggests that, in the Suga abrasion wear test, it is possible not only to compare the wear resistance of materials qualitatively at any applied load but also to compare the Rw quantitatively by converting the data obtained under different loads.

As-hardened	$W_l = 0.194 \times W_d + 0.208$ (R = 1.00)
L-H_{Tmax}	$W_l = 0.201 \times W_d + 0.176$ (R = 1.00)
H_{Tmax}	$W_l = 0.191 \times W_d + 0.066$ (R = 1.00)
H-H_{Tmax}	$W_l = 0.209 \times W_d - 0.106$ (R = 1.00)

W_l : Wear loss, W_d : Wear distance

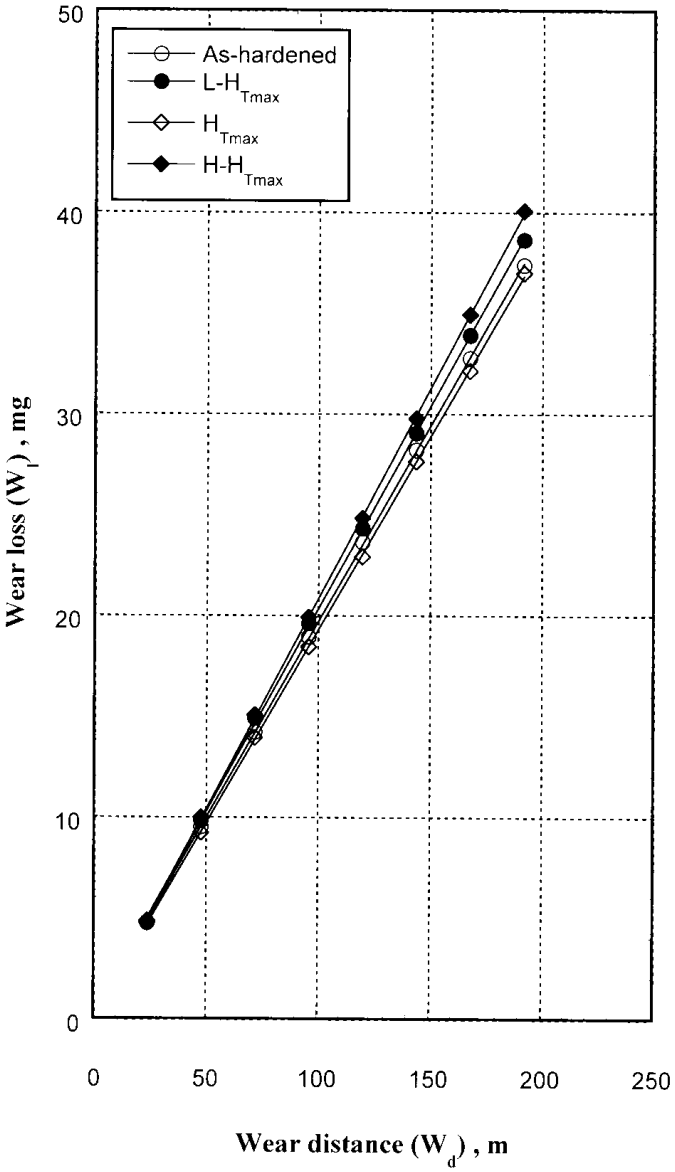

Fig. 5.3 Relationship between wear loss (W_l) and wear distance (W_d) of 1% Mo specimens heat-treated by different conditions. Suga abrasion wear test (two-body-type) with load 4.9 N (0.5 kgf).

As-hardened	W_l = 1.039 x W_d - 1.184 (R = 1.00)
L-H_{Tmax}	W_l = 1.049 x W_d + 0.431 (R = 1.00)
H_{Tmax}	W_l = 1.018 x W_d + 0.281 (R = 1.00)
H-H_{Tmax}	W_l = 1.075 x W_d + 0.434 (R = 1.00)

W_l : Wear loss, W_d : Wear distance

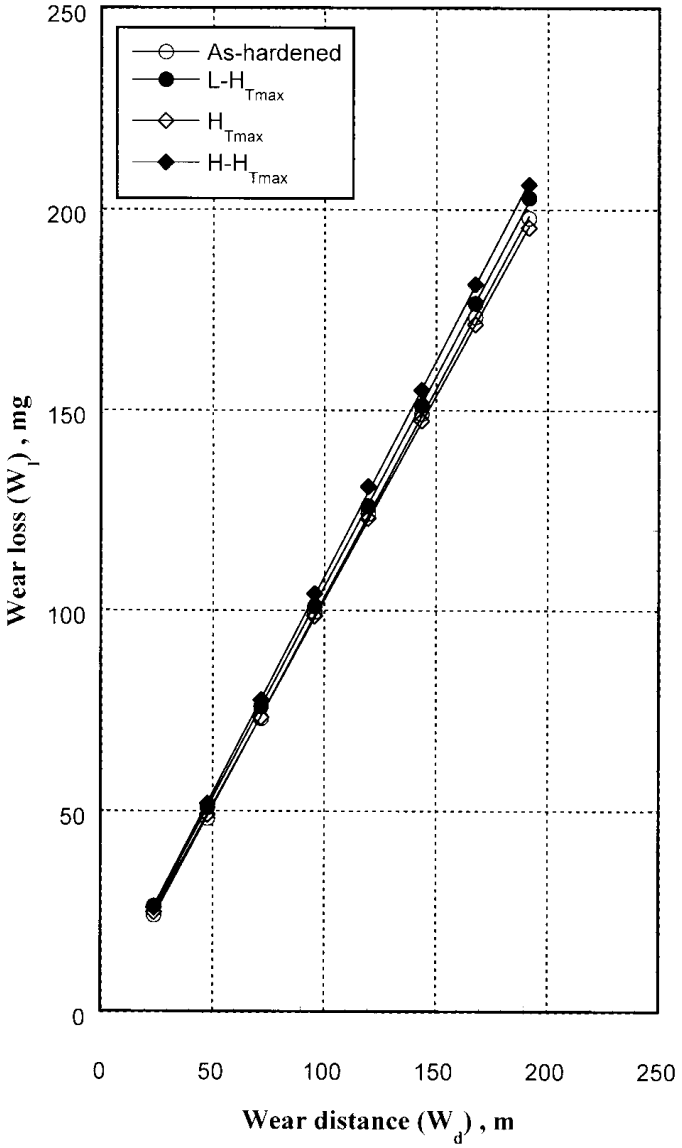

Fig. 5.4 Relationship between wear loss (W_l) and wear distance (W_d) of 1% Mo specimens heat-treated by different conditions. Suga abrasion wear test (two-body-type) with load 29.4 N (3 kgf).

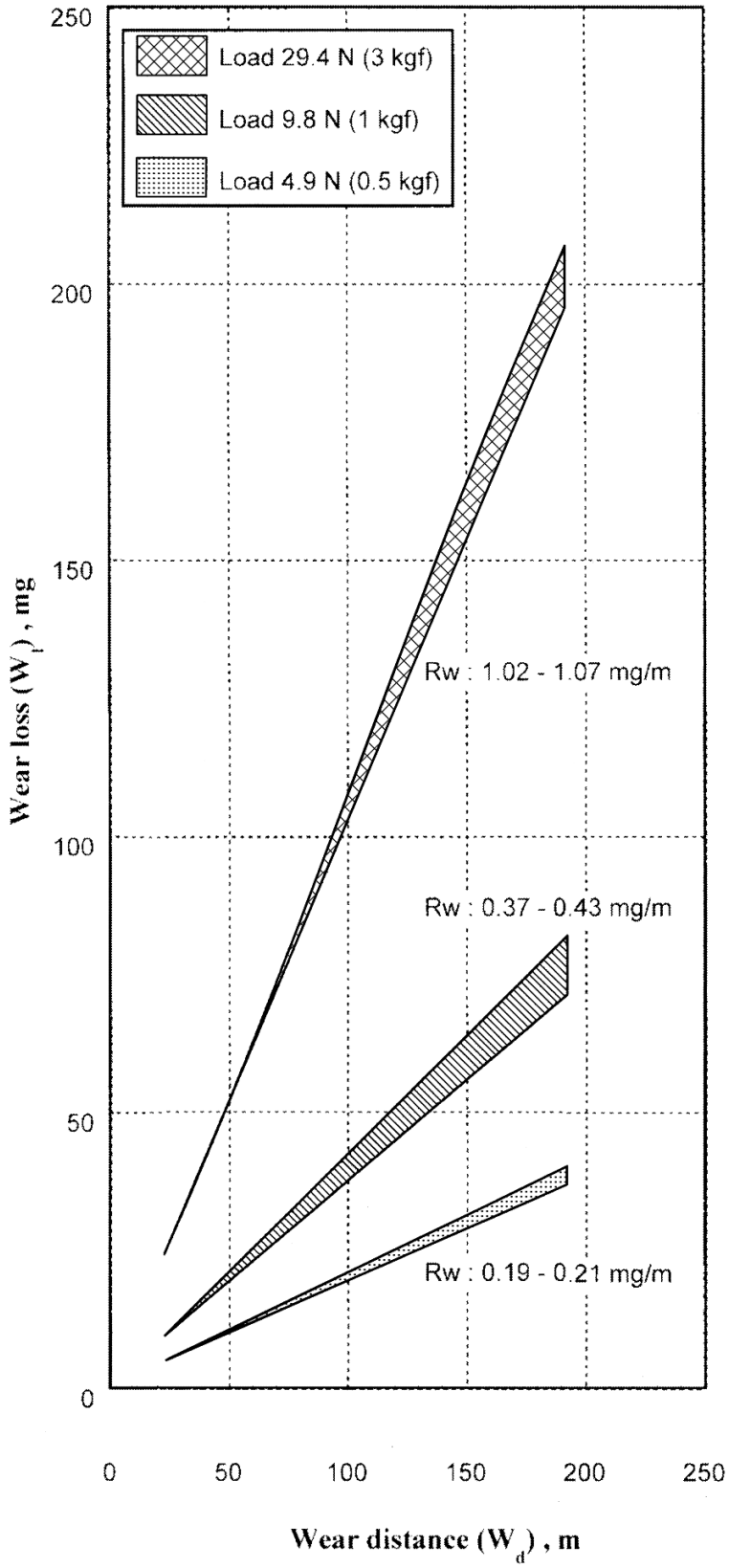

Fig. 5.5 Comparison of relationships between wear loss (W_l) and wear distance (W_d) of 1% Mo specimen under different loads of Suga abrasion wear test (two-body-type).

As-hardened	Rw = 0.034 x L + 0.036 (R = 1.00)
L-H_{Tmax}	Rw = 0.033 x L + 0.052 (R = 1.00)
H_{Tmax}	Rw = 0.033 x L + 0.030 (R = 1.00)
H-H_{Tmax}	Rw = 0.034 x L + 0.062 (R = 1.00)

Rw : Wear rate, L : Load

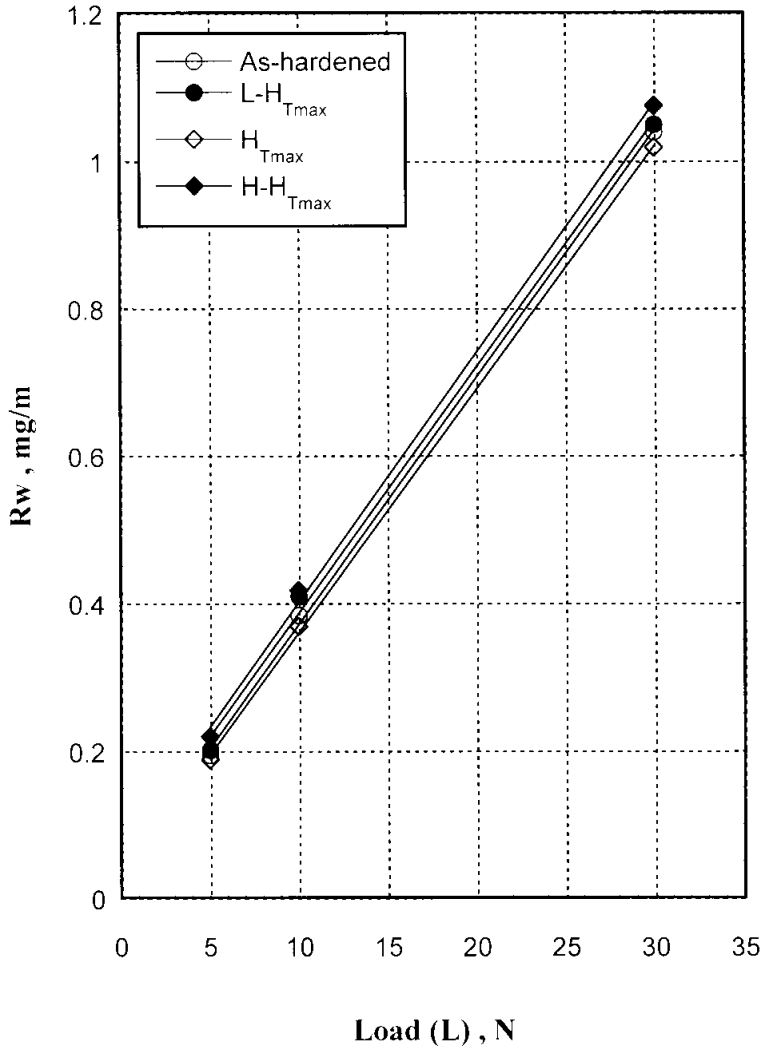

Fig. 5.6 Effect of load (L) on wear rate (Rw) of 1% Mo specimens with different heat treatment. Suga abrasion wear test (two-body-type).

5.2 Correlation between Wear Rate (Rw) and Hardness, Volume Fraction of Retained Austenite (V_γ) and Mo content

5.2.1 Effect of macro-hardness on wear rate (Rw)

The macro-hardness is the sum of matrix hardness and hardness of eutectic structure. In this section, the effect of macro-hardness on wear rate (Rw) is discussed.

Relationship betweens Rw and macro-hardness by Suga abrasion wear test and Rubber Wheel abrasion wear test are respectively shown in Fig. 5.7 and 5.8. The Rw values decrease in proportion to the macro-hardness without scattering regardless of heat treatment condition and Mo content. The relations are expressed by next equations,

for Suga abrasion wear test,

$$Rw = -4.2 \times 10^{-4} \times HV30 + 0.72 \qquad (R = 0.87) \qquad \text{[Eq. 5.1]}$$

and for Rubber Wheel abrasion wear test,

$$Rw = -1.6 \times 10^{-4} \times HV30 + 0.19 \qquad (R = 0.73) \qquad \text{[Eq. 5.2]}$$

It is clear from above relations that the higher macro-hardness provides better wear resistance. In order to clarify the sensitivity of hardness, the slopes of lines in Fig. 5.7 for Suga abrasion wear test and in Fig. 5.8 for Rubber Wheel abrasion wear test are calculated. The ratio of slopes in Eq. 5.1 and Eq. 5.2 is about 2.6. This means that the hardness affected the Rw 2.6 times more in Suga abrasion wear test than that in Rubber Wheel abrasion wear test

.

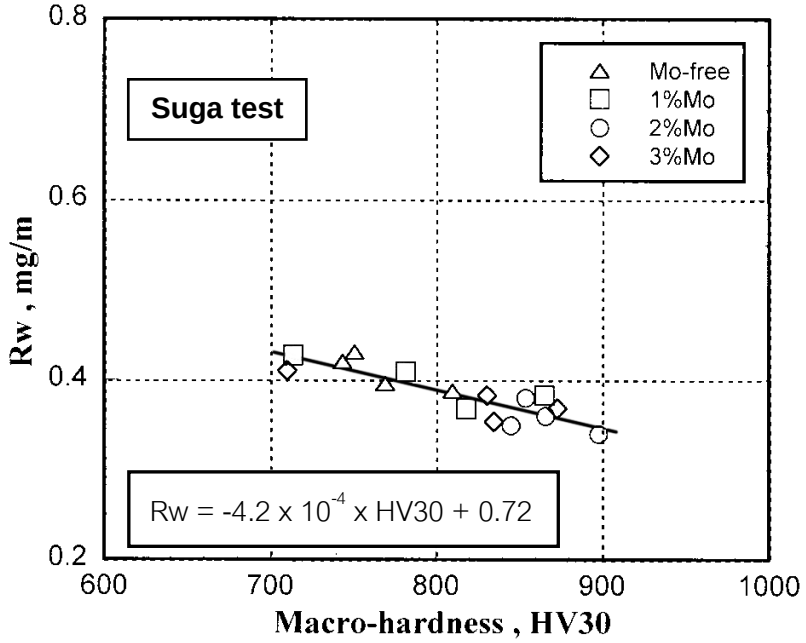

Fig. 5.7 Relationship between wear rate (Rw) and macro-hardness of heat-treated specimens with different Mo content. Suga abrasion wear test (two-body-type) with load 9.8 N (1 kgf).

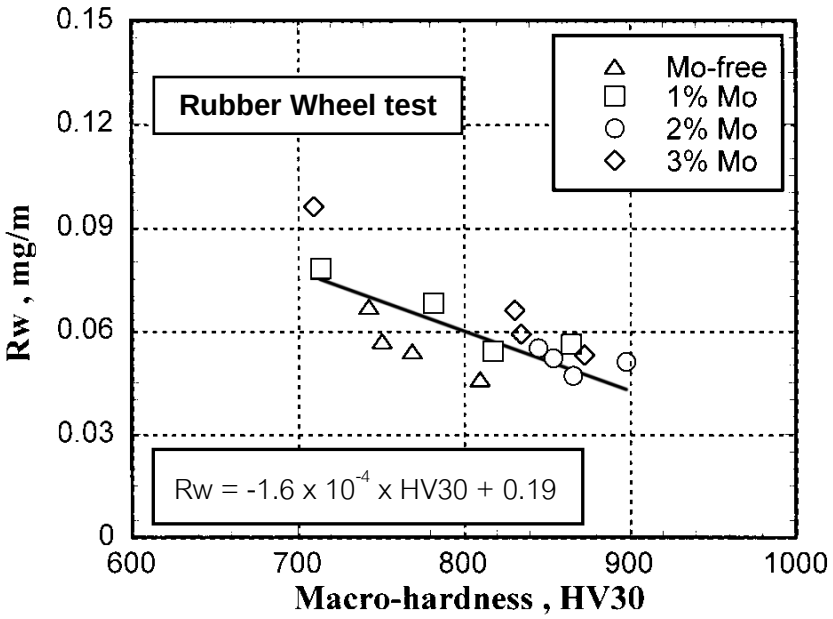

Fig. 5.8 Relationship between wear rate (Rw) and macro-hardness of heat-treated specimens with different Mo content. Rubber Wheel abrasion wear test (three-body-type) with load 85.3 N (8.7 kgf).

From Fig. 5.7 and Fig. 5.8, it can be said that the hardness has strong effect on the Rw and it seems that the Rw decreases clearly as the hardness increases. This could be due to the microstructure. The hardness of heat-treated specimen rises due to an increase in the amount of martensite and precipitated carbides in the matrix. It was reported that the martensite wore by cutting mechanism, and the wear resistance is improved by marginal with increasing the hardness. [37] Under high stress wear condition, the martensite offers high abrasion wear resistance due to the high strength enough to support eutectic carbides and thus, diminishes carbide fracture. In addition, the secondary carbides increase the matrix strength through a dispersion hardening effect, and this also lead to the improvement of the wear resistance.

5.2.2 Effect of volume fraction of retained austenite (V_γ) on wear rate (Rw)

The amount of retained austenite also affects the wear resistance of high Cr cast iron. The relationship between Rw and V_γ is respectively shown in Fig. 5.9 for Suga abrasion wear test and Fig. 5.10 for Rubber Wheel abrasion wear test. Though, the data are scattering a little, Rw decreases gradually to the minimum point and then increases again as V_γ increases. The smallest Rw is obtained at about 10% V_γ in both Suga and Rubber Wheel abrasion wear tests. This suggests that a certain amount of V_γ improves the abrasion wear resistance. This result agrees with the results from the other researches using different wear test methods, pin-on-disc test, which is about 20% V_γ. [45] The decrease in the Rw with raising the V_γ is considered due to the work hardening effect of retained austenite. In the case of very low V_γ value, some pearlite possibly appears there which reduces the wear resistance. In the case of high V_γ value, excessive retained austenite reduces not only the hardness but also work hardening effect. Resultantly, the Rw increases gradually as the V_γ rises.

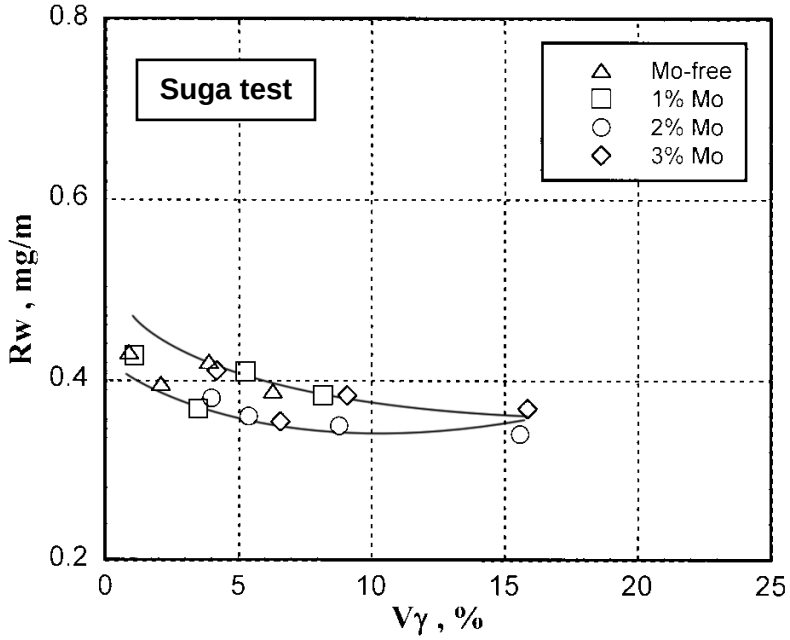

Fig. 5.9 Relationship between wear rate (Rw) and volume fraction of retained austenite (V_γ) of heat-treated specimens with different Mo content. Suga abrasion wear test (two-body-type) with load 9.8 N (1 kgf).

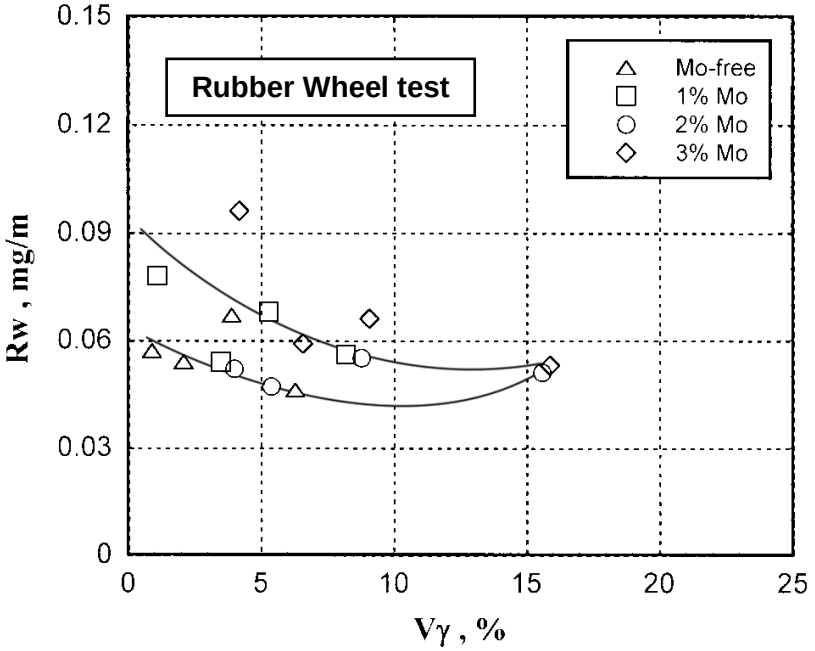

Fig. 5.10 Relationship between wear rate (Rw) and volume fraction of retained austenite (V_γ) of heat-treated specimens with different Mo content. Rubber Wheel abrasion wear test (three-body-type) with load 85.3 N (8.7 kgf).

5.2.3 Effect of Mo content on wear rate (Rw)

From Chapter IV, it became clear that the hardness varies depending on the Mo content. Therefore, the Mo content should affect the Rw. The effect of Mo content on Rw is shown in Fig. 5.11 for Suga abrasion wear test and Fig. 5.12 for Rubber Wheel abrasion wear test.

In the Suga abrasion wear test, the Rw decreases gradually, in other words, the wear resistance increases with an increase in the Mo content (See Fig. A.4 Rw vs. Mo content of H_{Tmax} specimen in appendix). It can explain that Mo increases the hardness of both eutectic carbide and matrix. Under high stress abrasion, the abrasive particle with extremely high hardness cut through both eutectic carbides and matrix. So, an increase of hardness by Mo addition could prevent the crack propagation. As a result, the Rw decreases with raising the hardness as explained in the previous section. [39] Anyway, it can be said that the Mo gives a positive effect on the wear resistance of high Cr cast iron under two-body-type abrasion wear.

In Rubber Wheel abrasion wear test, by contrast, Mo does not show significant effect on Rw. The Rw values in Rubber Wheel abrasion wear test are little scattered and it seems independent on the Mo content (See Fig.A.5 Rw vs. Mo content of H_{Tmax} specimen in appendix). Although Mo raises the macro-hardness, the Rw values are almost same. It is known that the stress concentration on the worn surface in this test is quite low and the hardness of abrasive particle about 1200 HV is smaller than that of eutectic M_7C_3 carbide which is about 1500-1800 HV. [46] Therefore, the matrix regions with lower hardness wore preferentially. From this viewpoint, the matrix hardness could be the major effect on the Rw. The average values of matrix hardness in Table 4.2 are 737 HV30 for Mo-free, 722 HV30 for 1% Mo, 780 HV30 for 2% Mo and 733 HV30 for 3% Mo specimens, respectively. It is found that the matrix hardness is almost the same except for 2% Mo specimen. Therefore, it is not a surprise that the Rw do not change so much by Mo addition.

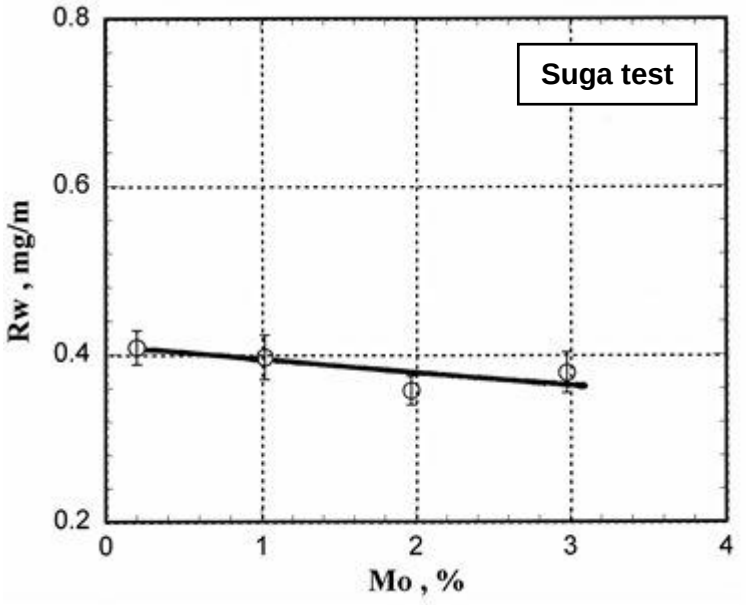

Fig. 5.11 Effect of Mo content on wear rate (Rw). Suga abrasion wear test (two-body-type) with load 9.8 N (1 kgf).

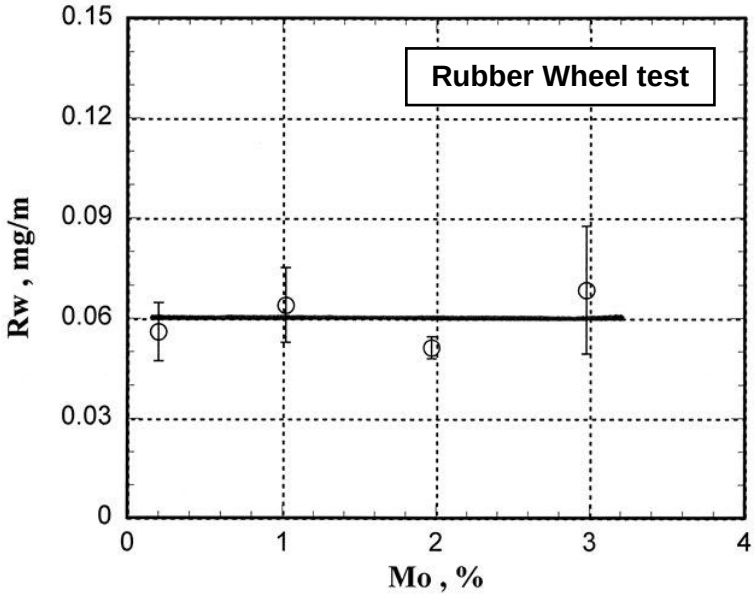

Fig. 5.12 Effect of Mo content on wear rate (Rw). Rubber Wheel abrasion wear test (three-body-type) with load 85.3 N (8.7 kgf).

5.3 Mechanism of Abrasion Wear

In order to comprehend the wear behavior during abrasion wear test, the worn surface of specimens is adopted for surface observation by SEM or FE-SEM and OM.

5.3.1 Suga (Two-body-type) abrasion wear

The worn surfaces of test piece after Suga abrasion wear test were observed by SEM. The SEM photographs are shown in Fig. 5.13. It is clear that the worn surface shows many wear tracks in the same direction of wear test. The worn surface consists of grooving, pitting and scratching with small number of tearing. It is found from the observation that pitting is usually observed in the eutectic region, so the surface of eutectic area is rougher, and the severe wear of grooving are observed in both matrix and eutectic regions. The cross-sectional microstructures perpendicular to wear direction are shown in Fig. 5.14. The surface is quite smooth when observed using OM. This is because the abrasive particles could indent into both of matrix and carbides. However, when observed at higher magnification by FE-SEM, it is found the wear of matrix is more violent than that of eutectic carbide, particularly in the dendrite region where is unprotected by carbides.

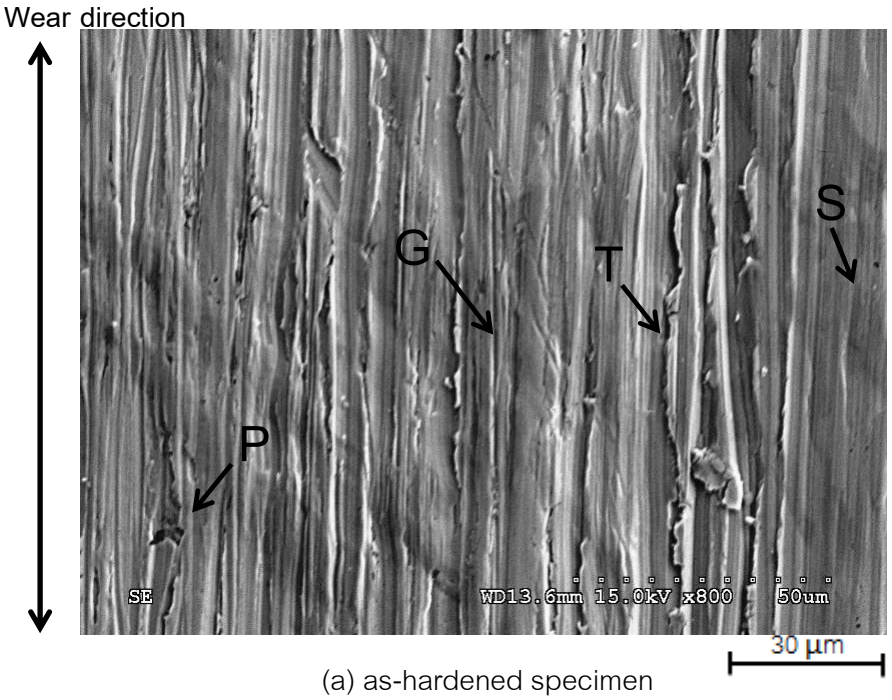

(a) as-hardened specimen

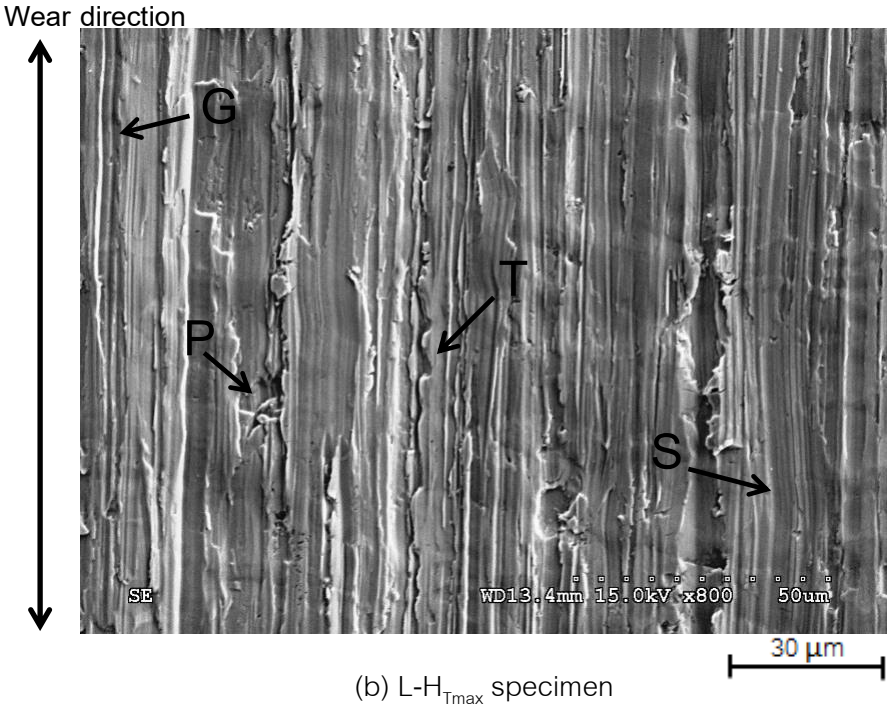

(b) L-H_{Tmax} specimen

Fig. 5.13 SEM microphotograph of worn surface of 26% Cr cast iron containing 1% Mo. Suga abrasion wear test (two-body-type) with load 9.8 N (1 kgf) and at wear distance 192 m.

Note ; G:Grooving, P:Pitting, S:Scratching and T:Tearing.

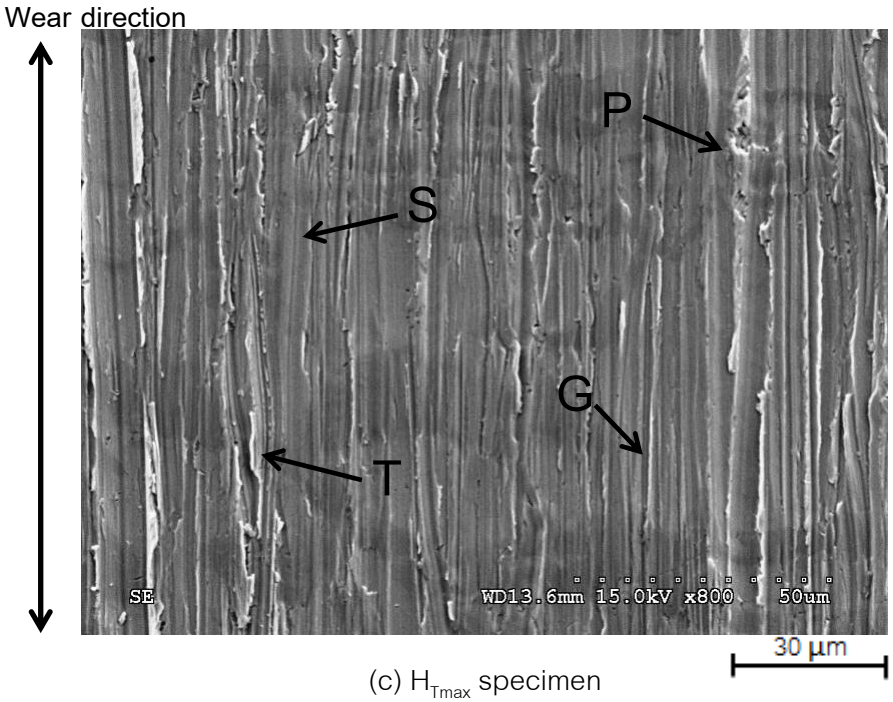

(c) H_{Tmax} specimen

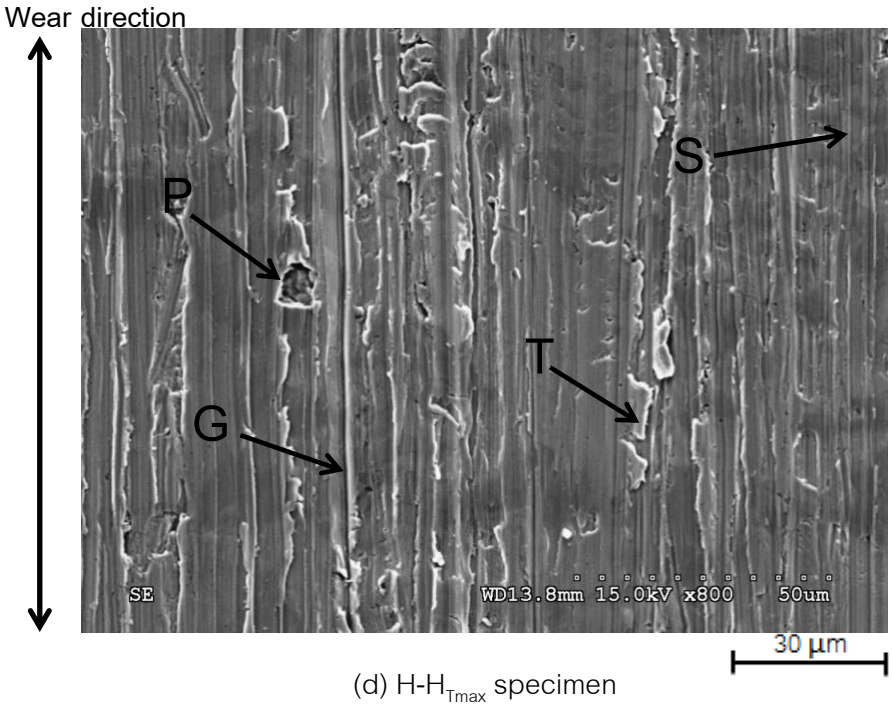

(d) H-H_{Tmax} specimen

Fig. 5.13 SEM microphotograph of worn surface of 26% Cr cast iron containing 1% Mo. Suga abrasion wear test (two-body-type) with load 9.8 N (1 kgf) and at wear distance 192 m.

Note ; G:Grooving, P:Pitting, S:Scratching and T:Tearing.

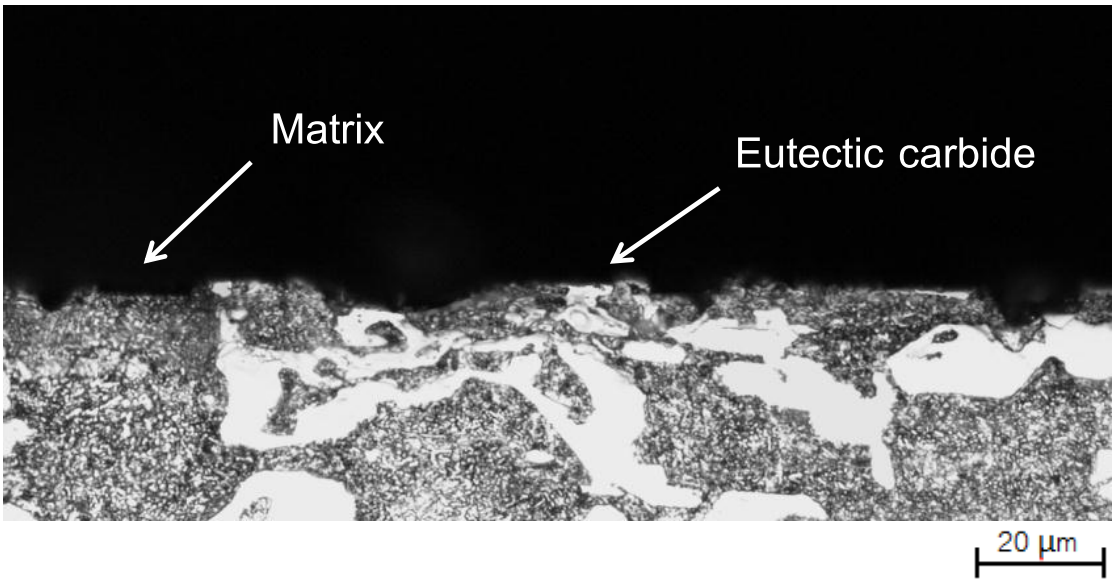

a) by OM

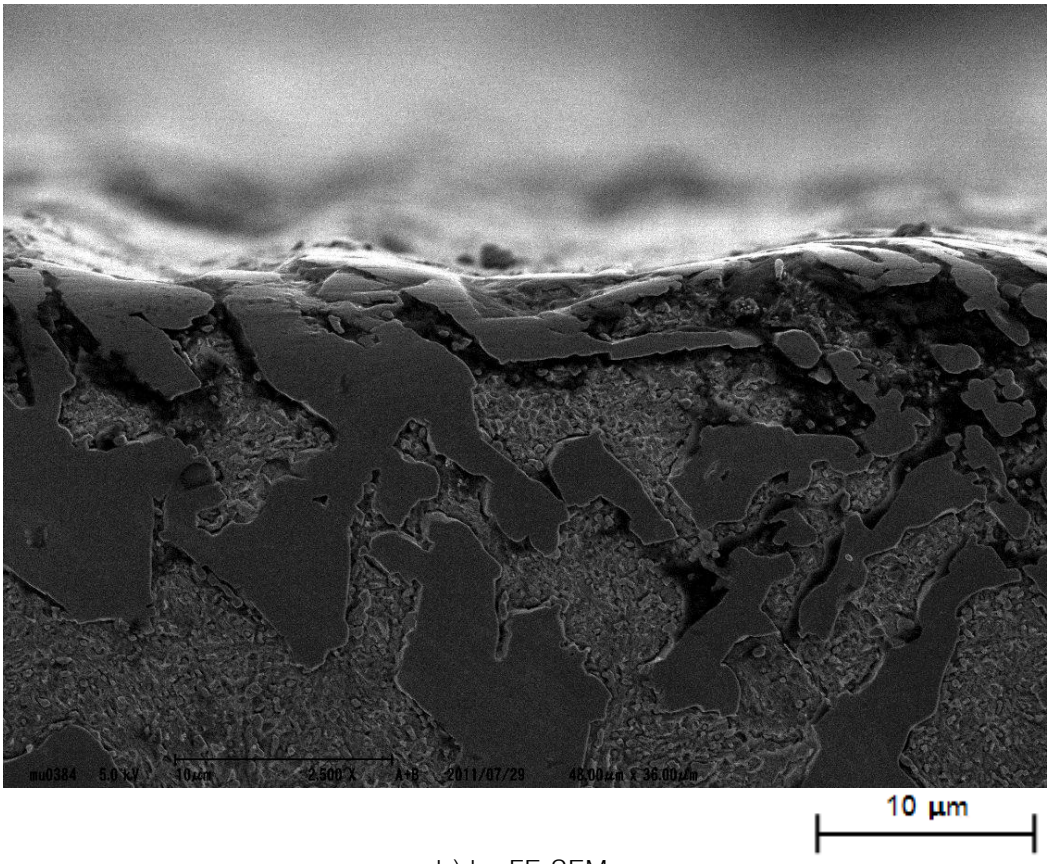

b) by FE-SEM

Fig. 5.14 Cross-sectional microstructures of worn surface by Suga abrasion wear test (two-body-type).

5.3.2 Rubber Wheel (Three-body-type) abrasion wear

Worn surfaces observation of test piece after Rubber Wheel abrasion wear test were carried out and the microphotographs are shown in Fig. 5.15. The lines which wear direction cannot observe. This is because the abrasive particles move freely on the surface of test piece. The worn surface consists of pitting in dendrite area and scratching in the eutectic area. It seems that the matrix has concave surface and was worn preferentially than eutectic carbide. This is confirmed by distribution of Fe and Cr elements on the worn surface of H-H_{Tmax} test piece of 26%Cr-2%Mo cast iron shown by Fig. 5.16. The area of high concentration of Cr is eutectic carbides and that of high concentration of Fe is matrix. It can be said that the removal rate of matrix is not only related to the total wear rate but also the rate of carbide fracture. The matrix removes first followed by the fracture of carbides. The cross-sectional microstructures taken by OM and FE-SEM are shown in Fig. 5.17. The microphotographs prove that the worn surface is in a wave shape and the matrix is worn more than eutectic areas.

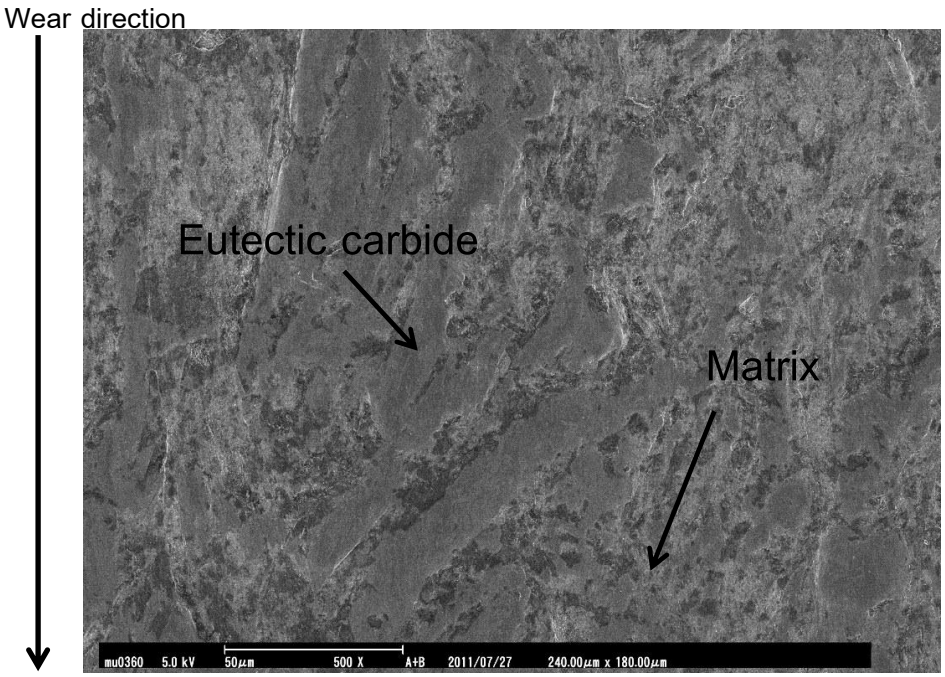

(a) as-hardened specimen

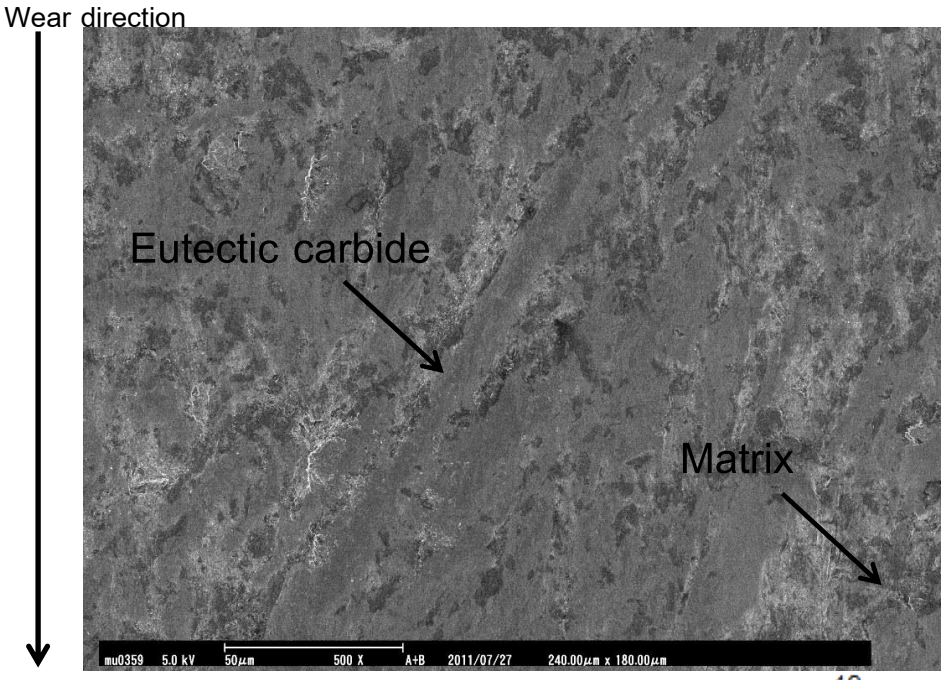

(b) L-H_{Tmax} specimen

Fig. 5.15 FE-SEM microphotograph of worn surface at wear distance 3142 m of 26% Cr cast iron with 2% Mo. Rubber Wheel abrasion wear test (three-body-type) with load 85.3 N (8.7 kgf).

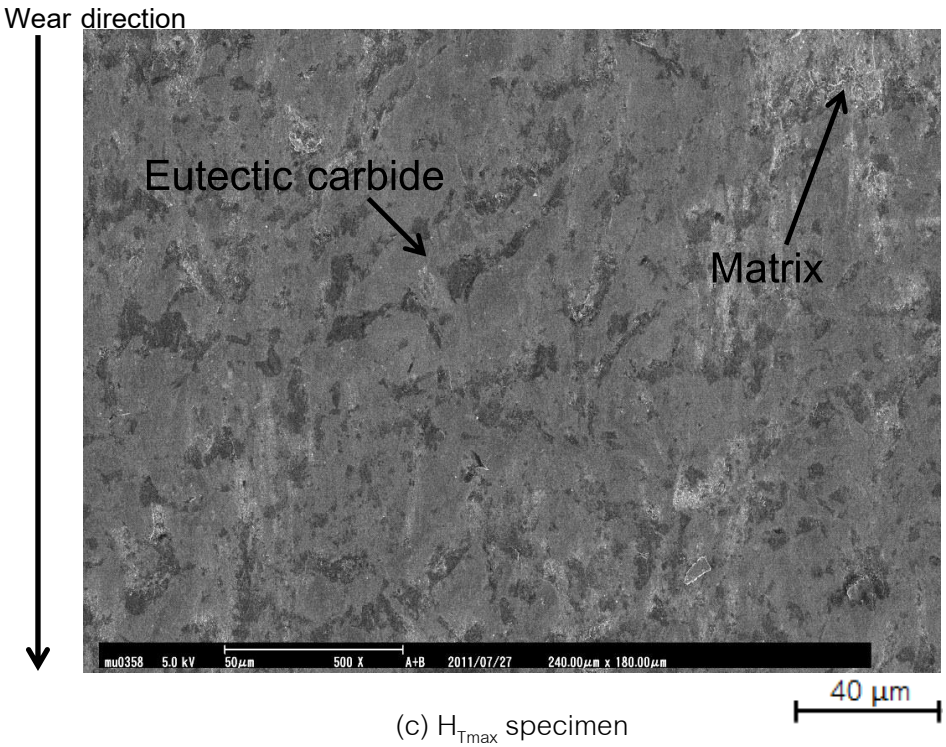

(c) H_{Tmax} specimen

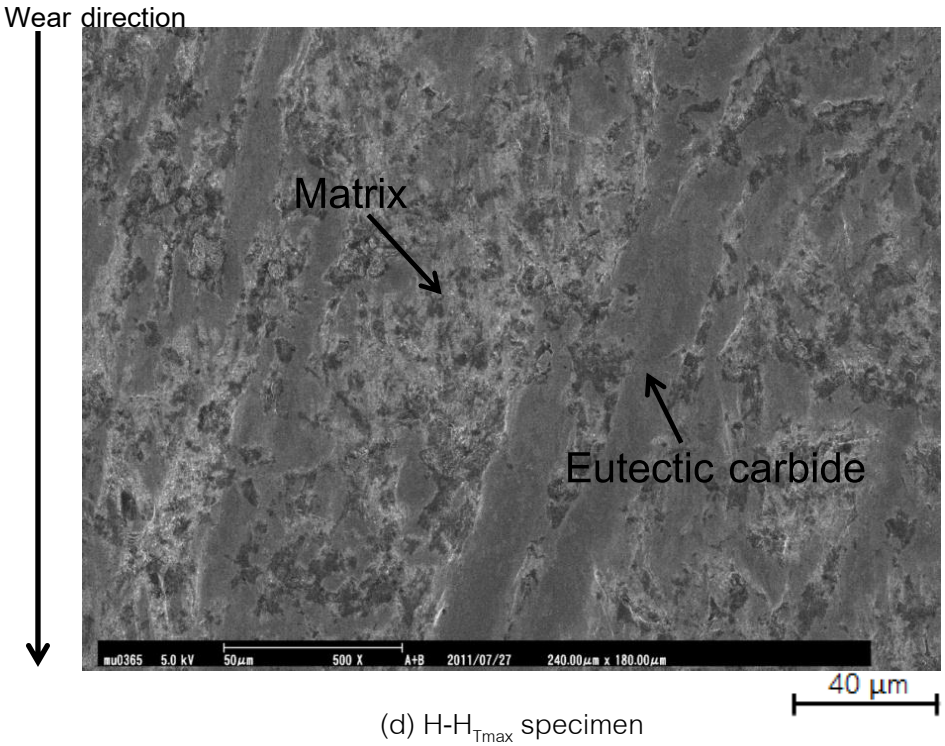

(d) H-H_{Tmax} specimen

Fig. 5.15 FE-SEM microphotograph of worn surface at wear distance 3142 m of 26% Cr cast iron with 2% Mo. Rubber Wheel abrasion wear test (three-body-type) with load 85.3 N (8.7 kgf).

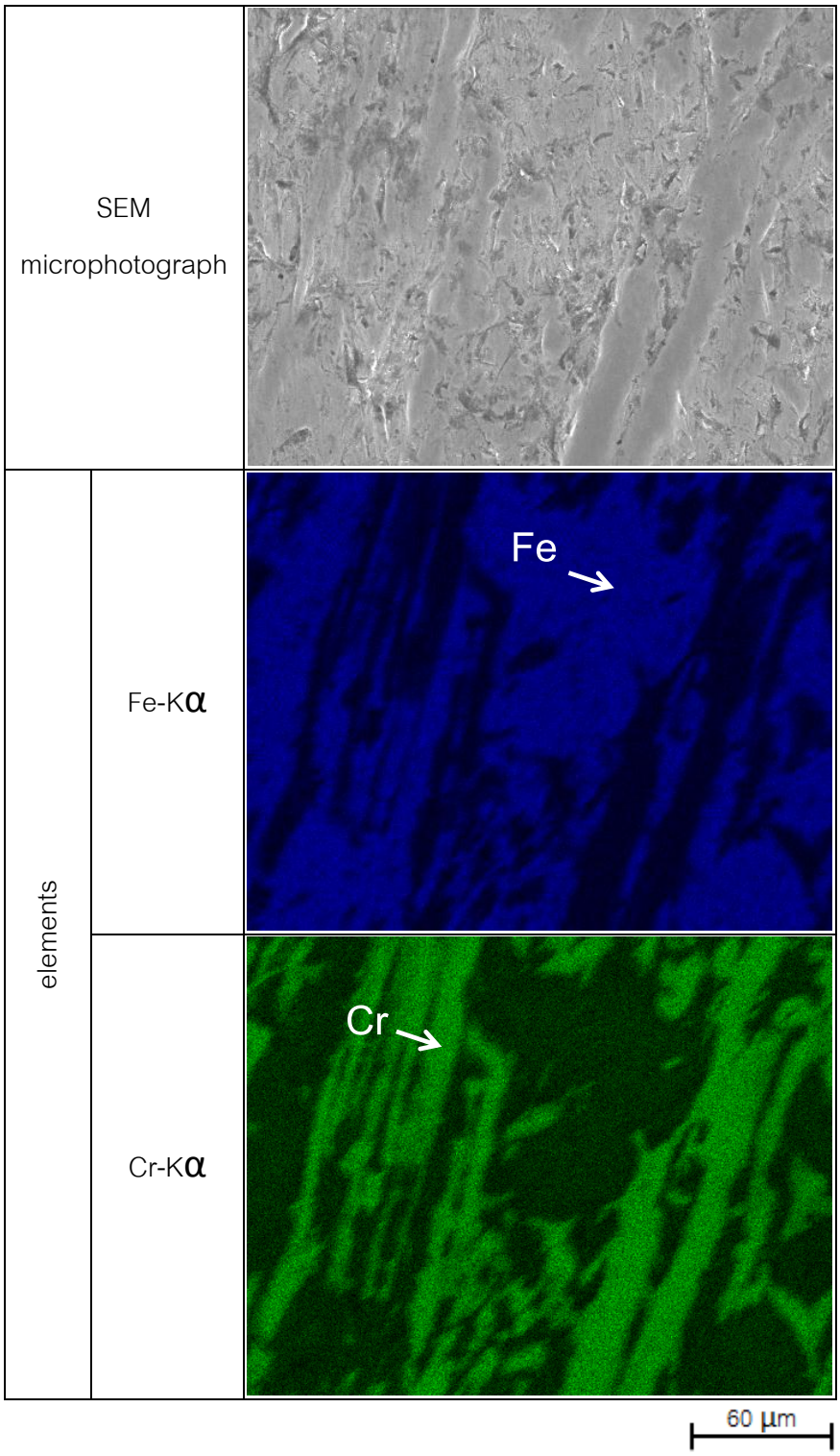

Fig. 5.16 SEM microphotograph and EDS X-ray images of Fe and Cr elements on worn surface of H-H_{Tmax} specimen of 26% Cr cast iron with 2% Mo. Rubber Wheel abrasion wear test (two-body-type) with load 85.3 N (8.7 kgf) and at wear distance 3142 m.

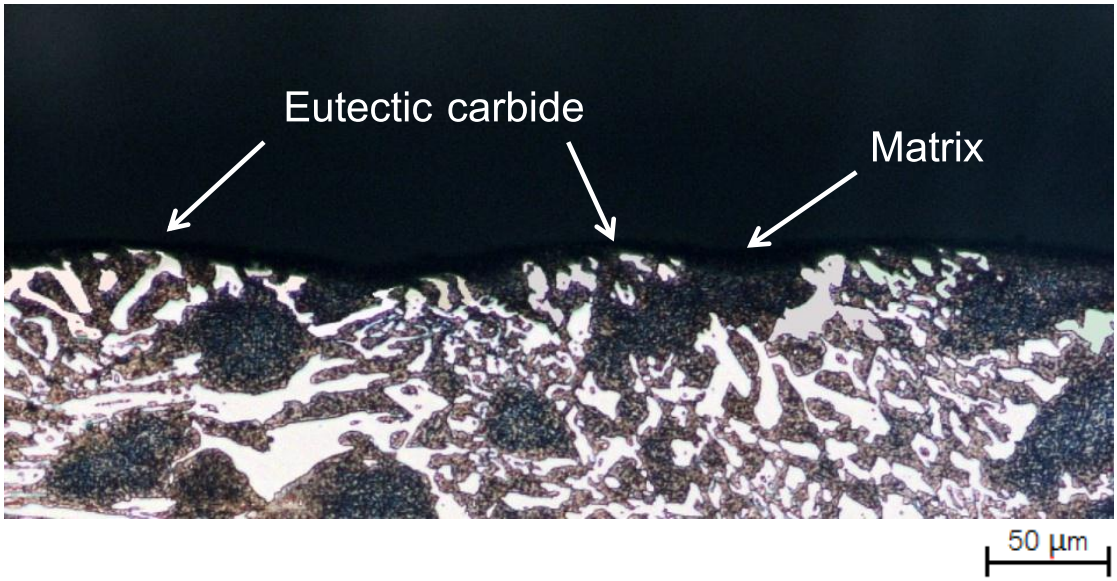

a) by OM

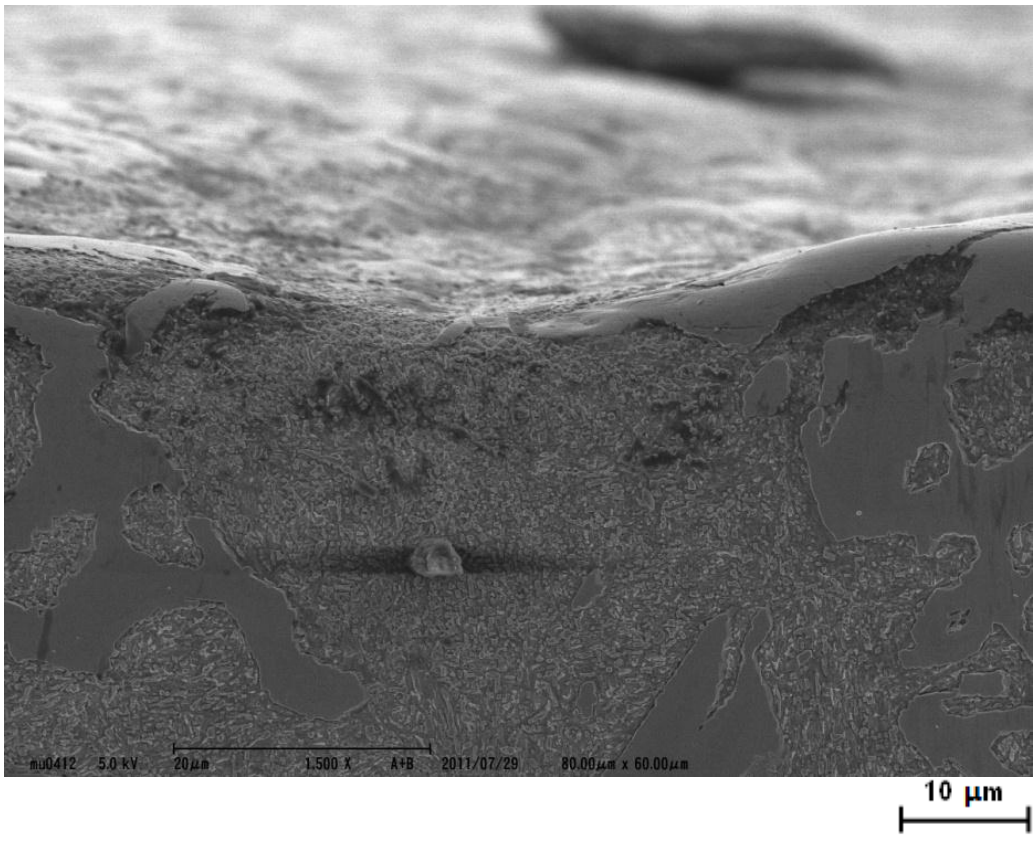

b) by FE-SEM

Fig. 5.17 Cross-sectional microstructures of worn surface by Rubber Wheel abrasion wear test (three-body-type).

5.4 Comparison of Abrasion Wear Resistance between 26% Cr and 16% Cr Cast Irons

It is believed that the macro-hardness of material determines the wear performance, the harder the materials, the more the wear resistance. From the experimental results, it was found that many factors influences on the wear resistance of materials, for example hardness, V_γ, load, microstructure, etc.. Under the same wear condition, the microstructure plays an important role to the wear resistance. In high Cr cast iron, the microstructure varies depending on the chemical composition and heat treatment condition. The wear behavior of 16% Cr cast iron with Mo was reported by the previous study.[18] The results of the investigation are introduced here listing in Table 5.2-5.5. Therefore, it is worth comparing that the wear behaviors of two kinds of high Cr cast irons, 16% or 26% Cr and nil to 3% Mo at under the same wear condition.

The relationship between the hardness and V_γ for 16% and 26% Cr cast irons is shown in Fig. 5.18. It is found that the hardness increases first and then decreases as the V_γ increases. The maximum hardness value is obtained at about 10-15% V_γ. This tells that the hardness is not always independent on the V_γ value.

The effect of Mo content on the micro-hardness is shown in Fig. 5.19. The micro-hardness is varied by Mo content. At the same Mo content, the micro-hardness value between 16% and 26% Cr cast irons are close each other. The maximum micro-hardness is obtained in 2% Mo cast iron.

Table 5.2 Chemical compositions of 16% Cr cast irons. [18]

Specimens	Alloy (mass%)				
	C	Cr	Si	Mn	Mo
Mo-free	2.96	15.93	0.51	0.55	0.22
1% Mo	2.95	16.00	0.50	0.55	1.06
2% Mo	2.97	15.96	0.54	0.59	1.95
3% Mo	2.91	15.91	0.47	0.55	2.98

Table 5.3 Macro-hardness, micro-hardness and volume fraction of retained austenite (V_γ) of heat-treated 16% Cr cast irons varying Mo content. [18]

Specimen		Macro-hardness (HV30)	Micro-hardness (HV0.1)	V_γ , %
Mo content	Heat treatment condition			
Mo-free	As-hardened	822	696	25
	L-H_{Tmax}	755	731	21
	H_{Tmax}	786	764	6
	H-H_{Tmax}	748	727	2
1% Mo	As-hardened	811	722	34
	L-H_{Tmax}	744	728	32
	H_{Tmax}	831	780	5
	H-H_{Tmax}	718	697	2
2% Mo	As-hardened	808	779	29
	L-H_{Tmax}	760	737	27
	H_{Tmax}	849	818	13
	H-H_{Tmax}	838	808	6
3% Mo	As-hardened	824	808	40
	L-H_{Tmax}	762	724	37
	H_{Tmax}	816	764	5
	H-H_{Tmax}	654	545	2

Note ; L-H_{Tmax} : tempered at lower temperature than that at which H_{Tmax} is obtained.

H_{Tmax} : maximum tempered hardness.

H-H_{Tmax} : tempered at higher temperature than that at which H_{Tmax} is obtained.

Table 5.4 Wear rate (Rw) by Suga abrasion wear test (two-body-type) of heat-treated 16% Cr cast irons varying Mo content. Load : 9.8 N(1kgf). [18]

Specimen	Wear rate (Rw) , mg/m			
	As-hardened	L-H_{Tmax}	H_{Tmax}	H-H_{Tmax}
Mo-free	0.45	0.50	0.51	0.52
1% Mo	0.48	0.50	0.45	0.51
2% Mo	0.47	0.49	0.45	0.48
3% Mo	0.44	0.44	0.43	0.56

Table 5.5 Wear rate (Rw) by Rubber Wheel abrasion wear test (three-body-type) of heat-treated 16% Cr cast irons varying Mo content. Load : 85.3 N (8.7 kgf). [18]

Specimen	Wear rate (Rw) , mg/m			
	As-hardened	L-H_{Tmax}	H_{Tmax}	H-H_{Tmax}
Mo-free	0.053	0.066	0.057	0.074
1% Mo	0.047	0.058	0.058	0.078
2% Mo	0.051	0.064	0.049	0.049
3% Mo	0.058	0.071	0.069	0.113

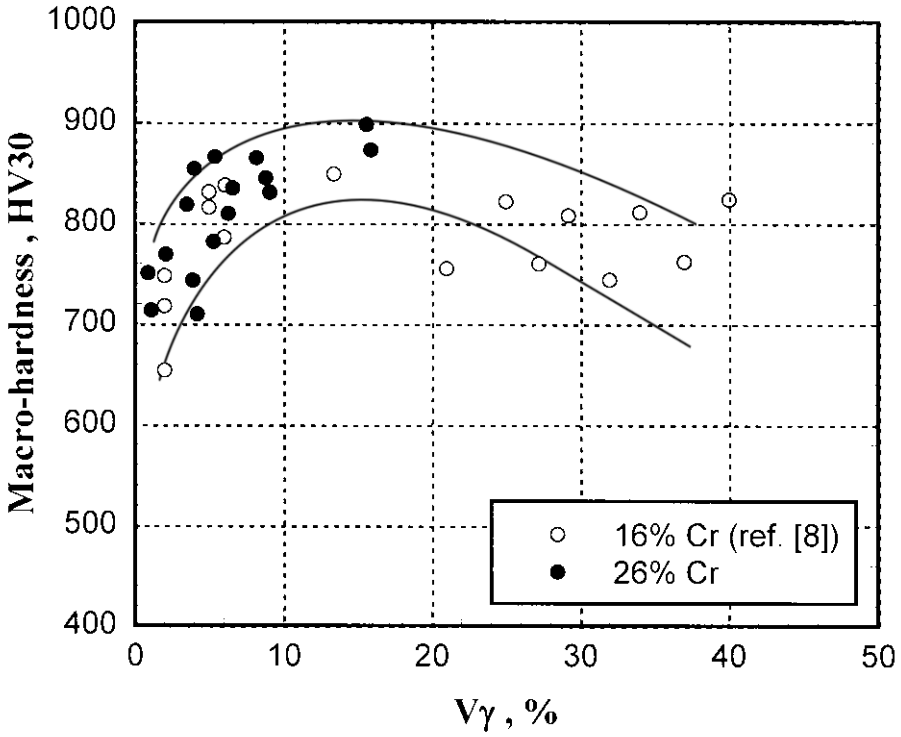

Fig. 5.18 Relationship between macro-hardness and volume fraction of retained austenite (V_γ) of 16% Cr and 26% Cr cast irons with different Mo content

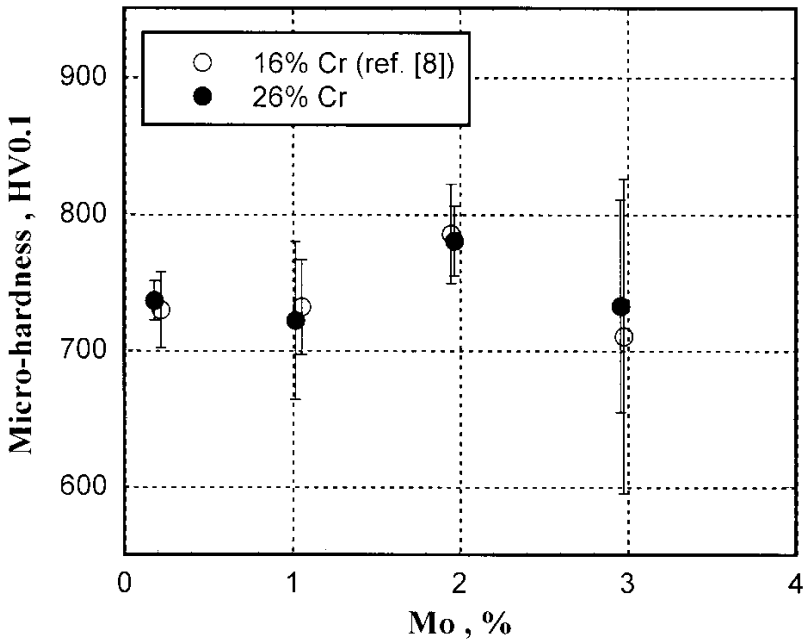

Fig. 5.19 Effect of Mo content on micro-hardness between 16% Cr and 26% Cr cast irons with different Mo content.

5.4.1 Effect of macro-hardness on wear rate (Rw)

Relationship between Rw and hardness of 16% and 26% Cr cast irons by Suga and Rubber Wheel abrasion wear test are shown in Fig. 5.20 and 5.21, respectively. Under high stress condition like Suga abrasion wear test, it is found that the Rw decreases with increasing the hardness in both the 16% and 26% Cr cast irons and the decreasing rate is almost the same. At the same hardness level, the Rw value of 16% Cr cast iron is higher than that of 26% Cr cast iron. That is to say, the wear resistance of 26% Cr cast iron is higher than that of 16% Cr cast iron. This can be explained as followed,

According to Fig. 5.19, the matrix hardness is almost the same between 16% and 26% Cr cast irons at the same Mo content. Therefore, the Rw should be depended by the hardness of eutectic structure and carbide morphology. The carbide morphology of 16% Cr cast iron is thicker and more interconnected in comparison with that of 26% Cr cast iron which is thin or fine and more discontinuous. [3] It was reported that the hardness of carbide also increases with an increase in the Cr content. [16] Therefore, the hardness of eutectic carbide in 26% Cr cast iron must be higher than that in 16% Cr cast iron. When the abrasives with high hardness are used, the harder and tougher carbides must show the better wear resistance when the amount of eutectic carbide is almost same. Another reason is that the small size of carbide may reduce the average free portion among carbides and this leads to improving the protection of the matrix.

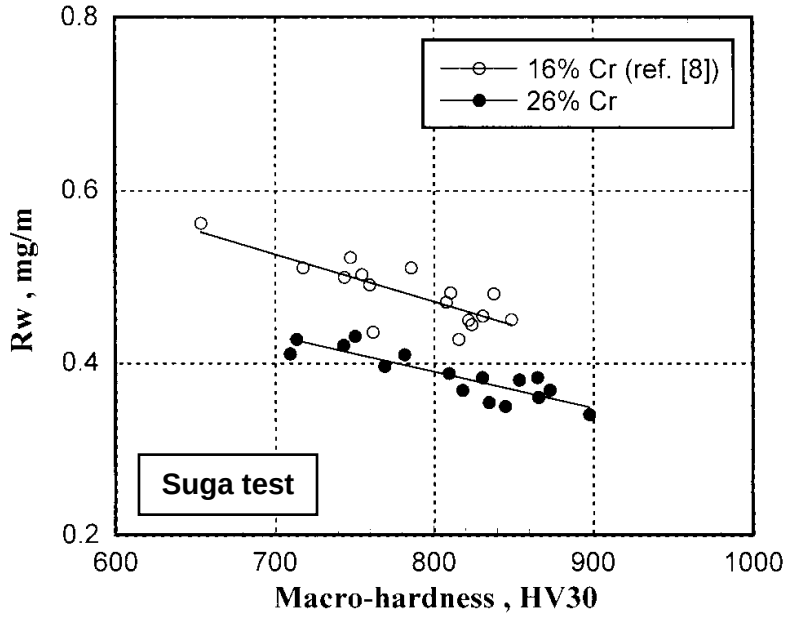

Fig. 5.20 Relationship between wear rate (Rw) and macro-hardness of 16% Cr and 26% Cr cast irons varying Mo content. Suga abrasion wear test (two-body-type) with load 9.8 N (1 kgf).

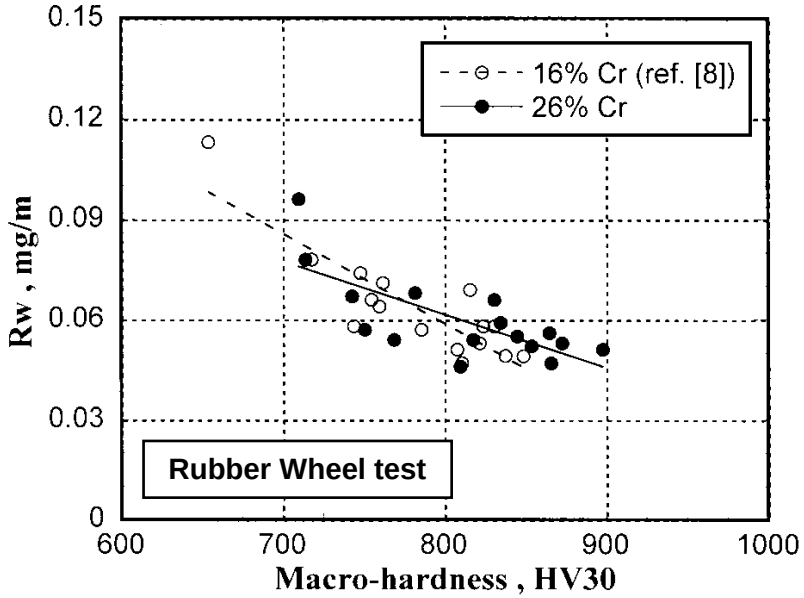

Fig. 5.21 Relationship between wear rate (Rw) and macro-hardness of 16% Cr and 26% Cr cast irons varying Mo content. Rubber Wheel abrasion wear test (three-body-type) with load 85.3 N (8.7 kgf).

The results by Rubber Wheel abrasion wear test is shown by Fig. 5.21. The linear relations between Rw and macro-hardness in both of 16% and 26% Cr cast irons are obtained. The Rw decreases as the hardness increases. Though, the difference of behavior between 16% and 26% Cr cast irons does not appear clearly, the relationship between Rw and macro-hardness seems to be very similar, but the fitting lines drawn by KaleidaGraph software may show a little difference in the inclination. The decreasing rate of Rw in the 16% Cr cast iron is a little greater than that in the 26% Cr cast iron. In the range of low hardness, the Rw value of 16% Cr cast iron is larger than that of 26% Cr cast iron. However, it becomes inversely when the hardness rises over 800 HV30. It is considered that a large amount of retained austenite in the as-hardened state contributes more to the secondary hardening. An increase in the amount of secondary carbides and martensite in the matrix makes the matrix stronger and improves the wear resistance.

To clarify the sensitivity of hardness to the Rw, the slopes of each line in Fig. 5.20 and Fig. 5.21 are considered. In Suga abrasion wear test, the sensitivity of hardness to the Rw is similar between 16% and 26% Cr cast irons. In the Rubber wheel abrasion wear test, on the other hand, the sensitivity of hardness to the Rw of 16% Cr cast iron is about 70% greater than that of 26% Cr cast iron.

Here, it can be concluded that the total hardness or macro-hardness has strong effect on the high stress abrasion test like Suga abrasion wear test. On the other side, the matrix hardness or micro-hardness influences on the Rw in low stress abrasion wear test like Rubber Wheel abrasion wear test.

5.4.2 Effect of volume fraction of retained austenite (V_γ) on wear rate (Rw)

From the discussions concerning the effect of hardness on the Rw, it appears that the matrix structure provides a mechanical support to the carbides. This is because the matrix strength is related to the degree of protection to the abrasives given by the carbides. If the carbides protect the matrix from abrasive particles, the matrix works only to provide the mechanical support. On the other hand, if the matrix is not protected and preferentially removed by abrasion process, the carbides may spall and be fractured. Therefore, it could be said that the wear resistance of the matrix will control the wear rate of carbides and the poor wear resistance or unsupporting matrix will bring about the fracture of carbide. In this section, the effect of retained austenite on the Rw is clarified, and here, the sensitivity of the Rw received from the V_γ in Suga and Rubber Wheel abrasion wear tests were highlighted in Fig. 5.22 and 5.23, respectively. It is clear from both figures that the Rw is influenced greatly by the V_γ.

As for the results of Suga abrasion wear test shown in Fig. 5.22, it is found that the Rw decreases as the V_γ increases up to 15% for 16% Cr cast iron and 10% for 26% Cr cast iron. Overall in the V_γ value, the 26% Cr cast iron shows higher wear resistance than that of 16% Cr cast iron regardless of Mo content. Over 15% V_γ, the Rw gradually increases. This suggests that it is difficult to explain the Rw by the V_γ values only. Another reason is that the eutectic carbide in the 26% Cr cast iron is harder than that in the 16% Cr cast iron, and the morphology of eutectic carbide is quite different between both cast irons. [1,2,13] As mentioned earlier in Suga abrasion wear test, the harmony of both the matrix and eutectic carbides must give a strong effect on the wear rate (Rw), which is in turn the wear performance.

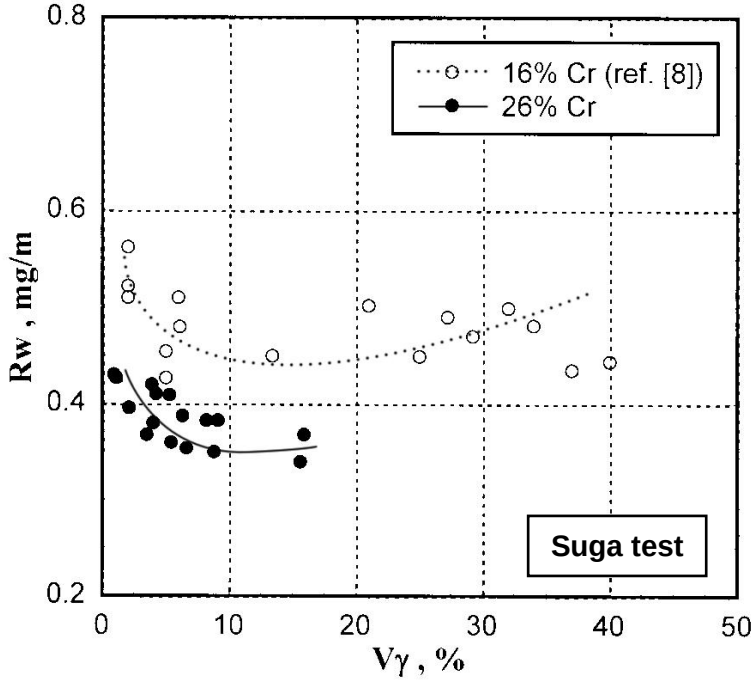

Fig. 5.22 Relationship between wear rate (Rw) and volume fraction of retained austenite (V_γ) of 16% Cr and 26% Cr cast irons varying Mo content. Suga abrasion wear test (two-body-type) with load 9.8 N (1 kgf).

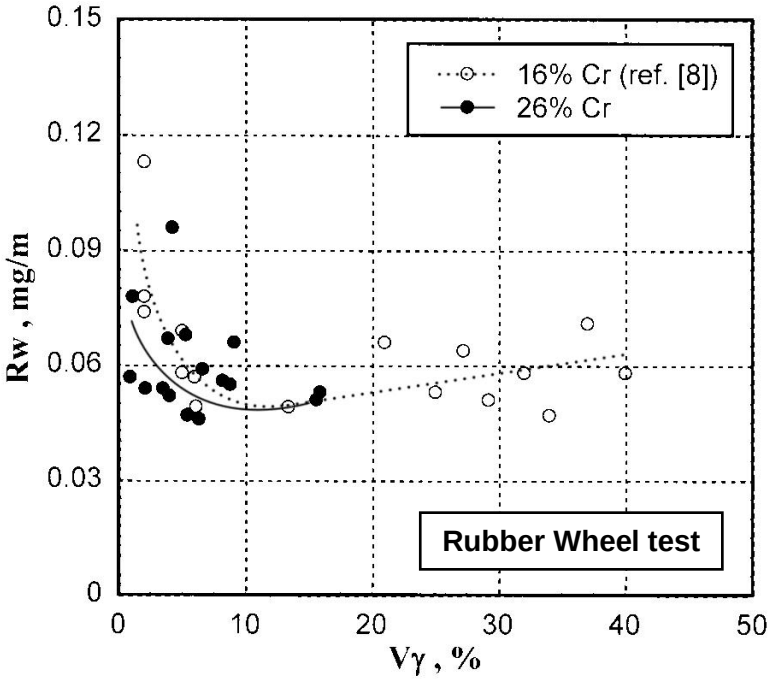

Fig. 5.23 Relationship between wear rate (Rw) and volume fraction of retained austenite (V_γ) of 16% Cr and 26% Cr cast irons varying Mo content. Rubber Wheel abrasion wear test (three-body-type) with load 85.3 N (8.7 kgf).

As for the results of Rubber Wheel abrasion wear test shown in Fig. 5.23, the minimum value of the Rw is obtained near 10% V_γ in both of 16% and 26% Cr cast irons. [8] However, the difference in the Rw between 16% and 26% Cr cast irons is small or looks rather little under the same Rw values less than 20% V_γ. It is also found that the Rw is almost the same at over 10% V_γ. In this case, the amount of retained austenite which determines the matrix hardness does influence on the Rw. The major effect could be due to a much more formation of strain induced martensite. At high V_γ value, however, the effect of work hardening is small because of more stable austenite. In the cases less than 10% V_γ, the Rw of the 16% Cr cast iron is larger than that in the 26% Cr cast iron. The difference is likely to be involved with higher grade of secondary hardening.

5.4.3 Effect of Mo content on wear rate (Rw)

From the wear test results, it was clarified that Mo influences on the hardness and the amount of retained austenite of the cast iron. Therefore, Mo content should affect the Rw. The effect of Mo content on the Rw in Suga and Rubber Wheel abrasion wear tests of 16% and 26% Cr cast irons are shown in Fig. 5.24 and 5.25, respectively.

In Fig. 5.24 for Suga abrasion wear test, the Rw decreases gradually with an increase in the Mo content (See Fig. A.6 Rw vs. Mo content of H_{Tmax} specimen in appendix). This can be explained that Mo retards the pearlite transformation and contributes to improve the hardness of both the eutectic carbide and matrix. At higher Mo content, the Mo_2C carbides precipitate and they increase the wear resistance. It is also found that the decreasing rate of the Rw by an increase in Mo content is very similar between 16% and 26% Cr cast irons. At the same Mo content, the Rw of 26% Cr cast iron is much smaller than that of 16% Cr cast iron.

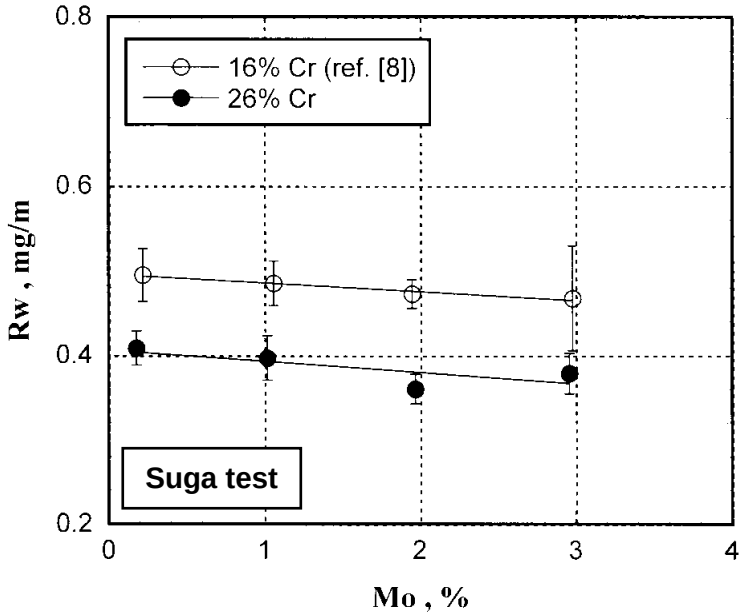

Fig. 5.24 Effect of Mo content on wear rate (Rw) in 16% Cr and 26% Cr cast irons varying Mo content. Suga abrasion wear test (two-body-type) with load 9.8 N (1 kgf).

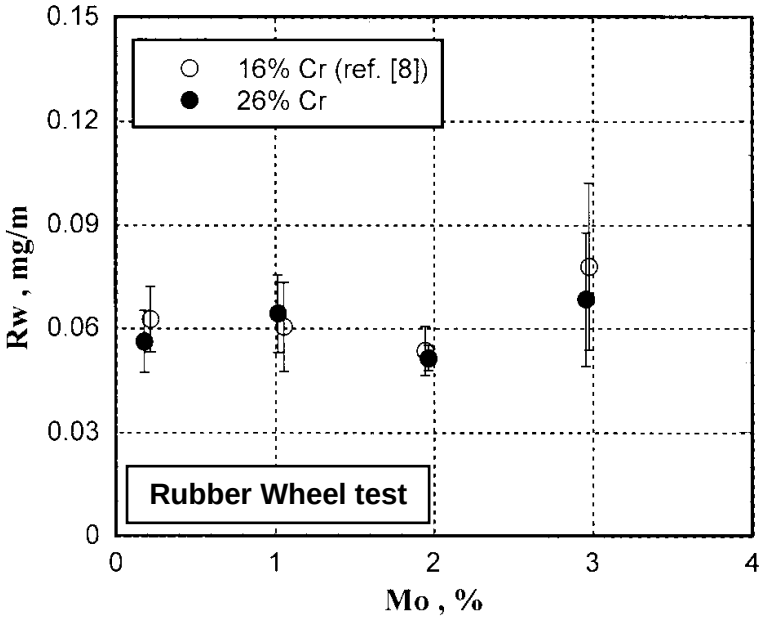

Fig. 5.25 Effect of Mo content on wear rate (Rw) in 16% Cr and 26% Cr cast irons varying Mo content. Rubber Wheel abrasion wear test (three-body-type) with load 85.3 N (8.7 kgf).

In the case of Rubber Wheel abrasion wear test shown in Fig. 5.25, the relation of Rw vs. Mo content is not clear (See Fig. A.7 Rw vs. Mo content of H_{Tmax} specimen in appendix). As mentioned before, the matrix hardness plays an important role on the Rw in this test. It was reported that the solubility limit of Mo in austenite is about 0.5%. [46] At high Mo content, most of Mo is consumed to form the eutectic M_7C_3 and/or M_2C carbides. So, an increase in the Mo content did not show significant effect on the difference in the micro-hardness as shown in Fig. 5.19. When the relation is compared between 16% and 26% Cr cast irons, the Rw of 26% Cr cast iron seems to be a little lower than that in 16% Cr cast iron except for 1% Mo cast iron. It can be explained from the viewpoint of partition coefficient that the Mo concentration in the matrix of 26% Cr cast iron is greater than that of 16% Cr cast iron. [47] From this viewpoint, therefore, the special secondary carbides of M_2C or M_6C could precipitate more in the matrix and they improved the matrix strength. As a result, the Rw of 26% Cr cast iron is smaller than that of 16% Cr cast iron, in turn, the wear resistance or wear performance of 26% Cr cast iron is better than that of 16% Cr cast iron.

CHAPTER VI
CONCLUSIONS

Abrasion wear behavior of heat-treated hypoeutectic 26% Cr cast irons without and with Mo was investigated. After annealing, the specimens were hardened from 1323 K (As-H) and tempered at three levels of temperatures, a temperature giving the maximum hardness (H_{Tmax}), and lower and higher temperatures than the H_{Tmax} temperature (L-H_{Tmax}, H-H_{Tmax}). The effects of hardness, volume fraction of retained austenite (V_γ), heat treatment condition, Mo content and matrix structure on the wear behavior were clarified. The following conclusions have been drawn from the experimental results and discussions.

6.1 Behavior of hardness according to heat treatment

6.1.1 In as-cast state, the hardness decreased up to 1% Mo but it decreased slightly when Mo content increased over 1%.

6.1.2 In as-hardened state, the hardness increased gradually with an increase in Mo content.

6.1.3 In tempered state, the hardness showed an evident secondary hardening and a peak of hardness (H_{Tmax}) was obtained. It is due to the precipitation of secondary carbides and the transformation of destabilized retained austenite into martensite during cooling.

6.2 Behavior of volume fraction of retained austenite (V_γ) according to heat treatment

6.2.1 In as-cast state, the V_γ increased up to 1% Mo but it increased very slightly when Mo content is increased more than 1%.

6.2.2 In as-hardened state, the V_γ was more when Mo was increased.

6.2.3 In tempered state, the V_γ value decreased as the tempering temperature increased.

6.3 Effect of Mo content on hardness and volume fraction of retained austenite (V_γ)

6.3.1 In as-hardned state, the hardness varied with Mo content. The hardness and V_γ increased with an increase in Mo content.

6.3.2 In tempered state, the hardness and V_γ were high in Mo-bearing specimens than Mo-free specimen.

6.4 Abrasion wear

6.4.1 The results of two-body-type abrasion wear tested by Suga abrasion wear test

a) Linear relationship between wear loss and wear distance was obtained.

b) When wear rate (Rw) was expressed by a slope of each straight line, the largest wear resistance or smallest Rw was obtained in the as-hardened specimens for both Mo-free and 2% Mo cast irons and in the specimens with H_{Tmax} for both 1% and 3% Mo cast irons. The smallest wear resistance was obtained in the specimen with H-H_{Tmax} regardless of Mo content.

c) The Rw decreased to the lowest value and then increased as the V_γ increased. The smallest Rw appeared in the specimen with 10% V_γ.

d) The Rw decreased with increasing macro-hardness and Mo content .

6.4.2 The results of three-body-type abrasion wear tested by Rubber Wheel abrasion wear test

a) A linear relationship was obtained between wear loss and wear distance.

b) The largest wear resistance or the smallest Rw was obtained in as-hardened specimens for both Mo-free and 3% Mo cast irons, and in the specimens with H_{Tmax} for both 1% and 2% Mo cast irons. The smallest wear resistance was obtained in the specimens with L-H_{Tmax} for both Mo-free and 2% Mo cast irons and in the specimens with H-H_{Tmax} for both 1% and 3% Mo cast irons.

c) The Rw decreased as the macro-hardness increased, and the smallest Rw appeared in the specimen with 10% V_γ, regardless of Mo content.

d) The Rw decreased with increasing macro-hardness, and Rw was independent on Mo content.

6.4.3 Behavior of abrasion wear

a) Two-body-type abrasion wear by Suga abrasion wear test was approximately eight times more sevear than three-body-type abrasion wear by Rubber Wheel abrasion wear test.

b) The Rw increased in propotion to the applied load.

c) The sensitivity of hardness to the Rw is same between 16% and 26% Cr cast irons in Suga abrasion wear test. In Rubber Wheel abrasion wear test, however, the sensitivity of hardness to the Rw of 16% Cr cast iron was about 70% larger than that of 26% Cr cast iron.

d) The macro-hardness showed a strong effect on the Rw in Suga abrasion wear test and the Rw decreased with an increase in macro-hardness. On the other hand, the micro-hardness had a major effect on the Rw in Rubber Wheel abrasion wear test.

e) Because of harder and tougher chromium carbides in 26% Cr cast irons, 26% Cr cast iron showed better wear resistance than the 16% Cr cast iron does.

f) Worn surface consisted of grooving, pitting, scratching and tearing. The matrix was preferably worn much more than the eutectic carbide.

REFERENCES

[1] Laird, G., Gundlach, R., and Rohring, K. Abrasion-Resistance Cast Iron Handbook. USA: American Foundry Society, 2000.

[2] Matsubara, Y., Ogi, K., and Matsuda, K. Eutectic solidification of high chromium cast iron-eutectic structures and their quantitative analysis. AFS Transaction 89 (1981): 183-196.

[3] Inthidech, S., Sricharoenchai, P., and Matsubara, Y. Effect of alloying element on heat treatment behavior of hypoeutectic high chromium cast iron. Materials Transactions 47 (2006): 72-81.

[4] Sare, I.R., and Arnold, B.K. The effect of heat treatment on gouging abrasion resistance of alloy white cast iron. Metallurgical and Materials Transaction A 26A (1995): 357-370.

[5] Kim, C. X-Ray method of measuring retained austenite in heat treat white cast irons. Journal of Heat Treating 1 (1979): 43-51.

[6] Sudsakorn Inthidech. Heat Treatment Behavior of High Chromium Cast Iron for Abrasive Wear Resistance. Doctoral dissertation, Metallurgical Engineering, Faculty of Engineering, Chulalongkorn University, 2005.

[7] Inthidech, S., Aungsupaitoon, P., Sricharoenchai, P., and Matsubara, Y. Two-body-type abrasion wear behavior in hypoeutectic 16 % Cr cast irons with Mo. International Journal of Cast Metal Research 23 (2010): 164-172.

[8] Phasit Aungsupaitoon. Abrasion Wear Behavior of Hypoeutectic 16 Mass% Chromium Cast Iron Containing Molybdenum. Master's Thesis, Metallurgical Engineering, Faculty of Engineering, Chulalongkorn University, 2008.

[9] Tabrett, C.P., Sare, I.R., and Ghomashchi, M.R. Microstructure-property relation in high chromium white iron alloys. International Materials Reviews 41 (1996): 59-82.

[10] Davis, J.R. Metallurgy and Properties of High-Alloy White Irons. Cast Irons, pp. 107-122. Ohio: ASM International, 1996.

[11] Ikeda, M., et al. Effect of molybdenum addition on solidification structure mechanical properties and wear resistivity of high chromium cast irons. ISIJ International 32 (1992): 1157-1162.

[12] Thong, C.P., Suzuki, T., and Umeda, T. Eutectic solidification of high-chromium cast irons. Physical Metallurgy of Cast Iron IV (1989): 403-410.

[13] Powell, G.L.F. Morphology of eutectic M_3C and M_7C_3 in white iron castings. Metals Forum 3 (1980): 37-46.

[14] Dogan, Ö.N., Hawk, J.A., and Laird II, G. Solidification structure and abrasion resistance of high chromium white irons. Metallurgical and Materials Transactions A 28A (1997): 1315-1328.

[15] Dogan, Ö.N. Effect of chemical composition and superheat on macrostructure of high Cr white iron castings. Abrasion 2005: An International Conference on Abrasion Wear Resistant Alloyed White Cast Iron For Rolling and Pulverizing Mills, Sao Paulo, Brazil, Aug. 14-17, 2005, 179-188. Sao Paulo : Escola Politecnica da USP, 2005.

[16] Maratray, F., and Usseglio-Nanot, R. Factors affecting the structure of chromium and chromium-molybdenum white irons. Climax Molybdenum S.A. (1970): 10.

[17] Laird II, G. Microstructure of Ni-hard I, Ni-hard IV and high-Cr white cast irons. AFS Transactions 99 (1991): 339-357.

[18] Chung, R.J., et al. Effects of titanium addition on microstructure and wear resistance of hypereutectic high chromium cast iron Fe–25wt.%Cr–4wt.%C. Wear 267 (2009): 356-361.

[19] He-Xing, C., Zhe-Chuan, C., Jin-Cai, L., and Huai-Tao, L. Effect of niobium on wear resistance of 15%Cr white cast iron. Wear 166 (1993): 197-201.

[20] Tylczak, J.H., and Oregon, A. Abrasive wear. ASM Handbook 18 (1992): 337-351.

[21] Chattopadhyay, R. Abrasion. Surface Wear: Analysis, Treatment, and revention, pp. 72-79. Ohio: ASM International, 2001.

[22] Trope, W.R., and Chicco, B. The Fe-rich corner of the metastable C-Cr-Fe liquidus surface. Metallurgical Transactions A 16A (1981): 11-19.

[23] Dupin, P., Saverna, J., and Schissler, J.M. A structural study of chromium white cast iron. AFS Trans 90 (1982): 711-718.

[24] Bedolla-Jacudine, A. Microstructure of vanadium-, niobium,-and titanium-alloyed high-chromium white cast irons. International Journal of Cast Metals Research 13 (2001): 343-361.

[25] Rickard, J. Some experiments concerning the as-cast grain size in 30% chromium cast irons. BCIRA Journal 8 (1960): 200-216.

[26] Powell, G.L.F., Carlson, R.A., and Randle, V. The morphology and microtexture of M_7C_3 in Fe-Cr-C and Fe-Cr-C-Si alloys of near eutectic composition. Journal of Materials Science 29 (1994): 4889-4896.

[27] Laird, G., and Powell, G.L.F. Solidification and solid-state transformation mechanisms in Si alloyed high-chromium white cast irons. Metallurgical Transactions A 24A (1993): 981-988.

[28] Matsubara, Y., Ogi, K., and Matsuda, K. Influence of alloying elements on the eutectic structures of high chromium cast iron. Journal of the Japan Foundrymen's Society (IMONO) 51 (1979): 545-550.

[29] Tang, X.H., et al. Variations in microstructure of high chromium cast irons and resultant changes in resistance to wear, corrosion and corrosive wear. Wear 267 (2009): 116-121.

[30] Liang, G.Y., and Su, J.Y. The effect of rare earth elements on the growth of eutectic carbides in white cast irons containing chromium. Cast Metals 4 (1991): 83-88.

[31] Shen, J., and Zhou, Q.D. Solidification behavior of boron-bearing high-chromium cast iron and the modification mechanism of silicon. Cast Metals (1988): 79-85.

[32] Pearce, J.T.H. Structure and wear performance of abrasion resistant chromium cast irons. AFS Transactions 92 (1984): 599-622.

[33] Gunldlach, R.B., and Doane, D.V. Alloy cast irons. ASM Handbook 1 (1990): 222-268.

[34] Sare, I.R., and Arnold, B.K. The influence of heat treatment on the high-stress abrasion resistance and fracture toughness of alloy white cast irons. Metallurgical Transactions A 26A (1995): 1785-1793.

[35] Inthidech, S., et al. Behavior of hardness and retained austenite in heat treatment of high chromium cast iron for abrasive wear resistance. AFS Transaction (2004): 899-910.

[36] Sare, I.R., and Arnold, B.K. The influence of heat treatment on the high-stress abrasion resistance and fracture toughness of alloy white cast irons. Metallurgical Transactions A 26A (1995): 1785-1793.

[37] Powell, G.L.F., and Bee, J.V. Secondary carbide precipitate in an 18wt%Cr-1wt%Mo white iron. Journal of Materials Science 31 (1996): 707-711.

[38] Maratray, F., and Poulalion, A. Austenite retention in high-chromium white iron. AFS Transactions 90 (1982): 795-804.

[39] Stachowiak, G.W, and Batchelor, A.W. Engineering Tribology. USA: Elsevier, 2005.

[40] Zum Gahr, K., and Doane, D.V. Optimizing fracture toughness and abrasion resistance in white cast irons. Metallurgical Transactions A 11A (1980): 613-620.

[41] Watson, J.D., Mutton, P.J., and Share, I.R. Abrasive wear of white cast iron. Metal forum 3 (1980): 74-88.

[42] Radulovic, M., Fiset, M., Peev, K., and Tamovic, M. The influence of vanadium on fracture toughness and abrasion resistance in high chromium white cast irons. Journal of Materials Science 29 (1994): 5085-5094.

[43] Albertin, E., and Sinatora, A. Effect of carbide fraction and matrix microstructure on the wear of cast iron balls tested in a laboratory ball mill. Wear 250 (2001): 492-501.

[44] Share, I.R. Abrasion resistance and fracture toughness of white cast irons. Metals technology 6 (1979): 412-419.

[45] Blickensderfer, R., and Laird, G. A pin-on-drum abrasive wear test and comparison with other pin test. Journal of testing and evaluation 16 (1988): 516-526.

[46] Yamamoto, K., Sasaguri, N., and Matsubara, Y. Influence of alloying element on high temperature hardness of M_7C_3 carbide in high chromium white iron. Abrasion 2011: An International Conference on Abrasion Wear Resistant Alloyed White Cast Iron For Rolling and Pulverizing Mills, Liege, Belgium, Aug. 22-23, 2011, 201-209. Liege : Rue Hayette, 2011.

[47] Ono, Y., Murai, N., and Ogi, K. Partition coefficients of alloying elements to primary austenite and eutectic phases of chromium irons for rolls. ISIJ International 32 (1992): 1150-1156.

APPENDIX

Characterization of Molybdenum Carbide

In 2% and 3% Mo specimens, it was found the morphology of eutectic carbide that could be molybdenum carbide in the observation by OM and SEM. As shown in Fig. A.1-A.3, the distribution of alloy taken by EDS-SEM show that this carbide has very high concentration of Mo, so, it could be eutectic carbide of molybdenum carbide and considered to be Mo_2C carbide

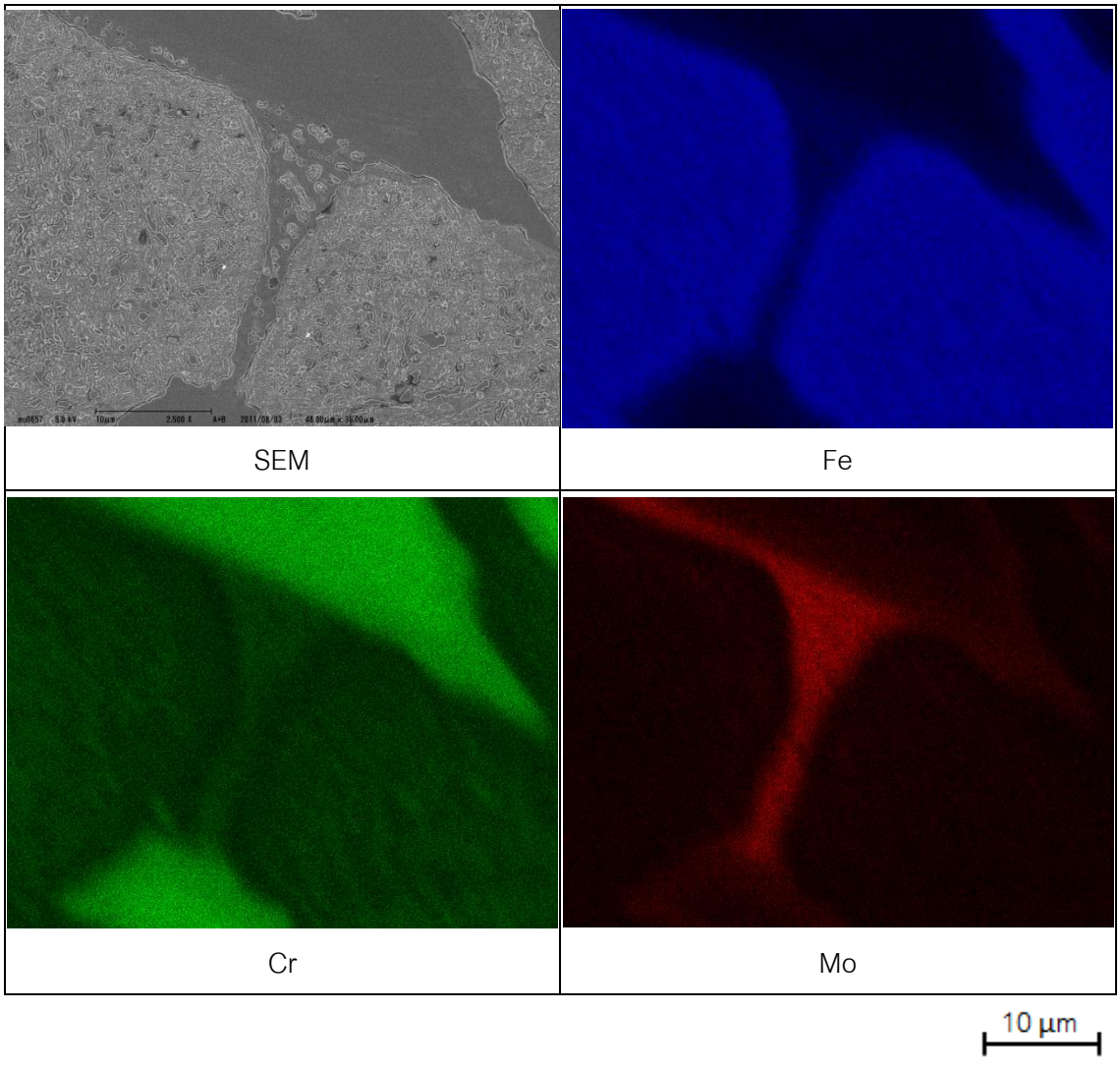

Fig. A.1 SEM microphotograph and distribution of alloying elements taken by EDS analysis of 26% Cr cast iron containing 3% Mo.

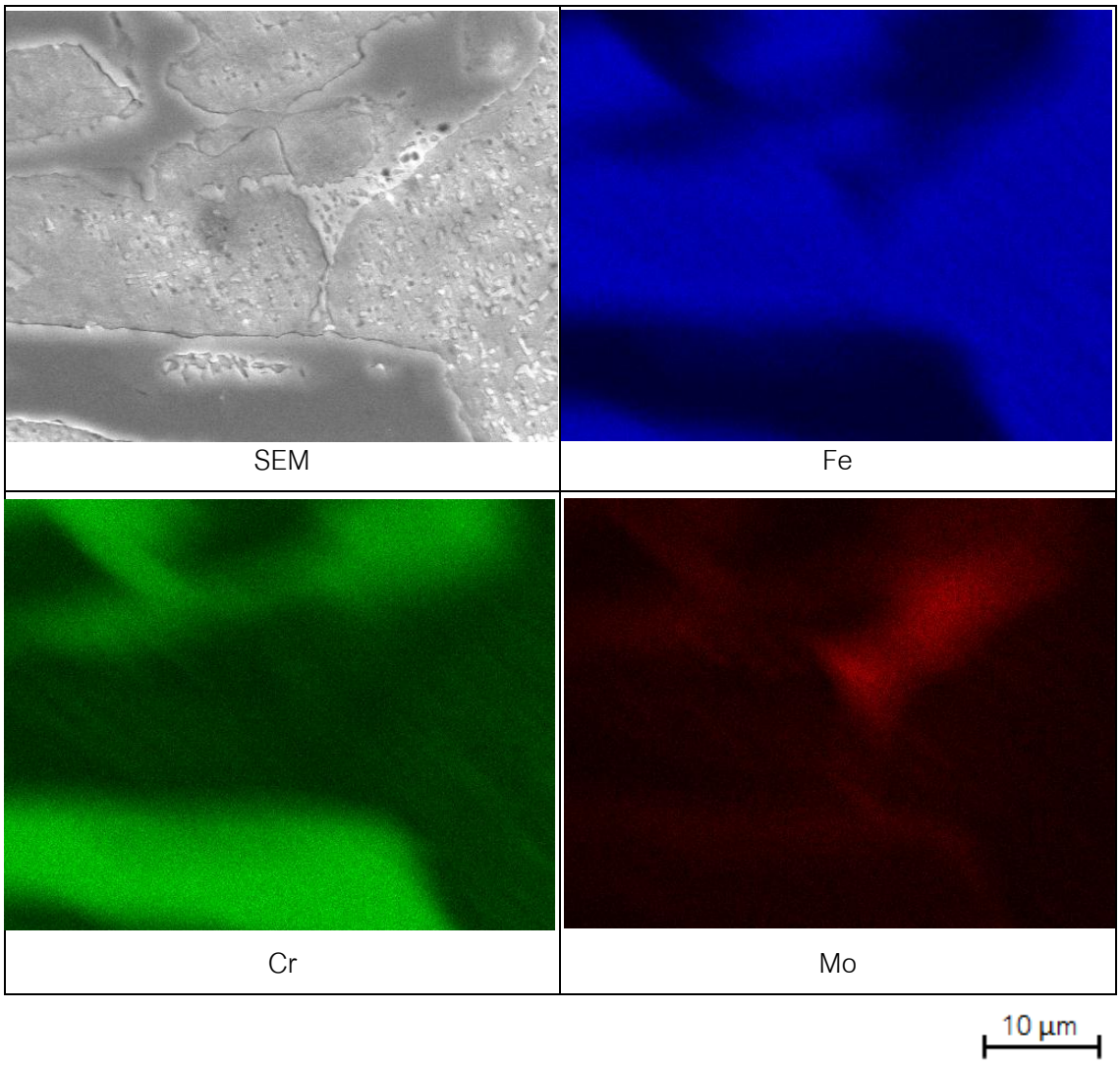

Fig. A.2 SEM microphotograph and distribution of alloying elements taken by EDS analysis of 26% Cr cast iron containing 3% Mo.

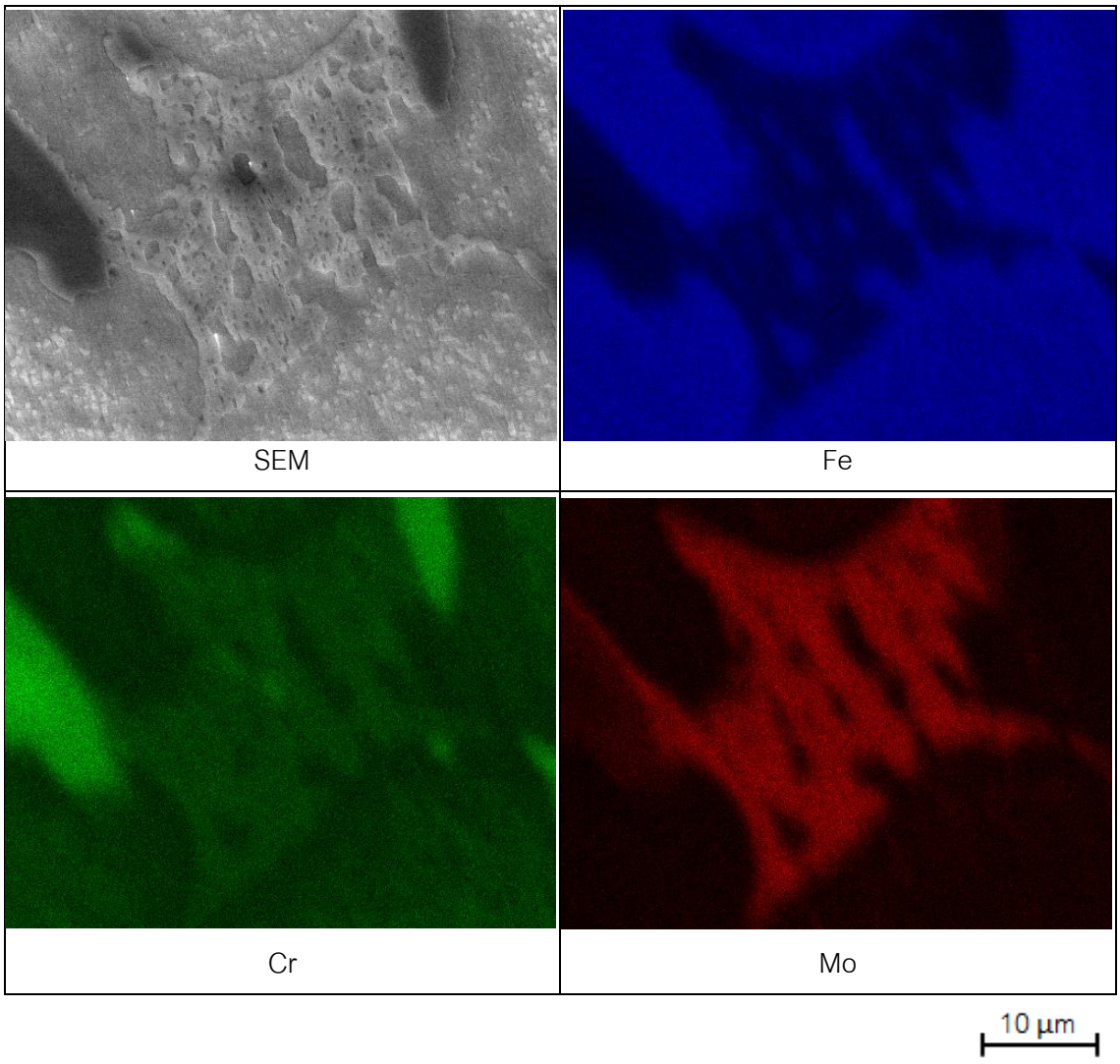

Fig. A.3 SEM microphotograph and distribution of alloying elements taken by EDS analysis of 26% Cr cast iron containing 3% Mo.

Effect of Mo content on wear rate of H_{Tmax} specimen

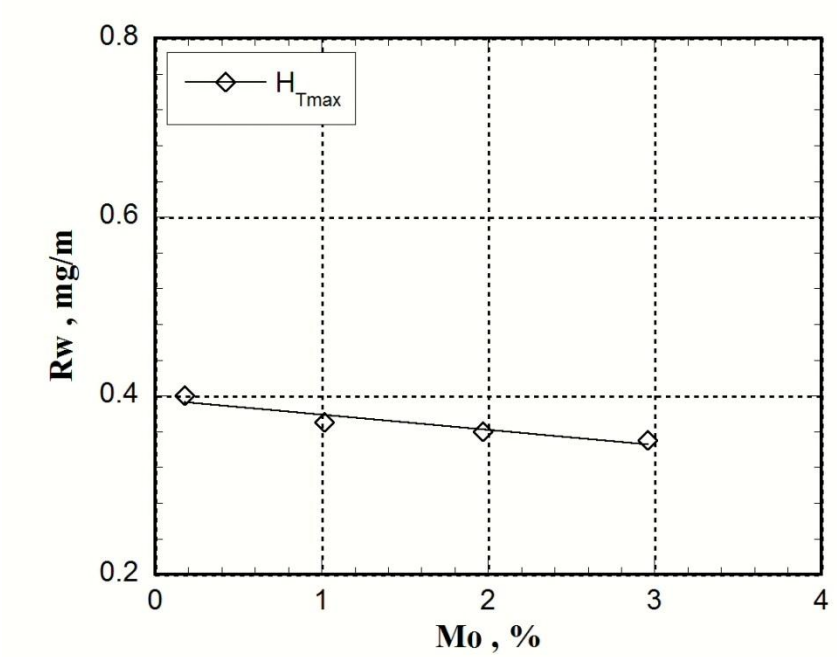

Fig. A.4 Effect of Mo content on wear rate (Rw) of H_{Tmax} specimen. Suga abrasion wear test (two-body-type) with load 9.8 N (1 kgf).

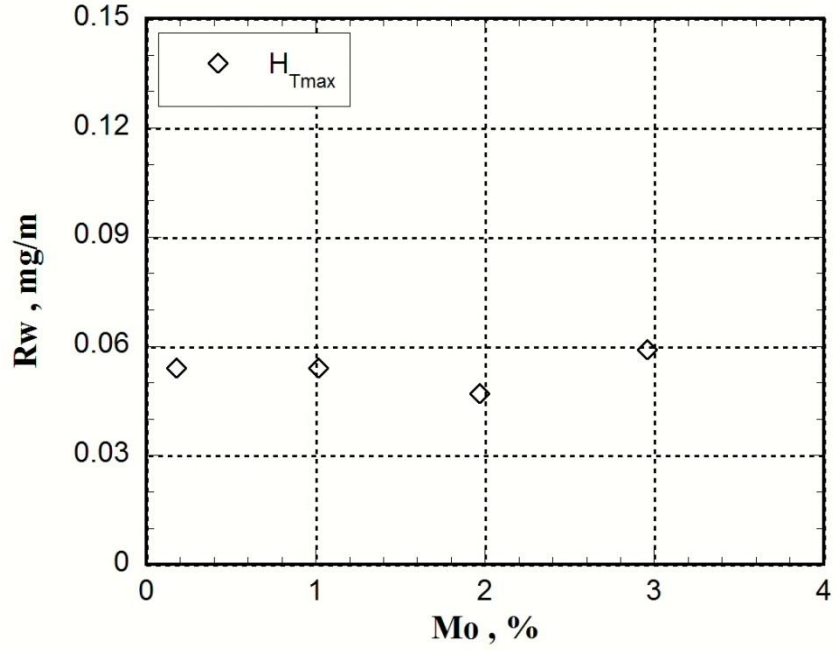

Fig. A.5 Effect of Mo content on wear rate (Rw) of H_{Tmax} specimen. Rubber Wheel abrasion wear test (three-body-type) with load 85.3 N (8.7 kgf).

Effect of Mo content on wear rate comparing with 16% Cr cast iron

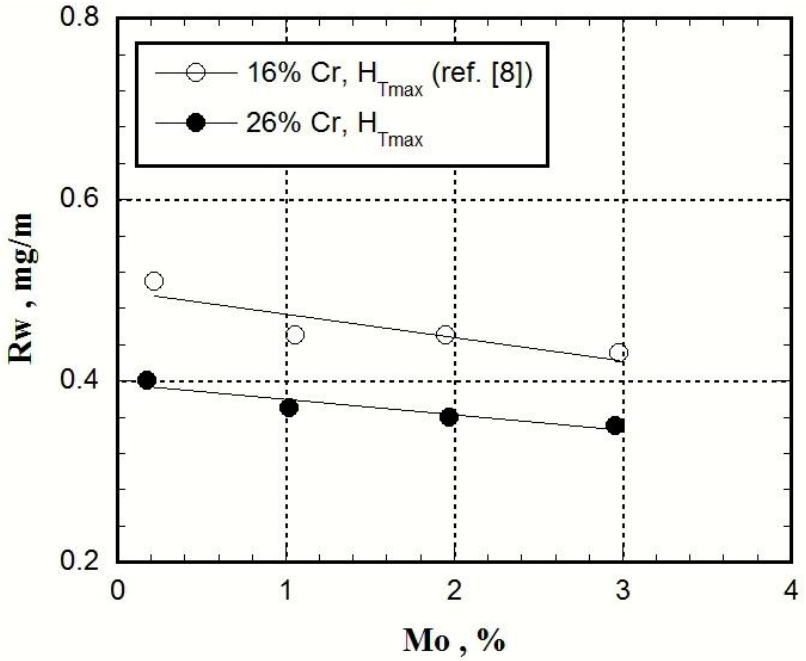

Fig. A.6 Effect of Mo content on wear rate (Rw) in 16% Cr and 26% Cr cast irons with H_{Tmax} varying Mo content. Suga abrasion wear test (two-body-type) with load 9.8 N (1 kgf).

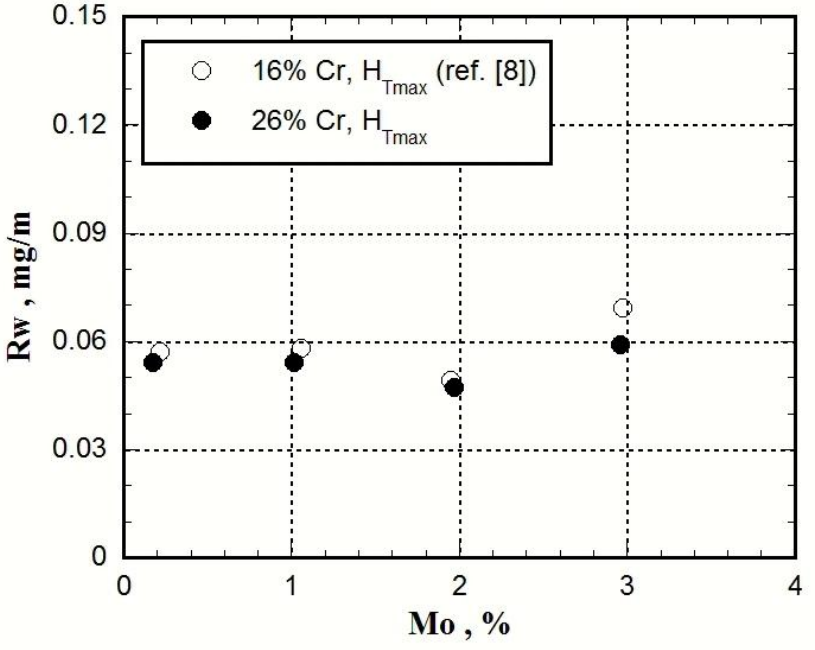

Fig. A.7 Effect of Mo content on wear rate (Rw) in 16% Cr and 26% Cr cast irons with H_{Tmax} varying Mo content. Rubber Wheel abrasion wear test (three-body-type) with load 85.3 N (8.7 kgf).

Biography

My name is Attasit Chooprajong. I was born on July 28, 1986 in Nakhon si thammarat. I graduated from Chulalongkorn University with Bachelor degree of Engineering in 2008. I was a researcher student at Department of Materials Science and Engineering, Kurume National College of Technology, Japan in 2011.